Equalization of Doubly Selective Channels Using Iterative and Recursive Methods

---

Thesis submitted to the University of Wales in candidature for the degree of Doctor of Philosophy.

Sajid Ahmed

September 2005

Cardiff School of Engineering
University of Wales, Cardiff

ProQuest LLC
789 East Eisenhower Parkway
P.O. Box 1346
Ann Arbor, MI 48106-1346

To my parents for their prayers and assistance,
my brothers and sisters for their encouragement
and my wife for her continuous moral support.

Abstract

Novel iterative and recursive schemes for the equalization of time-varying frequency selective channels are proposed. Such doubly selective channels are shown to be common place in mobile communication systems, for example in second generation systems based on time division multiple access (TDMA) and so-called beyond third generation systems most probably utilizing orthogonal frequency division multiplexing (OFDM).

A new maximum likelihood approach for the estimation of the complex multipath gains (MGs) and the real Doppler spreads (DSs) of a parametrically modelled doubly selective single input single output (SISO) channel is derived. Considerable complexity reduction is achieved by exploiting the statistical properties of the training sequence in a TDMA system. The Cramér-Rao lower bound for the resulting estimator is derived and simulation studies are employed to confirm the statistical efficiency of the scheme.

A similar estimation scheme is derived for the MGs and DSs in the context of a multiple input multiple output (MIMO) TDMA system. A computationally efficient recursive equalization scheme for both a SISO and MIMO TDMA system which exploits the estimated MGs and DSs is derived on the basis of repeated application of the matrix inversion lemma. Bit error rate (BER) simulations confirm the advantage of this scheme over equalizers which have limited knowledge of such parameters.

For OFDM transmission over a general random doubly selective SISO channel, the time selectivity is mitigated with an innovative relatively low complexity iterative

method. Equalization is in effect split into two stages: one which exploits the sparsity in the associated channel convolution matrix and a second which performs a posteriori detection of the frequency domain symbols. These two procedures interact in an iterative manner, exchanging information between the time and frequency domains. Simulation studies show that the performance of the scheme approaches the matched filter bound when interleaving is also introduced to aid in decorrelation.

Finally, to overcome the peak to average power problem in conventional OFDM transmission, the iterative approach is extended for single carrier with cyclic prefix (SCCP) systems. The resulting scheme has particularly low complexity and is shown by simulation to have robust performance.

Abbreviations and Acronyms

AML	Approximate Maximum Likelihood
AMPS	Advanced Mobile Phone System
AWGN	Additive White Gaussian Noise
BER	Bit Error Rate
BW	Band Width
CCM	Channel Convolution Matrix
CDMA	Code Division Multiple Access
CIR	Channel Impulse Response
CP	Cyclic Prefix
CRLB	Cramér-Rao Lower Bound
CSI	Channel State Information
DFE	Decision Feedback Equalizer
DQPSK	Differential Quadrature Phase Shift Keying
DS	Doppler Shift
EDGE	Enhanced Data rates for GSM Evolution
ETACS	European Total Access Communication System
FDD	Frequency Division Duplex
FDE	Frequency Domain Equalization
FDMA	Frequency Division Multiple Access
FFT	Fast Fourier Transform
FIR	Finite Impulse Response
FIM	Fisher Information Matrix
FO	Frequency Offset
FRLS	Fast-Recursive Least Squares

GMSK	Gaussian Minimum Shift Keying
GPRS	General Packet Radio Service
GSM	Global System for Mobile Communications
HSCSD	High Speed Circuit Switched Data
IBI	Inter-block Interference
IC	Interference Canceller
ICI	Inter-Carrier-Interference
iff	If and only if
IFFT	Inverse Fast Fourier Transform
IS-95	Interim Standard-95
ISI	Inter-Symbol-Interference
ITU	International Telecommunication Union
LS	Least-Squares
LTE	Linear Transversal Equalizer
LTI	Linear-Time-Invariant
LTV	Linear-Time-Variant
OFDM	Orthogonal Frequency Division Multiplexing
MCM	Multi-Carrier Modulation
MFB	Match Filter Bound
MIMO	Multiple Input and Multiple Output
MIP	Multipath Intensity Profile
MG	Multipath Gain
MLE	Maximum Likelihood Estimator
MMSE	Minimum Mean Square Error
MS	Mobile Station
MSE	Mean Square Error
MVUE	Minimum Variance Unbiased Estimator
NTT	Nippon Telephone and Telegraph System
OFDM	Orthogonal Frequency Division Multiplexing
PDC	Personnel or Pacific Digital Cellular

PSK	Phase Shift Keying
SCCP	Single Carrier with Cyclic Prefix
SISO	Single Input and Single Output
TD-SCDMA	Time Division Synchronized Code Division Multiple Access
TDD	Time Division Duplex
UMTS	Universal Mobile Telecommunications System
UWB	Ultra Wide Band
W-CDMA	Wide band Code Division Multiple Access
WSSUS	Wide Sense Stationary Uncorrelated Scattering

Operators

det(.)	Determinant of a matrix
diag(.)	Diagonal of matrix
E{.}	Expectation
Re(.)	Real Part of a Complex number
$(.)^T$	Transpose
$(.)^H$	Hermitian/Conjugate transposition
$\hat{x}$	Estimated sample
$\|.\|$	Absolute value
$\|\|.\|\|$	Euclidean norm
$\odot$	Schur-Hadamard Product
$\prod$	Interleaver
$\tilde{x}$	Interleaved sample
$\mathcal{O}(N)$	Order N

Publications

Journal Papers

1. S. Ahmed, S. Lambotharan, A. Jakobsson and J. A. Chambers, "Parameter estimation and equalization techniques for communication channels with multipath and multiple frequency offsets," *IEEE Trans. Commun.*, vol. 53, pp. 219-223, Feb. 2005.

2. S. Ahmed, S. Lambotharan, A. Jakobsson and J. A. Chambers, "MIMO frequency selective channels with multiple frequency offsets: estimation and detection techniques," *IEE Proc. Commun.*, vol. 53, pp. 489- 494, Aug. 2005.

3. S. Ahmed, M. Sellathurai, S. Lambotharan and J. A. Chambers, "Low complexity iterative method of equalization for single carrier with cyclic prefix in doubly selective channels," *accepted for IEEE Signal Processing Letters.*

4. S. Ahmed, M. Sellathurai, S. Lambotharan and J. A. Chambers, "Low complexity iterative method of equalization for OFDM in doubly selective channels, " *submitted to IEEE Trans. on Wireless Communications.*

Conference Papers

1. S. Ahmed, S. Lambotharan, A. Jakobsson and J. A. Chambers, "Parameter estimation and equalization techniques for MIMO frequency selective channels with multiple frequency offsets", *European Signal Processing Conference (EUSIPCO 2004)*, Vienna, Austria.

2. S. Ahmed, J. A. Chambers and S. Lambotharan, "Frequency offset estimation technique for frequency selective channel with multiple frequency offsets in DS-CDMA", *International Bhurban Conference on Applied Science and Technology (IBCAST 2004)*, Bhurban, Pak.

3. S. Ahmed, M. Sellathurai, S. Lambotharan and J. A. Chambers, "Low complexity iterative methods of equalization for OFDM," *European Signal Processing Conference (EUSIPCO 2005)*, Antalya, Turkey.

4. S. Ahmed, M. Sellathurai and J. A. Chambers, "Low complexity iterative method of equalization for OFDM in time varying Channels," *accepted for 39th Asilomar Conference on Signals, Systems and Computers,* California, USA.

Statement of Originality

As far as the author knows the majority of the work presented in chapter 3 to 6 represents original contribution to the area of parameter estimation and equalization. The originality is partially supported by four journal and four conference papers. The most significant contributions are given below:-

1. In chapter 3, and [1] an Approximate Maximum Likelihood (AML) estimator for a single input and single output multipath channel with distinct frequency offsets is proposed. The AML estimator splits the L-dimensional maximization problem into L one dimensional maximization problems. In this scenario to compensate for the effects of multiple frequency offsets, structural movements of the matrices are exploited in the design of the Minimum Mean Squared Error (MMSE) equalizer, in particular, repeated application of the matrix inversion lemma yields a low complexity equalizer.

2. In chapter 4, the parameter estimation and equalization of single input single output channel is extended to Miltiple Input Multiple Output (MIMO) multipath and distinct frequency offsets channels, the related work is presented in [2,3].

3. In chapter 5 and [4–6], a new iterative equalization method for a doubly selective Orthogonal Frequency Division Multiplexing (OFDM) channel is proposed. The proposed method exploits the sparsity of the channel convolution matrix to design a general MMSE equalizer. The transmitted time domain samples are estimated on the basis of interference cancellation. To cancel the interference the a posteriori mean values are found from the a posteriori mean values of frequency domain symbols.

4. In chapter 6 and [7], iterative equalization of a single carrier cyclic prefix scheme is proposed, which also exploits the sparsity of the channel convolution matrix to find the general MMSE equalizer and estimator. In contrast to frequency domain equalization of single carrier cyclic prefix, this algorithm benefits from not requiring a fast Fourier and inverse fast Fourier transform at the receiver.

Acknowledgment

First of all, I would like to thank my respected supervisor Prof. J. A. Chambers for his invaluable suggestions, guidance, patience and continuous encouragement throughout my research work, without which it would not have been possible to execute my research work.

I am also indebted to my co-supervisors Dr. S. Lambotharan and Dr. M. Sellathurai for their discussions, criticism and suggestions in writing up my research work and understanding the basics of my research work. I would especially like to express my appreciation to Dr. S. Lambotharan, whose enthusiasm to discover novel equalization techniques put me on the track for my PhD.

Special thanks to Dr. Andreas Jakobsson for his discussion on frequency offsets, help in learning the type-setting package LaTex and advice on how to write research papers.

I am very grateful to the Ministry of Science and Technology and Cardiff School of Engineering for supporting me financially to complete my PhD.

I am most grateful to my research companions both in King's College London and Cardiff University, Dr. Wenwu Wang, Dr. Yi Hui, Dr. Maria Jafari, Dr. Cenk Toker, Rab Nawaz, Shabbar Khan, Zhuo Zhang, Thomas Bowles, Qiang Yue, Li Zhang, Yonggang Zhang, Min Jing, Zaid, Abdul Rehman, Ahmed Izzidien, Lay Teen, Clive Cheong Took and Andrew Aubrey, for their great company and support.

CONTENTS

List of Figures

List of Tables

Chapter 1

INTRODUCTION

The notion of mobile communication essentially began in 1980. Since then, it has undergone significant change and experienced enormous growth. The mobile systems introduced in the 1980s were based on analogue communication techniques and are commonly referred to as first generation systems, they only supported voice services [8]. For first generation systems several standards were developed throughout the world such as Advanced Mobile Phone System (AMPS) in the United States, European Total Access Communications System (ETACS) in Europe and Nippon Telephone and Telegraph System (NTT) in Japan. The commonly used standards for first generation mobiles systems, throughout the world, and their key features are summarized in Table 1.1.

Region	Europe	North America	Japan
	ETACS	AMPS	NTT
Multiple access	FDMA	FDMA	FDMA
Duplexing	FDD	FDD	FDD
Down Link	935-960 MHz	869-894 MHz	870-885 MHz
Up Link	890-915 MHz	824-849 MHz	925-940 MHz
Channel Spacing	25 kHz	30 kHz	25 kHz
Data rate	8 kbps	10 kbps	0.3 kbps

Table 1.1. Air interfaces and spectrum allocation in first generation mobile systems.

In the 1990s digital transmission techniques were introduced and formed the second generation systems. They provided increased spectrum efficiency and higher quality of voice services than the first generation systems together with better data services [9]. The digital standards currently in use, such as Global System for Mobile communications (GSM) in Europe, Interim Standard-95 (IS-95) in the United States and Personnel or Pacific Digital Cellular (PDC) in Japan, are second generation systems. The most common standards used for second generation mobile systems in the world and their key features are summarized in Table 1.2.

Region	Europe	North America	North America	Japan
	GSM	TDMA (IS-54/136)	IS-95	PDC
Multiple access	TDMA	TDMA	CDMA	TDMA
Duplexing	FDD	FDD	FDD	FDD
Modulation	GMSK	$\pi/4$ DQPSK	QPSK/OQPSK	$\pi/4$ DQPSK
Down-link	935-960 MHz	869-894 MHz	869-894 MHz	810-826 MHz
Up-link	890-915 MHz	824-849 MHz	824-849 MHz	940-956 MHz
Channel spacing	200 kHz	30 kHz	1,250 kHz	25 kHz
Data/Chip rate	270.833 kbps	48.6 kbps	1.2288 Mcps	42 kbps

Table 1.2. Air interfaces and spectrum allocation for second generation mobile systems.

The initial second generation systems were originally designed for the delivery of only high quality voice services and their data handling capabilities were limited to several tens of kbps [10]. Therefore, for high data rates and more advance services, such as packet switched data, second generation systems were further upgraded and referred to as 2.5 generation systems. The three upgrade options for GSM include; Enhanced Data Rate for GSM Evolution (EDGE) that can provide data rates up to 500kbps within a GSM carrier spacing of 200kHz, General Packet Radio Services (GPRS), as the name implies, is a packet switch technique and High Speed Circuit Switched Data

(HSCSD), which is a circuit switched technique that allows a single mobile user to use consecutive time slots in the GSM standard for high data rate applications [11]. EDGE and GPRS are also the upgrade options for IS-136, while the cdma2000 standard is the upgrade option for IS-95. [12].

In the 21^{st} century, wireless mobile telephony is rapidly growing and providing new and improved multimedia services. High quality images and video will be transmitted and received; moreover, mobile telephony provides access to the web with high data rate requiring asymmetric access. Emerging requirements for high data rate services and better spectrum efficiency are the main drivers identified for the third generation mobile communication systems [9, 13]. The International Telecommunication Union (ITU) describes third generation networks as IMT-2000 and prescribes wideband CDMA as the air interface. The main objectives of the IMT-2000 standard are summarized as [11, 14]

- Data rate of 344 kbps for vehicular environment
- Data rate of 2 Mbps for indoor environment
- Higher spectrum efficiency as compared to existing system
- High flexibility to introduce new services

Today's research focuses on beyond third generation or fourth generation wireless systems, where mobile users may use portable computers. In the first phase the operating frequencies of fourth generation systems may be around 5.8GHz, and are likely to support [15]

- 2 Mbps for moving vehicles, and
- 2-600 Mbps for low mobility systems

This is the background to the evolution of mobile communication systems since 1980. To meet the demands for increased data rate services and improved spectrum effi-

Region	Europe	North America	China
	UMTS	CDMA-2000	TD-SCDMA
Multiple access	W-CDMA	MC-CDMA	CDMA
Duplexing	FDD/TDD	FDD	TDD
Data Rate	2Mbps	2Mbps	2Mbps
Downlink	2110-2170MHz	1930-1990MHz	2010-2025MHz
Uplink	1920-1980MHz	1850-1910MHz	2010-2025MHz
Channel spacing	5MHz	5MHz	5MHz
Chip Rate	3.84Mcps	3.6864Mcps	1.28Mcps

Table 1.3. Expected air interfaces and spectrum allocation for third generation mobile systems.

ciency advanced digital signal processing techniques must be exploited at the physical layer [16], the heart of which is the radio channel between the transmitter and receiver.

1.1 Channel Modelling

In wireless mobile systems, communication is not normally line of sight, particularly in an urban environment; instead, the received signal consists of a large number of reflected, refracted and scattered waves. Therefore, the signal travels from the transmitter to receiver via more than one path. Due to this multipath propagation, the transmitted signal arrives at the receiver at different time instances and with different amplitudes that may give rise to Inter-Symbol-Interference (ISI) [17]. An ISI producing channel is termed frequency selective. ISI is a fundamental limiting factor in the performance of high data rate communication, within the physical layer of a mobile communication system. If the channel is not changing significantly within the observation interval of time then the effects of ISI can be compensated for relatively easily by using an equalizer. In the noiseless case, an equalizer is designed such that the convolution of its impulse response with the channel impulse response should ide-

ally be a Kronecker delta function [17]. Such an equalizer may require knowledge of the channel impulse response, which is not usually available. Hence, to estimate the channel impulse response, the transmitter is generally required to send training data, already known at the receiver. Indirect equalization techniques, such as adaptive do not require CSI, can also be employed. These techniques learn the channel or its inverse without estimating it [18].

On the other hand, if the frequency selective channel is time-varying (also called time selective), it is referred to as a doubly selective channel. Time selectivity of the channel degrades the Bit-Error-Rate (BER) performance and increases the computational complexity of conventional receivers [1, 19]. However, time selectivity of the channel can be exploited to obtain time diversity benefit.

Therefore, the design of a relatively low complexity receiver that can provide significant improvement in BER performance over a conventional receiver in a frequency selective environment is the main motivation for this thesis. The causes of time variations in the channel are next discussed.

1.1.1 Sinusoidal time-varying channel

As previously discussed, from first generation to beyond third generation, the requirement for high data rates is continuously increasing. With the increase in data rate the operating frequency is also increasing. Mobility in the systems, at high operating frequencies yields significant Doppler Shifts (DSs). Therefore, even if in a given interval of time the channel is not changing due to mobility, the DS may introduce time selectivity in the channel. Consequently, the assumption that the channel is constant, in a given interval of time, does not hold true and affect the BER performance of the receiver. In order to improve the BER performance of the receiver, the effects of the time selectivity of the channel due to DS must be cancelled. In most of the available literature [20–23], it is commonly considered that all multipaths have identical DSs and can be compensated for relatively easily prior to MLSE or adaptive equalization.

However, the DS is defined as

$$f_d = \frac{f_c v_r}{c} \cos\theta \tag{1.1.1}$$

where v_r, is the speed of the mobile station (MS) in m/s, f_c is the carrier frequency in Hz, c is the velocity of light in m/s and θ is the angle of arrival in radians. This equation shows that if the relative speed between the base station and MS is constant, then the DS will be a function of the angle of arrival. Therefore, when the DS is significant it is necessary to account for it from each angle of arrival or multipath, which is one of the main motivations of this thesis. For example, consider a mobile user in a fast moving vehicle with a speed of approximately 250 km/h and a carrier frequency of 4 GHz. The DS at the base station for an arrival angle of zero degrees, is approximately 1 kHz, whilst for an arrival angle of 60 degrees becomes 0.5kHz. This results in phase deviations of approximately 18 and 9 degrees respectively for both arrival angles, in every bit period, for a bit rate of 20 kbit/s, and distinct sinusoidal time variations into each multipath of the channel. In this scenario, it is difficult to compensate for the effects of DSs prior to equalization and that must be accounted for in equalizer design.

Numerical Example: In order to examine the benefits of accounting for the distinct DSs in equalizer design, the above mentioned scenario is simulated. In the first case, the receiver assumes the same DS from each multipath and cancels the effects of DS prior to equalization, which is a general type of equalization for frequency offset compensation. In the second case, the receiver assumes distinct DSs from each multipath and accounts for them in the equalizer design. The BER performances of both cases are depicted in Figure 1.1. It can be noted that in the equalizer design accounting for distinct DSs from each multipath a better performance as compared to assuming identical DSs from each multipath is obtained. For example, at a fixed BER of 10^{-3}, a 2 dB improvement in SNR is required by the receiver assuming a single DS.

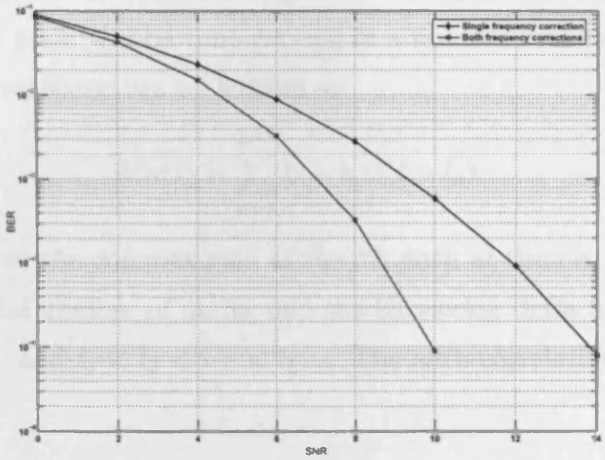

Figure 1.1. BER performance comparison of two receivers; one is assuming identical DS from each path and the second is accounting for multiple DSs from each multipath. For both simulations the length of the channel is kept equal to 2 and a 10 taps equalizer is used.

1.1.2 A general time-varying channel

In wireless mobile communications the channel is not stationary at all times, it may vary with respect to time. In wireless and wire-line communications data are transmitted in frames and it is assumed that the channel is not changing during one frame at least [17]. But, sometimes the channel does not remain constant even in one frame. Therefore, to describe time varying nature of the channels a more general time-varying channel is modelled. Wide Sense Stationary and Uncorrelated Scattering (WSSUS) model is the most commonly used channel model in wireless communications [17, 24, 25]. In the WSSUS model the channel is characterized by its delay (or multipath) power spectrum and the scattering function.

When an impulse is transmitted over a multipath channel the received signal is a train of impulses. The range of locations of impulses with sufficient strength reveals the

spreading of the channel. If the channel is time-varying then the complex strength of each impulse in the train will be time-varying in a random manner. For the WSSUS model the impulse response can be written as

$$h(n;l) = \sum_{p=0}^{L-1} h(n;l_p)\delta(l-l_p), \tag{1.1.2}$$

where $h(n,l)$ denotes the complex gain of the lth path at time n. L and $\delta(.)$ denote respectively the total number of paths, and the Kronecker delta function. Moreover, $l \in \{l_o\ l_1\ \cdots\ l_{L-1}\}$, and $l_o < l_1 < \cdots < l_{L-1}$. The auto-correlation of the channel is given by

$$E\{h(n_1;l_1)h^*(n_2;l_2)\} = r_{hh}(n_1-n_2;l_1-l_2) \tag{1.1.3}$$

where $(.)^*$ denotes the complex conjugate operator. Since, the multipaths are uncorrelated

$$E\{h(n_1;l_1)h^*(n_2;l_2)\} = r_{hh}(n_1-n_2;l_1)\delta(l_1-l_2), \tag{1.1.4}$$

and can be decomposed into time and multipath auto-correlation functions as,

$$r_{hh}(n_1-n_2;l) = r_{tt}(n_1-n_2)r_{pp}(l), \tag{1.1.5}$$

where $r_{tt}(n_1-n_2)$ and $r_{pp}(l)$ are respectively the auto-correlation of the lth path with respect to time and the auto-correlation of the channel (assuming time stationarity) with respect to multipath which is also called the Multipath Intensity Profile (MIP) [17].

Example: For a Rayleigh fading channel, $h(n,l)$ is a white Gaussian random variable with zero mean and $\sigma_l^2|_{l=0,1,\ldots,L-1}$ is the variance of the lth multipath. Moreover, $h(n,l)|_{l=0,1,\ldots,L-1}$ are independent. Therefore, for a Rayleigh fading channel

$$r_{tt}(n_1-n_2) = 0 \quad \text{if} \quad n_1-n_2 \neq 0 \tag{1.1.6}$$

$$= 1 \quad \text{if} \quad n_1-n_2 = 0 \tag{1.1.7}$$

$$\text{and} \quad r_{pp}(l) = \sigma_l^2. \tag{1.1.8}$$

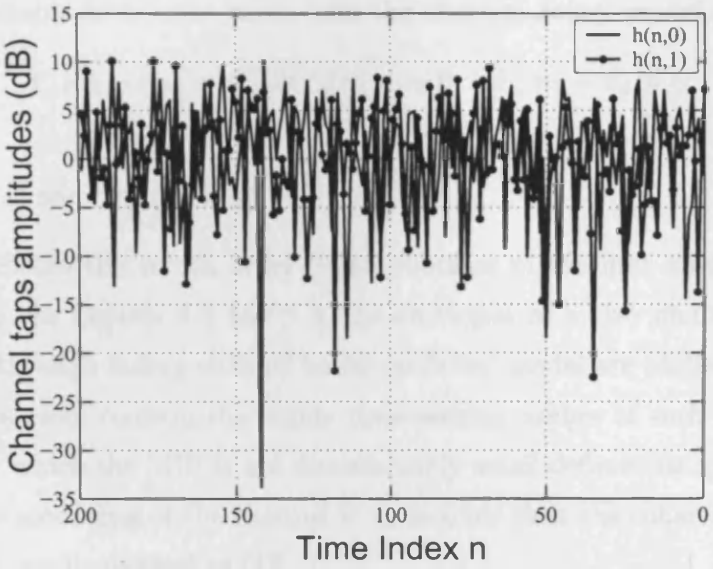

Figure 1.2. Time variations in the amplitudes of two multipaths of a Rayleigh fading channel.

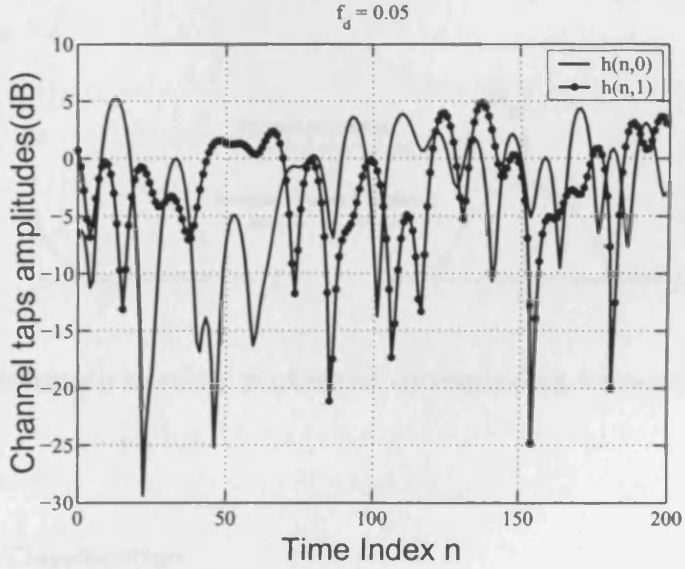

Figure 1.3. Time variations in the amplitudes of two multipaths of a Rayleigh fading channel based on Jakes' model.

If the coefficients $h(n,l)$ are taken from the classical Jakes' model [26] then

$$r_{tt}(n_1 - n_2) = J_o[2\pi f_d(n_1 - n_2)] \quad \text{if} \quad n_1 - n_2 \neq 0 \tag{1.1.9}$$

$$= 1 \quad \text{if} \quad n_1 - n_2 = 0 \tag{1.1.10}$$

$$\text{and} \quad r_{pp}(l) = \sigma_l^2,$$

where $J_o(\cdot)$ denotes the zeroth order Bessel function of the first kind and f_d is the normalized DS. In Figures 1.2 and 1.3, the envelopes of a two multipath Rayleigh fading and a Rayleigh fading channel based on Jakes' model are plotted with respect to time. These plots confirm the highly time-varying nature of such channels. The time width for which the MIP is not diminishingly small defines the spreading of the channel. If the spreading of the channel is T_s seconds then the coherence bandwidth of the channel can be defined as [27],

$$(BW)_h = \frac{1}{T_s}. \tag{1.1.11}$$

The relationship between the MIP, $r_{pp}(l)$, and its frequency spectrum, $R_{pp}(f)$, is shown in Figure 1.4

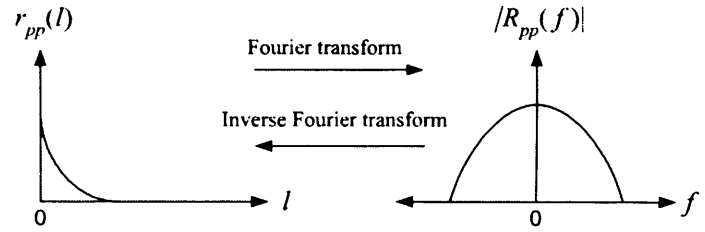

Figure 1.4. Multipath intensity profile and corresponding frequency domain representation.

1.2 Channel Classification

The MIP helps to describe the nature of the channel. A channel is said to be *frequency flat or non selective* if within the bandwidth, BW, occupied by the transmitted signal

the amplitude response of $R_{pp}(f)$ is constant. In the time domain, it can be said that the spreading time, T_s, is less than the symbol period, T. Flat fading does not introduce ISI. Therefore, such a channel satisfies

$$T_s << T. \tag{1.2.1}$$

On the other hand, a channel is said to be *frequency selective* if within the bandwidth, BW, occupied by the transmitted signal, the amplitude response $R_{pp}(f)$ is not flat for the entire bandwidth of the transmitted signal. Hence, each frequency component of the signal is amplified and phase shifted differently. Here, the multipath propagation spreads the transmitted signal over an interval of time which is longer than the symbol period, which can cause ISI. For frequency selective fading the channel satisfies

$$T_s >> T \tag{1.2.2}$$

i.e. the spreading of one symbol by the channel overlaps its neighbors.

1.3 Outline of the Thesis

Overview: This thesis proposes relatively low complexity equalization methods for time-varying frequency selective channels for communication systems that are based on Time Division Multiple Access (TDMA), Multiple Input Multiple Output (MIMO), Orthogonal Frequency Division Multiplexing (OFDM) and Single Carrier with Cyclic Prefix (SCCP) technologies. In the first two contribution chapters (chapters 3 and 4), the time variations in the multipaths of the channels are sinusoidal, while, in last two contribution chapters (chapters 3 and 4), a more general and realistic time-varying multipath channel is considered. This evolution corresponds to my period of research study. The following sub-sections review briefly what can be found in each of the five contribution chapters.

Chapter 3 studies parameter estimation and equalization for a Single Input Single Output (SISO), TDMA based communication system, such as GSM, where it is assumed that each multipath of the channel has distinct DS and thereby makes the

problem different from the identical DS problem. Here, unlike the identical DS problem [20,28,29], the distinct DSs cannot be compensated for prior to equalization and must be accounted for in equalization. In order to design an equalizer the complex Multipath Gains (MGs) and DSs are required. Presence of the distinct DSs converts the estimation of these parameters into a complicated $L+1$ dimensional optimization problem, where L is the length of the channel. Therefore, in order to estimate the MGs and DSs, the correlation property of the transmitted training signal sequence is exploited which thereby splits the $L+1$ dimensional estimation problem into $L+1$ one-dimensional problems. A maximum likelihood estimation approach is used to find the complex MGs and DSs. Moreover, to estimate the DSs the proposed algorithm does not require explicit knowledge of the MGs of the channel but requires knowledge of the support L of the channel. Then, to assess the performances of the proposed estimators the benchmark Cramér Rao lower bound (CRLB) for DSs and MGs [30] is derived.

As distinct DSs introduce time selectivity into the channel, adaptive and blind adaptive equalizers yield poor BER performance as the equalizer taps need to be updated after every symbol interval. Further, it has been shown that the conventional minimum mean square error (MMSE) equalizer is computationally cumbersome as the effective channel convolution matrix (CCM) changes deterministically between symbols, due to the multiple DSs. By exploiting the structural property of these variations, and using multiple application of the matrix inversion lemma, a computationally efficient recursive algorithm for the equalizer design is proposed.

Chapter 4 extends the work presented in chapter 3 to MIMO frequency selective channels with each multipath having distinct DS. The MIMO technology uses multiple antennas at both the transmit and the receive sides to obtain spatial diversity. Recent research in communication theory has shown that large gains in diversity, capacity and reliability of communications over wireless channels could be achieved by exploiting such spatial diversity and will play a key role in future high rate wireless

communications provided there is rich scattering environment [31,32]. The parameter estimation for flat fading channels in MIMO is studied in [33]. In this chapter the parameters in a MIMO system, allowing for a frequency selective channel between each transmit and receive antenna and each multipath, possibly having distinct DSs, are estimated. The training signals transmitted by all the antennas are assumed to be spatially and temporally uncorrelated. Therefore, by exploiting this property, MGs and DSs are estimated. In order to assess the performances of the estimators the benchmark CRLB is derived and used to compare the performances of the estimators.

Again, as in chapter 3, by exploiting the structural property of the variations in the CCM in this case, the computationally efficient recursive algorithm reduces the dimension of the matrix to find the inverse of the matrix that is needed to find the equalizer coefficient values from $n_R M \times n_R M$ to $n_R \times n_R$, where n_R is the number of receive antennas and M is the number of equalizer taps, as addressed in [2,3].

Chapter 5 studies the equalization of a general time-varying channel for an OFDM based system. Here in contrast to previous work, each multipath of the channel is randomly time varying. For this scenario the approach discussed in chapters 3 to 4 can not be applied, since the CCM does not change deterministically. To combat the effects of time selectivity of the channel in an OFDM system, Schniter in [19] preprocessed the received signal by multiplying with window coefficients that render the Inter-Carrier-Interference (ICI) response sparse, and thereby squeeze the significant coefficients into the $2D+1$ central diagonals of an ICI matrix. Here, it is found that $D = f_d N + 1$, where f_d is the DS in the carrier frequency and N is the number of carriers used to transmit an OFDM symbol. The complexity of this algorithm increases as the DS increases. In contrast to this work, examining the time domain model of the received OFDM signal reveals that the CCM is already sparse and has similar structure to that after preprocessing of the received samples in [19]. In this case, the number of non-zero elements in a row depends on the length of channel taps L, which

for a wireless channel is typically small, for example 5. Therefore, in this chapter, a new low complexity iterative method is addressed to compensate for the effects of time selectivity of the channel. The method splits the equalization into two stages. The first stage exploits the sparsity present in the CCM to estimate the time domain transmitted samples and the second stage performs the a posteriori detection of the frequency domain symbols. Both the stages exchange their information iteratively. The performance of the algorithm is compared with the match filter bound.

Chapter 6 studies the equalization of a single carrier with cyclic prefix (SCCP) scheme in a time varying frequency selective channel. A SCCP is an alternative to OFDM. OFDM is an attractive technique for transmission over frequency selective channels since it allows low complexity channel equalization at the receiver. However, OFDM requires an expensive and efficient transmitter amplifier at the front end, due to high peak-to-average power ratio (PAPR). Single carrier with cyclic prefix (SCCP) is a closely related transmission scheme that possesses most of the benefits of OFDM but does not require an expensive linear amplifier that can operate linearly over a wide range of signal amplitudes. Although similar to OFDM, in a time invariant multipath environment an SCCP system is very robust, it is sensitive to the time selective fading characteristics of the wireless channel. Time selectivity of the channel disturbs the orthogonality of the channel matrix, thereby degrading the system performance significantly and increasing the computational complexity of the receiver. On the other hand, time selectivity introduces temporal diversity that can be exploited to improve the performance. In this chapter, working with time domain samples, a low complexity iterative algorithm is proposed to compensate for the effects of time selectivity of the channel, which exploits the sparsity present in the CCM and a Maximum a Posteriori (MAP) detection in an iterative fashion, as in [7].

Finally, in chapter **Chapter 7** conclusions are drawn and future research directions are suggested.

Throughout the thesis, MATLAB is used to simulate all the problems.

Chapter 2

PARAMETER ESTIMATION AND EQUALIZATION

In many radio communication systems such as wireless mobile, wire-line telephone and optical transmission there may be more than one path, also called multipaths, between the transmitter and the receiver. In mobile telephony these multipaths may be due to the reflections and refractions from the buildings and other obstacles between the transmitter and receiver [17]. In wireline telephony that may be due to the dispersive nature of the wires [34, 35]. Multipaths may give rise to ISI, which limits high data rate transmission. Therefore, in a multipath environment to detect correctly the transmitted data, generally, a complex equalizer is designed that sometimes requires the Channel Impulse Response (CIR) i.e. the complex channel MGs. In order to estimate the CIR, generally, a training sequence is embedded in the transmitted signal sequence. In this chapter, a brief background to the technology of equalization and parameter estimation is presented.

2.1 Basic Baseband Model of a Communication System

Almost all baseband digital communication systems consist of three basic building blocks, the transmitter, the channel and the equalizer (receiver) as shown in Figure 2.1. In the figure, $x(n)$ is the transmitted symbol, $\{h(n)\}$ is the MGs sequence, $v(n)$ is the additive noise sample, $r(n)$ is the received sample, $\{w(n)\}$ are equalizer

coefficients, $\hat{x}(n)$ is the estimated signal after equalization and n is the discrete time index.

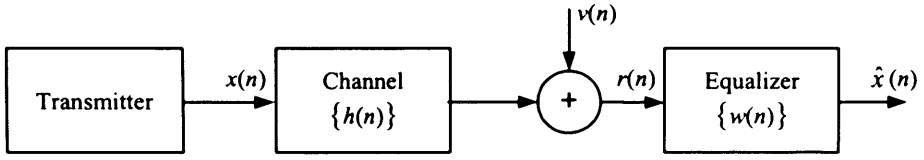

Figure 2.1. Baseband model of a digital communication system, consisting of the transmitter, channel and equalizer (receiver).

In the basic baseband model of a digital communication system, the transmitter is one of the most important parts of a digital communication system. The main function of the transmitter is to convert the raw data into an appropriate form suitable for transmission, e.g., the voice signal is sampled and encoded into binary signals to transmit. The original band of frequencies occupied by the encoded binary signals is called a baseband signal. The baseband signal has wide frequency spectrum centered at zero frequency, which is bandlimited before transmission with a filter called a transmit filter. Usually the binary signals contain low frequencies, which are difficult to propagate. Hence, signals centered around higher frequencies are preferred. The second function of the transmitter is therefore to shift the frequency spectrum of the bandlimited signal to some higher frequency centered at f_c called the carrier frequency. To shift the frequency spectrum to a higher frequency, the bandlimited signal is multiplied by the high frequency sinusoidal signal of frequency f_c [17]. The output signal is termed as the passband and the mapping of the baseband signal into the passband signal is called modulation.

The transmitted signal passes through the channel that can be considered as a Finite Impulse Response (FIR) filter and arrives at the receiver. The received signal is again passed through a filter called the receive filter matched to the frequency band of the transmitter. In general, the effects of the transmit filter, the transmission medium and the receive filter are included in the channel model $h(n)$ with finite time support.

Therefore, if the support of the modelled channel is L and the sampling rate at the receiver is equal to the symbol transmission rate then the received signal can be written as

$$r(n) = \sum_{l=0}^{L-1} h(l)x(n-l) + v(n) \tag{2.1.1}$$

Before proceeding, the following assumptions are made that are imposed throughout this thesis.

- The transmitted symbols $\{x(n)\}$ are independently and identically distributed (i.i.d).
- The additive noise samples $\{v(n)\}$ are zero mean white circularly Gaussian with variance σ_v^2.
- The channel is an FIR filter of support L.

Let the multipath component $h(m)$ possess the highest relative amplitude in the sequence $\{h(n)\}$, this multipath is termed as main multipath, multipaths before and after the main multipath are respectively called pre- and post-cursors. The energy of the wanted signal is conveyed mainly by the contribution of the main path. In addition to that the received signal is also contributed to by the convolution of pre- and post-cursors. Therefore, the received signal in (2.1.1) can be written as

$$r(n) = h(m)x(n-m) + \sum_{\substack{l=0 \\ l\neq m}}^{L-1} h(l)x(n-l) + v(n), \tag{2.1.2}$$

the term $\sum_{\substack{l=0 \\ l\neq m}}^{L-1} h(l)x(n-l)$ is the interference from the other symbols due to pre- and post-cursers and is called ISI. In the noiseless case, if $h(m)$ is known then the decision device at the receiver may reconstruct the transmitted signal $x(n)$ iff

$$|h(m)| > \sum_{\substack{l=0 \\ l\neq m}}^{L-1} |h(l)|, \tag{2.1.3}$$

however, if this condition is not satisfied an error may occur. The ISI effects can be cancelled by employing an equalizer that accumulates the energy transmitted for $x(n)$, reduces the energy from other transmitted symbols and produces a decision variable, $\hat{x}(n)$. Ideally,

$$\hat{x}(n) = x(n) + \nu(n) \tag{2.1.4}$$

where $\nu(n)$ is additive colored noise with the same variance as $v(n)$. If equalization is effective, a decision device can determine $x(n)$ with the same reliability as if the channel did not introduce any ISI. If $\{w(n)\}$ is the impulse response sequence of the equalizer then ideally in the absence of additive noise the following identity will hold

$$\begin{aligned} h(n) * w(n) &= \delta(n) \\ &= 1 \quad n = 0 \\ &= 0 \quad n \neq 0 \end{aligned} \tag{2.1.5}$$

although in practice a non zero delay and complex amplitude scaling can be tolerated.

2.2 Equalization Techniques

Equalization techniques have been developed since the 1960s/70s, [36–38], and the research in this area is continuously evolving to provide better performance. One of the reason for this on going research is due to the ever increasing demands for higher capacity and efficient bandwidth utilization of the channel. Channel equalization techniques to mitigate the effects of bandlimited time dispersive channel may be subdivided into two general types linear and nonlinear equalization. Furthermore, associated with each type of equalizer is one or more structures for implementing the equalizer. In this chapter, the most commonly used equalizers in practice are briefly reviewed.

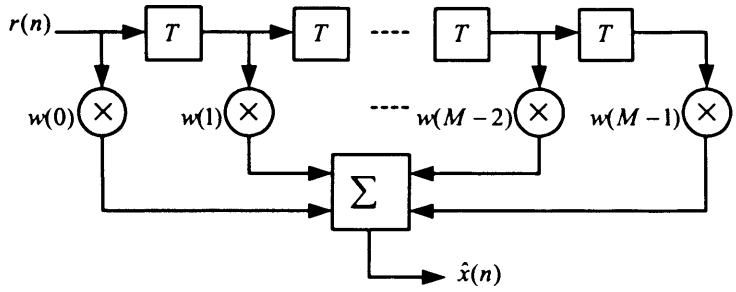

Figure 2.2. Linear Transversal Equalizer

2.2.1 Linear Transversal Equalization

A basic structure of a Linear Transversal Equalizer (LTE) is shown in Figure 2.2. In such equalizers the current and past values of the received signal are linearly weighted by equalizer coefficients, $w(l)$, and assumed to produce the estimate of the transmitted signal as an output that can be written as [17]

$$\hat{x}(n) = \sum_{l=0}^{M-1} w^*(l) r(n-l) = \mathbf{w}^H \mathbf{r}(n) \tag{2.2.1}$$

where $(.)^H$ denotes the conjugate transpose operation, M is the length of equalizer taps, $\mathbf{w} = [w(0) \;\; w(1) \;\; \cdots \;\; w(M-1)]^T$ is the tap weight vector, $(.)^T$ denotes the transpose operation and $\mathbf{r}(n) = [r(n) \;\; r(n-1) \;\; \cdots \;\; r(n-M+1)]^T$ is the received signal vector to estimate $\hat{x}(n)$. The equalizer coefficients may be chosen to force the samples of the combined channel and equalizer impulse response to zero at all other than one of the T-spaced instances. Such an equalizer is termed zero forcing, clearly, when determining the equalizer tap weights this criterion neglects the effect of noise altogether [18]. A more robust criterion called the Minimum Mean Square Error (MMSE) is very commonly used. Here, the equalizer tap weights are chosen to minimize the mean squared error between the transmitted symbol and the output, the sum of all squares of all terms plus the power of the noise [18, 36]. The cost function for this criterion can be written as

$$\begin{aligned} J(\mathbf{w}) &= E\{|\hat{x}(n) - x(n-d)|^2\} \\ &= E\{|\mathbf{w}^H\mathbf{r}(n) - x(n-d)|^2\}, \end{aligned} \tag{2.2.2}$$

to find the filter tap weights, the minimization of this cost function with respect to $\mathbf{w}$ yields the equalizer tap weight vector

$$\mathbf{w} = \left(\mathbf{H}\mathbf{H}^H + \sigma_v^2\mathbf{I}_M\right)^{-1}\mathbf{H}\mathbf{i}_d. \tag{2.2.3}$$

Where

$$\mathbf{H} = \begin{bmatrix} h_o & 0 & \dots & 0 & 0 \\ h_1 & h_o & 0 & 0 & 0 \\ \vdots & \ddots & \ddots & 0 & 0 \\ h_{L-1} & \cdots & h_1 & h_o & 0 \\ \mathbf{0} & \dots & h_{L-1} & \dots & h_o \end{bmatrix}, \quad M \times (M + L - 2)$$

and $\mathbf{i}_d$ is the dth column vector of an identity matrix of size $(M + L - 2) \times (M + L - 2)$ and defines the delay in estimating the transmitted symbol. If the values of the channel impulse response (CIR) at the sampling instances are known, the M coefficients of the zero forcing and MMSE equalizer can be obtained from (2.2.3).
An LTE does not perform well in channels with deep spectral nulls in their frequency response characteristics [39]. In an attempt to compensate for channel distortion the LTE places a large gain in that null region, and as a consequence, significantly increases the noise in the received signal. Non-linear equalizers are, however, superior to linear equalizers in applications where the channel has deep nulls or distortion is too severe for an LTE.

2.2.2 Non-Linear Equalization

There are two very effective nonlinear equalization techniques that have been developed over the past three decades; the first one is maximum likelihood sequence

estimation and the second is decision feedback equalization [39]. In the following, the key features of each are briefly described.

a. Maximum Likelihood Sequence Detection: Maximum Likelihood Sequence Estimator (MLSE) was first proposed by Forney [40] in 1978, it is an optimal equalizer in the sense that it minimizes the probability of sequence error. In MLSE a dynamic programming algorithm known as the Viterbi algorithm is used to determine in a computationally efficient manner the most likely transmitted sequence from the received noisy and ISI-corrupted sequence [17,41]. Because the Viterbi decoding algorithm is the way in which the MLSE equalizer is implemented, the equalizer is often referred to as the Viterbi equalizer. The MLSE equalizer tests all possible data sequences, rather than decoding each received symbol by itself, and chooses the data sequence that is the most probable in all combinations. Therefore, for a memoryless channel, if $p(\mathbf{r};\mathbf{c})$ denotes the conditional probability of receiving $\mathbf{r}$, when code vector $\mathbf{c}$ corresponding to sequence $\{x(n)\}$ is transmitted. Then, the likelihood function, $p(\mathbf{r};\mathbf{c})$, can be written as

$$p(\mathbf{r};\mathbf{c}) = \frac{1}{(\pi\sigma_v^2)^N} \prod_{n=1}^{N} e^{-\frac{|r(n)-x(n)|^2}{\sigma_v^2}}. \tag{2.2.4}$$

The MLSE chooses the estimate vector, $\hat{\mathbf{c}}$, for which the likelihood function is maximum. In GSM, the MLSE is often used to mitigate the effects of the channel at the receiver and to achieve optimal performance [42]. The GSM system is required to mitigate the signal dispersion of approximately $15 - 20\mu$s and the bit duration in GSM system is 3.69μs [43]. Thus the memory of the channel is $4 - 6$ bit intervals long. For channels with memory the likelihood function to maximize can be written as

$$p(\mathbf{r}|\mathbf{h};\hat{\mathbf{c}}) = \frac{1}{(\pi\sigma_v^2)^N} \prod_{n=1}^{N} e^{-\frac{|r(n)-\mathbf{x}_n^T\mathbf{h}|^2}{\sigma_v^2}}. \tag{2.2.5}$$

where $\mathbf{x}_n = [x(n)\ x(n-1)\ \cdots\ x(n-L+1)]^T$ and $\mathbf{h} = [h(0)\ h(1)\ \cdots\ h(L-1)]^T$. The MLSE solution is to maximize the likelihood function jointly over the CIR sequence,

$\{h(n)\}$, and code vector $\mathbf{c}$ corresponding to the transmitted sequence $\{x(n)\}$. The main drawback of the MLSE is its search complexity, measured in number of states, which increases exponentially with the channel support and large constellation points in the modulation, such as 8PSK or 16PSK schemes. Let M be the order of modulation and L the support of the channel then the number of equalizer states will be M^L.

b. Decision Feedback Equalization: A basic structure of a Decision Feedback Equalizer (DFE) is shown in Figure 2.3. It is a nonlinear equalizer, which is widely used in situations where the ISI is very high [38]. It exploits the already detected symbols to cancel the ISI by feeding them back. As shown in the figure, the equalized signal is the sum of the outputs of the forward and feedback filters.

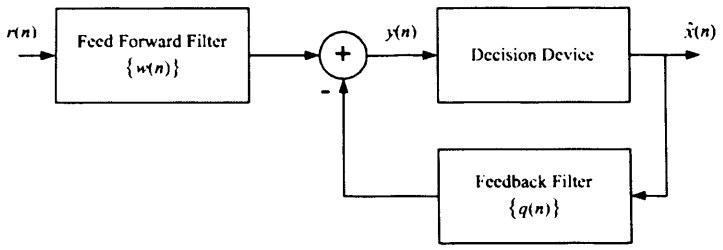

Figure 2.3. A basic structure of a DFE with forward and feedback filters.

The forward filter is just like the LTE. Decisions made on the equalized signals are fedback via a second LTE. The idea behind the decision feedback equalization approach is that if the previous or past symbols are known then in current decision the ISI contribution of these symbols can be removed by subtracting past symbols with appropriate weighting from the equalizer output. The combined output of a forward and feedback filter can be written as

$$y(n) = \sum_{k=0}^{N_f-1} w(k)r(n-k) - \sum_{l=1}^{N_b} q(l)\hat{x}(n-l) = \mathbf{w}^H\mathbf{r}(n) - \mathbf{q}^H\hat{\mathbf{x}}(n), \qquad (2.2.6)$$

which is quantized into a hard decision by a nonlinear decision device

$$\hat{x}(n) = \text{sign}[y(n)] \qquad (2.2.7)$$

where $\mathbf{w} = [w(0) \quad w(1) \quad \cdots \quad w(N_f - 1)]^T$ is the forward filter tap weight vector and $\mathbf{q} = [\ q(1) \quad q(2) \quad \cdots \quad q(N_b)\ ]^T$ is the feedback tap weight vector. The vectors $\mathbf{w}$ and $\mathbf{q}$ are chosen to minimize jointly the minimum mean square error

$$J(\mathbf{w}, \mathbf{q}) = E\{|y(n) - x(n)|^2\} \tag{2.2.8}$$

$$= E\left\{|\mathbf{w}^H \mathbf{r}(n) - \mathbf{q}^H \hat{\mathbf{x}}(n) - x(n)|^2\right\} \tag{2.2.9}$$

If the CCM is defined by

$$\mathbf{H} = \mathbf{H}_u + \mathbf{H}_c, \tag{2.2.10}$$

where $\mathbf{H}_u = [\ \mathbf{h}_1 \ \ \mathbf{h}_2 \ \cdots \ \mathbf{h}_k \ |\ \mathbf{0} \ \cdots \ \mathbf{0}\ ]$ and $\mathbf{H}_c = [\ \mathbf{0} \ \cdots \ \mathbf{0} \ |\ \mathbf{h}_{k+1} \ \cdots \ \mathbf{h}_{N-1}\ ]$ are respectively referred to uncancelled and cancelled symbols and $\mathbf{h}_k$ is the kth column of CCM $\mathbf{H}$. Then the expression for forward and feedback tap weights can be written as [44,45]

$$\mathbf{w} = \mathbf{R}_u^{-1} \mathbf{h}_k \tag{2.2.11}$$

$$\mathbf{q} = \mathbf{H}_c^H \mathbf{w} \tag{2.2.12}$$

where $\mathbf{R}_u = (\mathbf{H}_u \mathbf{H}_u^H + \sigma_n^2 \mathbf{I})$. The drawback of the DFE is that, at low SNR ratios, the already detected symbols may have higher probability of errors and when a particular incorrect decision is fed back, the DFE output reflects this error during the next few symbols due to incorrect decision on the feedback delay line. This phenomenon is called error propagation. It has been shown [18] that the DFE nearly always outperforms an LTE of equivalent complexity and offers ISI cancellation with reduced noise enhancement, hence it provides better BER performance as compared to an LTE [46,47].

2.2.3 Iterative Equalization based on Interference Cancellation

Iterative equalizers work on a similar principle to the DFE, in a way that the previously estimated symbols are fedback to cancel the interference caused by them in

current decisions [17]. In DFEs, previously estimated symbols are fedback and decision on current symbol is made only once. However, in iterative equalization the previously estimated symbols are fedback and decisions on the current symbol are made more than once. In iterative methods, once the estimation process is completed, it is started again to obtain more accurate estimates. Recalling (2.1.4), the received signal can be written as

$$r(n) = \sum_{l=0}^{L-1} h(l)x(n-l) + v(n) \tag{2.2.13}$$

The energy for $x(n)$ is received in L samples $\{r(n), r(n+1), ..., r(n+L-1)\}$. An interference canceller (IC) can be used to collects all the energy for $x(n)$ into a single sample as

$$\begin{aligned} \hat{x}(n) &= \sum_{l=0}^{L-1} h^*(l)r(n+l) \\ \hat{x}(n) &= x(n) + \sum_{k=1}^{L-1} q^*(k)x(n+k) + \sum_{k=1}^{L-1} q(k)x(n-k) + u(n) \end{aligned} \tag{2.2.14}$$

where

$$\begin{aligned} q(k) &= \sum_{l=k}^{L-1} h(l)h^*(l-k) \\ u(n) &= \sum_{k=0}^{L-1} h^*(k)v(n+k) \end{aligned}$$

From (2.2.14) it can be noted that $x(n)$ is interfered by $\{x(n-L+1), x(n-L+2), \ldots, x(n-1), x(n+1), \ldots, x(n+L-1)\}$. If Channel State Information (CSI) and the sequence $\{x(l)_{l\neq n}|\}$ is known then ISI can be completely eliminated, therefore

$$\begin{aligned} \hat{x}(n)_{IC} &= \hat{x}(n) - \sum_{k=1}^{L-1} q^*(k)x(n+k) - \sum_{k=1}^{L-1} q(k)x(n-k) \\ &= x(n) + u(n) \end{aligned} \tag{2.2.15}$$

In (2.2.15) $u(n)$ is a coloured noise with the same variance σ_v^2. An IC requires the knowledge of $\{x(n-L+1), x(n-L+2), \ldots, x(n-1)\}$ that are the past decisions,

an LTE can be used to provide these decisions. On the other hand, $\{x(n+1), x(n+2), \ldots, x(n+L-1)\}$ belong to the future decisions. Iterative methods tackle this problem by assuming no knowledge in the first iteration about the future decisions and estimate all the symbols, on this basis the estimate is less accurate. In the next iteration the iterative methods use the information about the future decision obtained in the first iteration to estimate the current symbols, which are likely to be more accurate as compared to the first iteration. This way after each iteration more and more accurate estimates are obtained. To detect the transmitted signals, the iterative interference cancellation is performed in chapters 5 and 6.

2.2.4 Adaptive Equalization

The channel equalization techniques mentioned in the previous section require the knowledge of CIR that is usually not known at the receiver and varies with time. For optimal performance, these equalizers should track to the time variations in the CIR. An equalizer that tracks the CIR variations and updates the equalizer tap weights accordingly is called an adaptive equalizer. Adaptive equalizers usually do not require the explicit CIR knowledge. However, during the training period a known signal is transmitted and a synchronized version of this training signal is generated at the receiver to find the equalizer coefficient values [18, 38]. At the end of the training period the optimal equalizer tap weights are continually updated. Adaptive equalizers can generally be classified into three categories. The first one involves the steepest descent methods [36], the second method incorporates the stochastic gradient method, also known as Least Mean Square (LMS) that was widely documented by Widrow [48]. The last one incorporates the Least-Squares (LS) algorithms. Among all adaptive algorithms the LMS algorithm is the most commonly used, for which the tap weight vector $\mathbf{w}$ is recursively estimated as follows

$$\mathbf{w}(n+1) = \mathbf{w}(n) + \mu e(n)\mathbf{r}(n), \tag{2.2.16}$$

where $\mathbf{w}(n) = [\ w_o(n)\ \ w_1(n)\ \ \cdots\ \ w_{M-1}(n)\ ]^T$ is the tap weight vector estimated at time index n, μ is the step size, $e(n) = d(n) - y(n)$ is the error between the transmitted and decoded signal at the output of an adaptive equalizer at time n, $d(n)$ is the training signal and $y(n) = \mathbf{w}^H(n)\mathbf{r}(n)$.

An adaptive equalizer can only track small variations in the channel. If the channel is fast time varying then the adaptive equalizer can not track the channel variations that degrade BER performance of the receiver, particularly, when higher constellation points modulation schemes are used [1]. Therefore, in fast time varying channels conventional block based equalization schemes have to be used that generally require explicit estimation of the channel parameters.

The efficient estimation of channel parameters is very important to decode the transmitted data accurately. Therefore, before continuing to the estimation techniques to design an estimator, it is very important to know wether the estimator being designed is unbiased or biased and if it is unbiased what is its variance about the true value. An estimator is said to be unbiased iff

$$E\{\hat{\theta}\} = \theta, \qquad a < \theta < b \tag{2.2.17}$$

where a and b represent the end values of an interval that the unknown parameter, θ, can take on. On the other hand an estimator is said to be biased if

$$E\{\hat{\theta}\} = \theta - b(\hat{\theta}) \tag{2.2.18}$$

where $b(\hat{\theta}) \neq 0$ is the bias in estimation.

2.3 Cramér Rao Lower Bound

To assess the performance of an unbiased estimator to have a lower bound on its variance is very useful. If an estimator attains this bound for every value of unknown parameter, θ, to be estimated, then, it is termed the Minimum Variance Unbiased (MVU) estimator. This lower bound provides the impossibility of determining an

estimator, having lower variance than the bound. Among various variance bounds the Cramér Rao Lower Bound (CRLB) is the easiest to find and most commonly used in practice. The theory of the CRLB allows the determination of the MVU estimator, if it exist. If $\hat{\theta}$ is the estimator of θ, then

$$\sigma_{\hat{\theta}}^2(\theta) \geq \text{CRLB}_{\hat{\theta}}(\theta) \tag{2.3.1}$$

where $\sigma_{\hat{\theta}}^2(\theta)$ represent the variance of the estimator, $\hat{\theta}$, that is the best that can be expected to be done with an unbiased estimator. In order to find the variance of an unbiased estimator, let us suppose an unbiased estimator, $\hat{\theta}$ of a scalar parameter θ. Then it can be written as

$$E\{\hat{\theta}\} = \int_{-\infty}^{\infty} \hat{\theta} p(\mathbf{r};\theta) d\mathbf{r} = \theta \tag{2.3.2}$$

where $\mathbf{r}$ represents the N sample receive vector. The regularity condition is

$$E\left\{\frac{\partial \ln p(\mathbf{r};\theta)}{\partial \theta}\right\} = 0 \qquad \forall\, \theta \tag{2.3.3}$$

where the $E\{.\}$ is evaluated with respect to $p(\mathbf{r};\theta)$. From (2.3.3) it can be written as

$$\int_{-\infty}^{\infty} p(\mathbf{r};\theta) \frac{\partial \ln p(\mathbf{r};\theta)}{\partial \theta} d\mathbf{r} = 0 \tag{2.3.4}$$

$$\int_{-\infty}^{\infty} p(\mathbf{r};\theta) \frac{1}{p(\mathbf{r};\theta)} \frac{\partial p(\mathbf{r};\theta)}{\partial \theta} d\mathbf{r} = 0 \tag{2.3.5}$$

$$\frac{\partial}{\partial \theta} \int_{-\infty}^{\infty} p(\mathbf{r};\theta) d\mathbf{r} = \frac{\partial 1}{\partial \theta} = 0 \tag{2.3.6}$$

Hence, the regularity condition holds true for every value of θ. Differentiation of (2.3.2) with respect to θ yields

$$\frac{\partial}{\partial \theta} \int_{-\infty}^{\infty} \hat{\theta} p(\mathbf{r};\theta) d\mathbf{r} = \int_{-\infty}^{\infty} \hat{\theta} \frac{\partial p(\mathbf{r};\theta)}{\partial \theta} d\mathbf{r} = 1 \tag{2.3.7}$$

Note that

$$\frac{\partial \ln p(\mathbf{r};\theta)}{\partial \theta} = \frac{1}{p(\mathbf{r};\theta)} \frac{\partial p(\mathbf{r};\theta)}{\partial \theta} \tag{2.3.8}$$

Therefore, using this result (2.3.7) can be written as

$$\int_{-\infty}^{\infty} \hat{\theta} \frac{\partial \ln p(\mathbf{r};\theta)}{\partial \theta} p(\mathbf{r};\theta) d\mathbf{r} = 1. \tag{2.3.9}$$

Equation (2.3.4) can be written as

$$\int_{-\infty}^{\infty} \theta \frac{\partial \ln p(\mathbf{r};\theta)}{\partial \theta} p(\mathbf{r};\theta) d\mathbf{r} = 0 \tag{2.3.10}$$

Subtracting (2.3.10) from (2.3.9) yields

$$\int_{-\infty}^{\infty} (\hat{\theta} - \theta) \frac{\partial \ln p(\mathbf{r};\theta)}{\partial \theta} p(\mathbf{r};\theta) d\mathbf{r} = 1. \tag{2.3.11}$$

The Cauchy Schwartz inequality is defined as

$$\left(\int w(\mathbf{r}) g(\mathbf{r}) h(\mathbf{r}) d\mathbf{r} \right)^2 \leq \int w(\mathbf{r}) g^2(\mathbf{r}) d\mathbf{r} \int w(\mathbf{r}) h^2(\mathbf{r}) d\mathbf{r}, \text{ provided } w(\mathbf{r}) \geq 0 \tag{2.3.12}$$

and equality holds when $g(\mathbf{r}) = c\ h(\mathbf{r})$, where c is a scalar and not a function of $\mathbf{r}$. Define,

$$\begin{aligned} w(\mathbf{r}) &= p(\mathbf{r};\theta)\ , \\ g(\mathbf{r}) &= (\hat{\theta} - \theta)\ , \\ h(\mathbf{r}) &= \frac{\partial \ln p(\mathbf{r};\theta)}{\partial \theta}\ . \end{aligned}$$

Squaring (2.3.11) and using the Cauchy Schwartz inequality [30], it can be written as

$$\left(\int_{-\infty}^{\infty} (\hat{\theta} - \theta) \frac{\partial \ln p(\mathbf{r};\theta)}{\partial \theta} p(\mathbf{r};\theta) d\mathbf{r} \right)^2 \leq \int_{-\infty}^{\infty} (\hat{\theta} - \theta)^2 p(\mathbf{r};\theta) d\mathbf{r} \int_{-\infty}^{\infty} \left(\frac{\partial \ln p(\mathbf{r};\theta)}{\partial \theta} \right)^2 p(\mathbf{r};\theta) d\mathbf{r}$$

$$1 \leq E\left\{ (\hat{\theta} - \theta)^2 \right\} E\left\{ \left(\frac{\partial \ln p(\mathbf{r};\theta)}{\partial \theta} \right)^2 \right\} \tag{2.3.13}$$

where $E\left\{ (\hat{\theta} - \theta)^2 \right\}$ is the definition of the variance of an estimator, $\hat{\theta}$, therefore

$$\sigma_{\hat{\theta}}^2(\theta) \geq \frac{1}{E\left\{ \left(\frac{\partial \ln p(\mathbf{r};\theta)}{\partial \theta} \right)^2 \right\}}. \tag{2.3.14}$$

In this expression for variance, the expected value of a square term, in the denominator, is to be found. However, it is more convenient to find the expected value of a unity power term. Therefore, by differentiating (2.3.4) with respect to θ the unity power equivalent of this square term can be found as

$$\int_{-\infty}^{\infty} \frac{\partial}{\partial\theta} p(\mathbf{r};\theta) \frac{\partial \ln p(\mathbf{r};\theta)}{\partial\theta} d\mathbf{r} = 0 \tag{2.3.15}$$

$$\int_{-\infty}^{\infty} \left(\frac{\partial \ln p(\mathbf{r};\theta)}{\partial\theta} \frac{\partial \ln p(\mathbf{r};\theta)}{\partial\theta} p(\mathbf{r};\theta) d\mathbf{r} + \frac{\partial^2 \ln p(\mathbf{r};\theta)}{\partial\theta^2} p(\mathbf{r};\theta) d\mathbf{r} \right) = 0 \tag{2.3.16}$$

$$\int_{-\infty}^{\infty} p(\mathbf{r};\theta) \left(\frac{\partial \ln p(\mathbf{r};\theta)}{\partial\theta} \right)^2 d\mathbf{r} = -\int_{-\infty}^{\infty} p(\mathbf{r};\theta) \frac{\partial^2 \ln p(\mathbf{r};\theta)}{\partial\theta^2} d\mathbf{r} \tag{2.3.17}$$

$$E\left\{ \left(\frac{\partial \ln p(\mathbf{r};\theta)}{\partial\theta} \right)^2 \right\} = -E\left\{ \frac{\partial^2 \ln p(\mathbf{r};\theta)}{\partial\theta^2} \right\} \tag{2.3.18}$$

Therefore, the variance of the estimator can be written as

$$\sigma_{\hat{\theta}}^2(\theta) \geq \frac{1}{-E\left\{ \frac{\partial^2 \ln p(\mathbf{r};\theta)}{\partial\theta^2} \right\}} \tag{2.3.19}$$

Equality is the so called CRLB and the condition for equality is

$$\frac{\partial \ln p(\mathbf{r};\theta)}{\partial\theta} = \frac{1}{c}(\hat{\theta} - \theta) \tag{2.3.20}$$

where c is a scalar constant whose value may depend on θ. Therefore, this equation implies that if the log-likelihood function can be written in this form then $\hat{\theta}$ will be the MVU estimator. By differentiating (2.3.20) again the value of $c(\theta)$ can be found as

$$\frac{\partial}{\partial\theta} \frac{\partial \ln p(\mathbf{r};\theta)}{\partial\theta} = \frac{\partial}{\partial\theta} \left(\frac{1}{c(\theta)} (\hat{\theta} - \theta) \right) \tag{2.3.21}$$

$$\frac{\partial^2 \ln p(\mathbf{r};\theta)}{\partial\theta^2} = -\frac{1}{c(\theta)} \tag{2.3.22}$$

$$c(\theta) = \frac{1}{-E\left\{ \frac{\partial^2 \ln p(\mathbf{r};\theta)}{\partial\theta^2} \right\}} \tag{2.3.23}$$

Therefore, if (2.3.20) can be written in general form

$$\frac{\partial \ln p(\mathbf{r};\theta)}{\partial\theta} = I(\theta)\left(g(\mathbf{r}) - \theta\right), \tag{2.3.24}$$

then $g(\mathbf{r})$ is the MVU estimator. The $I(\theta) = \frac{1}{c(\theta)}$ and is termed the Fisher information [30]. The CRLB derived in this section can easily be extended for vector parameters and will be used throughout the thesis to assess the performance of the estimators.

2.4 Channel Parameter Estimation

Generally, the parameter estimation in wireless channels includes the estimation of channel MGs, Frequency Offsets (FOs), phase shift and synchronization pulses. In this thesis, only the estimation of MGs and FOs is discussed and the remainder of the parameters are assumed to be known. Channel parameter estimation can be classified into two broad categories, supervised and non-supervised or blind.

2.4.1 Supervised Parameter Estimation

Supervised or training data assisted (TDA) is a practical parameter estimation technique in digital mobile communications, it can provide high performance in a fading environment with large constellations and it has a simple implementation [17,49,50]. Burst digital communication, where the data are transmitted in frames, is used in various wireless communications systems, such as TDMA, CDMA, and OFDMA. In the TDA parameter estimation technique a training signal sequence is embedded inside the data frames and is more suitable for applications requiring fast and reliable parameter estimation [21,51]. In the GSM frame structure, for example, the middle 26 bits in a time slot are dedicated for channel estimation as shown in Figure 2.4. Nevertheless, this method reduces the effective channel transmission rate as these extra bits do not contain useful data information bits. TDA parameter estimation can further be classified into two more categories, parametric, where the sample data follows a particular probability distribution, and non parametric, where the sample data does not follow any probability distribution. In the following the parametric and non-parametric approaches are briefly described.

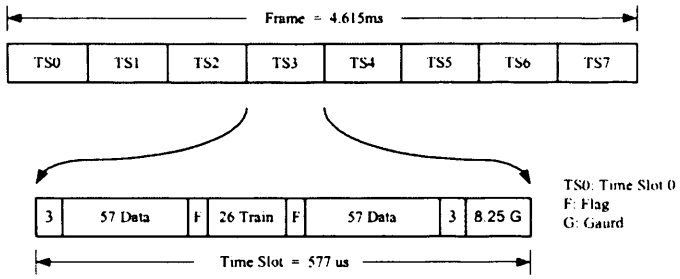

Figure 2.4. Frame structure of GSM communications.

Maximum Likelihood Estimation: Maximum likelihood estimation (MLE) is the most popular parametric technique to estimate the parameters. The MLE technique determines the parameters that maximize the probability (likelihood) of the received sample data. From a statistical point of view, the MLE technique is considered to be more robust, versatile, and yields estimators with good statistical properties and can be applied to most of the data models [30]. Moreover, it provides efficient methods for quantifying uncertainty through confidence bounds. Although the methodology of the MLE is simple, the implementation is computationally expensive. If $\mathbf{r} = [\ r(0)\ \ r(1)\ \ \cdots\ \ r(N-1)\ ]$ is a vector of N received samples with the Probability Density Function (PDF) $p(\mathbf{r}\ ;\boldsymbol{\theta})$, where $\boldsymbol{\theta} = [\ \theta_1\ \ \theta_2\ \ \cdots\ \ \theta_K\ ]$ is a vector of K unknown constant parameters to be estimated. Then, the likelihood function of the received samples can be written as

$$p(\mathbf{r};\boldsymbol{\theta}) = \prod_{i=0}^{N-1} p\left[r(i);\theta_1,\theta_2,...,\theta_K\right]. \tag{2.4.1}$$

As $\ln x$ is a monotonically increasing function of x between 0 and 1, taking the natural log of (2.4.1) will not affect the maximization, but simplify the problem, therefore

$$\ln[p(\mathbf{r};\boldsymbol{\theta})] = \sum_{i=0}^{N-1} \ln p\left[r(i);\theta_1,\theta_2,...,\theta_K\right] \tag{2.4.2}$$

Maximizing $\ln[p(\mathbf{r};\boldsymbol{\theta})]$, which is much easier to work with than $p(\mathbf{r};\boldsymbol{\theta})$, the MLEs of the elements of $\boldsymbol{\theta}$ are the simultaneous solutions of K equations such that,

$$\frac{\partial \ln[p(\mathbf{r};\boldsymbol{\theta})]}{\partial \theta_i} = 0 \; ; \quad i = 1, 1, ..., K \tag{2.4.3}$$

An MLE has three salient properties that are [30].

- It satisfies the condition $\lim_{N\to\infty} E\{\hat{\theta}\} = \theta$, i.e, it is asymptotically unbiased.
- The distribution of the maximum likelihood estimator is Gaussian.
- It asymptotically attains CRLB. This property of the estimator is termed as efficiency.

Increase in sample size of a maximum likelihood estimator decreases its variance, this property is termed as consistency. The draw back of the MLE is its complexity and it is difficult to apply for the signal models where the noise is not Gaussian.

Example 1: The N received samples in (2.1.1) can be written in vector form as

$$\mathbf{r} = \mathbf{X}\mathbf{h} + \mathbf{v} \tag{2.4.4}$$

where

$$\mathbf{r} = \begin{bmatrix} r(0) & r(1) & \cdots & r(N-1) \end{bmatrix}^T$$

$$\mathbf{X} = \begin{bmatrix} x(0) & x(-1) & \cdots & x(1-L) \\ x(1) & x(0) & \cdots & x(2-L) \\ \vdots & \ddots & \ddots & \cdots \\ x(N-1) & x(N-2) & \cdots & x(N-L) \end{bmatrix},$$

$$\mathbf{h} = \begin{bmatrix} h(0) & h(1) & \cdots & h(L-1) \end{bmatrix}^T$$

and $$\mathbf{v} = \begin{bmatrix} v(0) & v(1) & \cdots & v(L-1) \end{bmatrix}^T.$$

Here, $\{x(n)\}$ are transmitted training symbols that are known at the receiver. In order to estimate $\mathbf{h}$ in (2.4.4) the log-likelihood function of $\mathbf{r}$ can be written as

$$\begin{aligned} \ln p(\mathbf{r};\ \mathbf{h}) &= \ln \frac{1}{(\pi\sigma^2)^{N/2}}\, e^{-\frac{(\mathbf{r}-\mathbf{X}\mathbf{h})^H(\mathbf{r}-\mathbf{X}\mathbf{h})}{\sigma_v^2}} \\ &= \frac{-N}{2}\ln(\pi\sigma^2) - \frac{(\mathbf{r}-\mathbf{X}\mathbf{h})^H(\mathbf{r}-\mathbf{X}\mathbf{h})}{\sigma_v^2} \end{aligned} \tag{2.4.5}$$

To maximize the likelihood function, differentiating with respect to $\mathbf{h}$ (considering the log-likelihood function is a function of $\mathbf{h}$) yields

$$\begin{aligned} \frac{\partial \ln p(\mathbf{r};\mathbf{h})}{\partial \mathbf{h}^H} &= \frac{1}{\sigma_v^2}(\mathbf{X}^H\mathbf{r} - \mathbf{X}^H\mathbf{X}\mathbf{h}) \\ &= \frac{1}{\sigma_v^2}(\mathbf{X}^H\mathbf{X})\left\{(\mathbf{X}^H\mathbf{X})^{-1}\mathbf{X}^H\mathbf{r} - \mathbf{h}\right\} \end{aligned} \tag{2.4.6}$$

Comparing it with (2.3.24) or equating to zero yields the MVU estimator

$$\hat{\mathbf{h}} = (\mathbf{X}^H\mathbf{X})^{-1}\mathbf{X}^H\mathbf{r}. \tag{2.4.7}$$

Example 2: In this example, the joint estimation of $\mathbf{h}$ and FO is considered. Here, it is assumed that the support of the channel is L and each path experiences a DS of f_d. The received sample can be written as

$$r(n) = \sum_{l=0}^{L-1} h(l)x(n-l)e^{j2\pi f_d n} + v(n) \tag{2.4.8}$$

and N received samples in vector form can be written as

$$\mathbf{r} = \mathbf{E}_o\mathbf{X}\mathbf{h} + \mathbf{v} \tag{2.4.9}$$

where

$$\mathbf{E}_o = \begin{bmatrix} 1 & 0 & 0 & 0 \\ 0 & e^{j2\pi f_d} & 0 & 0 \\ 0 & 0 & \ddots & 0 \\ 0 & 0 & 0 & e^{j2\pi f_d(N-1)} \end{bmatrix} \tag{2.4.10}$$

The training signal matrix, $\mathbf{X}$, and MGs vector, $\mathbf{h}$, are defined in the previous example. Ignoring the constant terms, as they will not affect the maximization of the log-likelihood function, for the log-likelihood function to be maximum with respect to the unknown parameters then

$$\ln p(\mathbf{r}; \mathbf{h}; f_d) = -(\mathbf{r} - \mathbf{E}_o\mathbf{X}\mathbf{h})^H(\mathbf{r} - \mathbf{E}_o\mathbf{X}\mathbf{h}) \tag{2.4.11}$$

or the cost function to minimize is

$$\begin{aligned} J(\mathbf{h}; f_d) &= (\mathbf{r} - \mathbf{E}_o\mathbf{X}\mathbf{h})^H(\mathbf{r} - \mathbf{E}_o\mathbf{X}\mathbf{h}) \\ &= \mathbf{r}^H\mathbf{r} - \mathbf{r}^H\mathbf{E}_o\mathbf{X}\mathbf{h} - \mathbf{h}^H\mathbf{X}^H\mathbf{E}_o^H\mathbf{r} + \mathbf{h}^H\mathbf{X}^H\mathbf{X}\mathbf{h}. \end{aligned} \tag{2.4.12}$$

Note that $\mathbf{E}_o^H\mathbf{E}_o = \mathbf{I}$. To minimize the cost function with respect to $\mathbf{h}$, by assuming f_d constant, differentiate (2.4.12) with respect to $\mathbf{h}$

$$\frac{\partial J(\mathbf{h}; f_d)}{\partial \mathbf{h}} = -\mathbf{X}^H\mathbf{E}_o^H\mathbf{r} + \mathbf{X}^H\mathbf{X}\mathbf{h}, \tag{2.4.13}$$

equating it to zero yields

$$\hat{\mathbf{h}} = (\mathbf{X}^H\mathbf{X})^{-1}\mathbf{X}^H\mathbf{E}_o^H\mathbf{r}. \tag{2.4.14}$$

In this expression the matrix $\mathbf{E}_o$ is unknown and depends on f_d, therefore $\mathbf{h}$ can not be estimated. In order to estimate f_d, use of (2.4.13) in (2.4.12) yields the cost function to minimize with respect to f_d

$$J(f_d) = \mathbf{r}^H\mathbf{r} - \mathbf{r}^H\mathbf{E}_o\mathbf{X}(\mathbf{X}^H\mathbf{X})^{-1}\mathbf{X}^H\mathbf{E}_o^H\mathbf{r} \tag{2.4.15}$$

The training samples $\{x(n)\}$ are assumed uncorrelated, therefore $\mathbf{X}^H\mathbf{X} \approx N\mathbf{I}$. The minimization of (2.4.15) is equivalent to the maximization of the second term that can be written as

$$\mathbf{r}^H\mathbf{E}_o\mathbf{X}\mathbf{X}^H\mathbf{E}_o^H\mathbf{r} = \frac{\boldsymbol{\gamma}^H\boldsymbol{\gamma}}{N}$$

where

$$\boldsymbol{\gamma}^H = \left[\sum_{n=0}^{N-1} r(n)e^{j2\pi f_o n}x(n) \quad \cdots \quad \sum_{n=0}^{N-1} r(n)e^{j2\pi f_o n}x(n-L+1) \right],$$

and hence

$$\mathbf{r}^H\mathbf{E}_o\mathbf{X}\mathbf{X}^H\mathbf{E}_o^H\mathbf{r} = \frac{1}{N}\sum_{n=0}^{N-1}\sum_{l=0}^{L-1}\left|r(n)e^{j2\pi f_d n}x(n-l)\right|^2 = \phi(f_d), \tag{2.4.16}$$

and to estimate DS, f_d, the maximum likelihood solution can be written as

$$\hat{f}_d = \arg\max_f \phi(f) \tag{2.4.17}$$

The value of f that maximizes (2.4.17) will be the maximum likelihood estimator solution for f_d and can be used to estimate $\mathbf{h}$ in (2.4.14). In order to estimate f_d a grid search method can be used and the accuracy of the estimator depends on the frequency bin chosen, which is computationally very expensive. However, in practice a less computationally expensive approach called the Fast Fourier Transform (FFT) is used.

Least-Squares Estimation: Least-Squares (LSs) estimation is a non-parametric approach to estimate the parameters and is widely used in practice due to ease of implementation and optimality in Gaussian noise. Here, no probabilistic assumption about the data is needed other than the data. Therefore, it can be applied to almost all types of data model. The disadvantage of the least-squares estimator is that it does not guarantee the optimality of the estimator. A LSs estimator of an unknown parameter vector, θ, for a received signal model

$$r(n) = s(n;\theta) + v(n) \tag{2.4.18}$$

minimizes the Mean Square Error (MSE) between the the deterministic term $s(n;\theta)$ and received data, $r(n)$, as [30]

$$J(\theta) = \sum_{n=0}^{N-1}[r(n) - s(n;\theta)]^2 \tag{2.4.19}$$

Therefore, the estimator

$$\hat{\theta} = \arg\min_\theta J(\theta) \tag{2.4.20}$$

2.5 FO Estimation

In the above algorithms, to estimate FO, the training based estimation techniques were considered. However, the FO can be estimated without training data. In the following, some of the non-TDA estimation techniques are briefly discussed.

2.5.1 Frequency domain transformation

This is the easiest method to established the FOs and is a block based approach to estimate FOs. Here, the received signal samples are converted into the frequency domain by taking their discrete Fourier transform (DFT). If the received signal samples contain more than one FO then the Fourier transform gives peak values at the FOs provided there is sufficient separation between the offset frequencies. The amplitude of the received samples at different frequencies can be established by using the discrete Fourier transform relation given by [30, 52–54],

$$F(f) = \frac{1}{N}\sum_{n=0}^{N-1} r(n)e^{-j2\pi fn} \tag{2.5.1}$$

where $F(f)$ is the complex amplitude of the received signal at frequency f, $r(n)$, is the received signal sample and N is the number of received samples. The drawback of using this method is that in the presence of multiple frequency components in the received signal, it is difficult to find the source corresponding to a particular FO component. Secondly, this method does not give good performance in the presence of multipath fading channels.

2.5.2 Sub-space based FO estimation

Sub-space based estimation algorithms such as MUSIC and ESPRIT [55–57] can provide high resolution frequency estimation at the expense of increased computational complexity. Sub-spaced based algorithms require eigen or singular value decomposition of the received sample covariance matrix $\mathbf{R}$ to find the signal and noise orthogonal

sub-spaces i.e., $\mathbf{R} = \mathbf{V}\mathbf{\Lambda}\mathbf{V}^H$ and $\mathbf{V} = [\mathbf{V}_S \quad \mathbf{V}_N]$. Where $\mathbf{\Lambda}$ is a diagonal matrix of eigen values of the covariance matrix, while $\mathbf{V}_S$ and $\mathbf{V}_N$ contain the basis vectors for the signal and noise spaces respectively. An inner product of any two vectors from the orthogonal noise and signal subspaces yields zero and it is this property that is used to find the FOs of the signal. A draw back in using sub-space based algorithms is that as the number of frequency components in the received signal increases, the order of the associated covariance matrix increases. Therefore, to find the singular value decomposition of a high order covariance matrix extensive computation is required. The subspace based algorithm MUSIC computes the frequencies of the signal as the peaks in the MUSIC spectrum estimate given by [56]

$$S_{MUSIC}(f) = \frac{1}{\mathbf{s}^H(f)\mathbf{V}_N\mathbf{V}_N^H\mathbf{s}(f)} \tag{2.5.2}$$

where $\mathbf{s}(f)$ is the frequency scanning vector and is defined by

$$\mathbf{s}(f) = \begin{bmatrix} 1 & e^{-j2\pi f} & \ldots & e^{-j2\pi fM} \end{bmatrix}^T \tag{2.5.3}$$

and M is the order of the covariance matrix.

2.5.3 Un-supervised Parameter Estimation

In an un-supervised or blind parameter estimation technique, a training signal is theoretically assumed not to be needed. Hence, it has the potential to increase the overall capacity of the communication system. Here, the cost function based on some already known quantity, such as the modulus or energy of the transmitted signal is optimized to find some parameters. Blind algorithms generally take substantially more time to estimate the parameters and assume the channel is not changing rapidly. Therefore, they are not good for burst communication, where small numbers of bits are available. Although they have much potential where the channel is very slowly changing, as in fixed telephone networks. A number of blind parameter estimators is given in [58–60] and the references therein.

2.6 Summary

In this chapter, a foundation was provided to proceed to mitigate the effects of time-varying multipath channels. First of all the fundamental question: what are the causes and how the effects of multipath channels are mitigated was answered. To mitigate the effects of a multipath channel the technology of equalization was introduced and several linear, nonlinear and adaptive equalization techniques were discussed briefly. In fast fading channels, it was highlighted that it is difficult for an adaptive equalizer to track the channel variations, thereby degrading the BER performance of the system. Therefore, in the fast fading environment conventional equalizers are used that require the accurate knowledge of the channel. The performance of these equalizers depends on the variance of the channel parameter estimators, therefore, a bench mark on the variance of an unbiased estimator, the CRLB was derived to assess the performances of various unbiased estimators. Then some optimal and non-optimal parameter estimation techniques were discussed briefly.

Chapter 3

PARAMETER ESTIMATION AND EQUALIZATION IN SISO WITH FREQUENCY OFFSETS

Wireless transmission is impaired by signal fading, interference and additive noise. Moreover, the presence of FO introduces the time-variations into the multipath channel that degrade the BER performance of a communication system, particularly one based on the assumption that the channel is time-invariant. There are two main causes for FOs; poor synchronization between the transmitter and the receiver carrier frequencies and the motion-induced DS due to the relative motion between the mobile station and the local scatterers [61]. The reason for poor synchronization could be due to an error in the crystal oscillator frequency or due to temperature variations. If the FO is due to temperature variations, then it will be slowly time-varying as the temperature changes are not very abrupt and may take a longer time to cause the frequency of the oscillators to drift. The FO due to DS may be random and fast time-varying. Therefore, the overall FO, f_o, can be written as [62].

$$f_o = f_d + f_{se} \tag{3.0.1}$$

where f_d is the DS and f_{se} is the frequency synchronization error between the transmitter and the receiver local oscillator frequencies. The estimation of FO and its exploitation in equalization is crucial to enable accurate decoding of the transmitted

information. In this chapter, parameter estimation and a low complexity equalization technique for a TDMA based communication system is studied. For a TDMA communication system a SISO channel with each multipath possibly having distinct DS is considered. TDMA is a mechanism for sharing a channel, whereby several users have access to the whole channel bandwidth for a small period of time, which is called a time slot. The block of bits in one time slot is called a frame. For a Linear-Time-Invariant (LTI) channel, the adaptive equalizers do not require the explicit CSI and are very easy to implement. Therefore, the adaptive equalizers are commonly used to mitigate the effects of an ISI channel. Since a FO introduces time selectivity into the channel that degrades the BER performance of an adaptive equalizer, it is therefore necessary to estimate the FO and cancel its effects prior to adaptive equalization. In a TDMA system, it is difficult to estimate the FO due to the limited number of bits for training data; secondly, for voice, real time data are transmitted. Therefore, processing of the data must be completed before the arrival of the next frame. In a TDMA communication system, for example GSM, the duration of the time slot is only 0.576ms and each time slot contains 152 bits within which the middle 26 bits are dedicated for training data [43]. For a TDMA communication system, researchers have estimated FO by using different algorithms. Morelli [28] and Huseyin [63] have derived algorithms to estimate FO for a flat fading channel that are based on the autocorrelation of the channel. Channel estimates are noisy and require low pass filtering and the bandwidth of the low pass filter depends on Doppler spread. Therefore, such types of receivers require adaptive low pass filtering that makes these algorithms complicated. Krasny [29] has described optimal and sub-optimal algorithms based on maximum likelihood principle to find FO, where it is assumed that the channel is non-dispersive but it does not require any filtering. For a dispersive channel, in [64] FO together with the channel are estimated, this algorithm is based on channel impulse response estimation. In this method to estimate FO, channel estimation is also mandatory, the adaptive equalizers do not require channel information, hence, esti-

mation of the channel and FO increases the complexity of the receiver. Harish [20] proposed a maximum state accumulation technique of FO estimation that does not require an explicit estimation of the channel. All the above algorithms, assume that the FO is identical from each multipath.

In contrast to previous work, in this chapter, equalization for a single transmit and receive antenna, under a general framework that allows distinct FOs from each multipath, is addressed. Such a scenario may arise when either the receiver or the transmitter moves at high speed, thereby, resulting in distinct DSs for the multipaths due to different angle of arrival. In this scenario, most of the above FO estimation algorithms cannot be applied. Therefore, for this scenario, exploiting the correlation property of the transmitted training symbols, an Approximative Maximum Likelihood (AML) estimator is proposed. Here, unlike the identical DS problem, the distinct DSs can not be compensated for prior to equalization and have to be accounted for in equalizer design. Now, it is imperative to use the conventional block-based equalizer design. In multipath with distinct FO scenario, it is further shown that the conventional MMSE equalizer is computationally cumbersome as the effective CCM changes deterministically between symbols. However, by exploiting the structural property of these changes, a computationally efficient recursive algorithm for the equalizer design is proposed.

3.1 Problem statement

Consider a communication system employing a single transmit and receive antenna, and assume that the signal has propagated through L different paths, each having different FOs and complex MGs. If the sampling rate is equal to the symbol transmission rate then the received baseband signal can be written as

$$r(n) = \bar{r}(n) + v(n) = \sum_{l=0}^{L-1} h_l x(n-l) e^{j2\pi f_l n} + v(n), \tag{3.1.1}$$

where h_l and f_l denote respectively the unknown complex channel gain and the FO for the lth multipath of the channel. Herein, it is assumed that h_l and f_l are quasi-stationary, not changing significantly over the observed data frame, and only vary between data frames. Further, $x(n)$ is the transmitted signal with variance σ_x^2, and $v(n)$ is an additive circularly Gaussian distributed zero mean white (complex) noise with variance σ_v^2. Let $\mathbf{X}_{l,n}$ denote the $N \times N$ diagonal matrix formed from the vector $\mathbf{x}_{l,n}$ along the diagonal, with

$$\mathbf{x}_{l,n} = \left[\begin{array}{ccc} x(n-l) & \ldots & x(n-l-N+1) \end{array} \right]^T, \tag{3.1.2}$$

where N is the length of training symbols. Further, let $\mathbf{e}_{l,n}$ model the FO vector for the lth path,

$$\mathbf{e}_{l,n} = \left[\begin{array}{ccc} e^{j2\pi f_l n} & \ldots & e^{j2\pi f_l (n-N+1)} \end{array} \right]^T, \tag{3.1.3}$$

and form the $N \times L$ matrix $\mathbf{V}_n$ as

$$\mathbf{V}_n \triangleq \left[\begin{array}{ccc} \mathbf{v}_{0,n} & \ldots & \mathbf{v}_{L-1,n} \end{array} \right], \tag{3.1.4}$$

where $\mathbf{v}_{k,n} = \mathbf{x}_{k,n} \odot \mathbf{e}_{k,n}$, with $\odot$ denoting the Schur-Hadamard (elementwise) product. Hence, the vector constructed from N consecutive received samples can be expressed as

$$\begin{aligned} \mathbf{r}_n &\triangleq \left[\begin{array}{ccc} r(n) & \ldots & r(n-N+1) \end{array} \right]^T \\ &= \sum_{l=0}^{L-1} h_l \mathbf{X}_{l,n} \mathbf{e}_{l,n} + \mathbf{v}_n \\ &= \mathbf{V}_n \mathbf{h}_L + \mathbf{v}_n, \end{aligned} \tag{3.1.5}$$

where

$$\mathbf{h}_L = \left[\begin{array}{ccc} h_0 & \ldots & h_{L-1} \end{array} \right]^T$$

and

$$\mathbf{v}_n = \left[\begin{array}{ccc} v(n) & \ldots & v(n-N+1) \end{array} \right]^T.$$

Here, the problem of interest is given $\mathbf{r}_n$ and the training symbols $\{x(n)\}$, estimate the unknown parameter vector

$$\begin{aligned}\boldsymbol{\theta} &= \begin{bmatrix} h_0 & \dots & h_{L-1} & f_0 & \dots & f_{L-1} \end{bmatrix}^T \\ &\triangleq \begin{bmatrix} \mathbf{h}_L^T & \mathbf{f}_L^T \end{bmatrix}^T \end{aligned} \tag{3.1.6}$$

where $\mathbf{f}_L = [f_0\ f_1\ \dots\ f_{L-1}]^T$. Here, no explicit knowledge on the channel length is required, other than the knowledge on its upper bound. For an over modelled system, the estimates of the additional channel coefficients would be close to zero and in this way the channel length can potentially be determined. In the next section, to estimate the unknown MGs and FOs a computationally efficient approach is presented.

3.2 Estimation of multipath gains and frequency offsets

In this section, an approximative maximum likelihood (AML) estimator of the complex MGs and the FOs is outlined. Consider that the received signal, as expressed in (3.1.5), is only a function of the complex MGs and FOs. The likelihood function, of the received sample vector, to be maximized can be written as

$$p(\mathbf{r}_n|\boldsymbol{\theta}) = \frac{1}{(\pi\sigma_v^2)^N} e^{\frac{-(\mathbf{r}_n - \mathbf{V}_n\mathbf{h}_L)^H(\mathbf{r}_n - \mathbf{V}_n\mathbf{h}_L)}{\sigma_v^2}} \tag{3.2.1}$$

where the probability of an event occurring can be between 0 and 1, and $\ln x$ is a monotonically increasing function for $x \in \{0, 1\}$. Therefore, the log-likelihood function will not have any effect on the maximization problem, the log-likelihood function can be expressed as (ignoring the constant terms)

$$\ln p(\mathbf{r}_n|\boldsymbol{\theta}) = -\frac{1}{\sigma_v^2}(\mathbf{r}_n - \mathbf{V}_n\mathbf{h}_L)^H(\mathbf{r}_n - \mathbf{V}_n\mathbf{h}_L). \tag{3.2.2}$$

Maximization of (3.2.2) with respect to $\mathbf{h}_L$ yields [30]

$$\hat{\mathbf{h}}_L = (\mathbf{V}_n^H\mathbf{V}_n)^{-1}\mathbf{V}_n^H\mathbf{r}_n \triangleq \mathbf{V}_n^\dagger\mathbf{r}_n, \tag{3.2.3}$$

where $\mathbf{V}_n^{\dagger}$ denotes the Moore-Penrose pseudo-inverse. The FOs are estimated by minimizing the cost function, $J(\mathbf{f}_L)$, obtained by substituting equation (3.2.3) into (3.2.2),

$$J(\mathbf{f}_L) = \mathbf{r}_n^H \mathbf{r}_n - \mathbf{r}_n^H \mathbf{\Pi}_{\mathbf{V}_n} \mathbf{r}_n, \tag{3.2.4}$$

where $\mathbf{\Pi}_{\mathbf{V}_n} = \mathbf{V}_n \mathbf{V}_n^{\dagger}$ is the projection onto the range space of $\mathbf{V}_n$. By choosing the training sequence, $x(n)$, such that $E\left\{ x^*(n-l)x(n-p) \right\} = \delta_{p-l}$, where δ_k denotes the Kronecker delta function and $(\cdot)^*$ the conjugate, the n-dimensional minimization problem in (3.2.4) may be decoupled into n one-dimensional problems, which significantly reduces the complexity of the minimization. Note that $\mathbf{V}_n^H \mathbf{V}_n$ will be dominated by the large diagonal terms, with almost negligible contribution from the off-diagonal terms, if $x(n)$ is chosen as a pseudo-random sequence (as in the case of a training signal). Thus, $\mathbf{V}_n^H \mathbf{V}_n \approx \sum_{n=0}^{N-1} |x(n)|^2 \mathbf{I} \triangleq \kappa \mathbf{I}$, where κ is constant over the frame considered, enabling the minimization of (3.2.4) to be approximated as the maximum of

$$\begin{aligned} J'(\mathbf{f}_L) &= \mathbf{r}^H \mathbf{V}_n \mathbf{V}_n^H \mathbf{r}_n \\ &= \sum_{p=0}^{L-1} \left| \sum_{n=0}^{N-1} r^*(n) x(n-p) e^{j2\pi f_p n} \right|^2 \end{aligned} \tag{3.2.5}$$

This is a difficult joint multi-dimensional optimization problem. Therefore, the FO of an arbitrary individual path s between a transmit and a receive antenna is considered, for which the contribution to (3.2.5) is

$$\begin{aligned} \psi_s(n) &= r^*(n) x(n-s) e^{j2\pi f_s n} \\ &= Q_s + c_1(n) + c_2(n) \end{aligned} \tag{3.2.6}$$

where

$$\begin{aligned} Q_s &= h_s^* |x(n-s)|^2, \\ c_1(n) &= v^*(n)x(n-s)e^{j2\pi f_s n}, \\ c_2(n) &= \sum_{\substack{p=0 \\ p\neq s}}^{L-1} h_p^*(p)x^*(n-p)x(n-s)e^{j\Delta 2\pi f_p n} \\ \Delta f_p &= f_s - f_p \end{aligned}$$

Moreover, as $E\{x(n-u)x(n-v)\} = 0$ for $u \neq v$,

$$\begin{aligned} \left|\sum_{n=0}^{N-1} \psi_s(n)\right|^2 &\approx N^2|h_s|^2|x(n-s)|^4 + N\sum_{\substack{p=0 \\ p\neq s}}^{L-1}|h_p|^2|x(n-p)|^2|x(n-s)|^2 \\ &= N^2\rho_s + N\rho_i \\ &\approx N^2\rho_s \text{ (For large N)} \end{aligned} \tag{3.2.7}$$

Therefore, provided that the ratio between the signal component for which the parameters are to be estimated, $\rho_s = |h_s|^2|x(n-s)|^4$, to the interfering components $\rho_i = \sum_{\substack{p=0 \\ p\neq s}}^{L-1}|h_p|^2|x(n-p)|^2|x(n-s)|^2$, is greater than $1/N$, the joint multi-dimensional maximization problem in (3.2.5) can be reduced over all possible frequencies to the maximization of the following for each individual frequency

$$\hat{f}_s = \arg\max_f \left|\sum_{n=0}^{N-1} r^*(n)x(n-s)e^{j2\pi fn}\right|^2 \tag{3.2.8}$$

which can be efficiently evaluated using the fast Fourier transform (FFT). Once the FOs are estimated, the MGs, $\mathbf{h}_k$, can be estimated using (3.2.3).

3.3 Numerical Example for Variance of Estimators

In order to assess the performance of the proposed AML estimator, a two-tap channel with FOs $f_0 = 0.003$ and $f_1 = 0.005$ is considered. This is reasonable as the

maximum DS for a vehicular speed of 250 km/h (RA250 channels as defined in GSM standards) at a carrier frequency of 1800 MHz is 416Hz, which corresponds to 0.005 when normalized to the symbol rate of 100 kHz as in GSM [43]. The number of training samples to estimate MGs and FOs is $N = 100$. Training samples are assumed binary alphabets. Figures 3.1 and 3.2 show that the mean-square estimation error as obtained from 10^4 Monte-Carlo simulations attains the Cramér-Rao lower bound (CRLB), derived in the Appendix 3A. The complex channel gains h_0 and h_1 have been assumed to be constant throughout a burst, but may change between the frames.

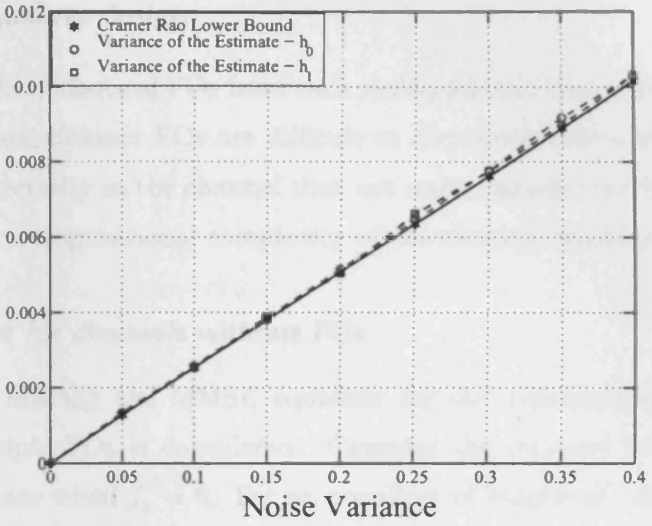

Figure 3.1. Comparison of the variance of the estimates of h_0 and h_1 with the CRLB

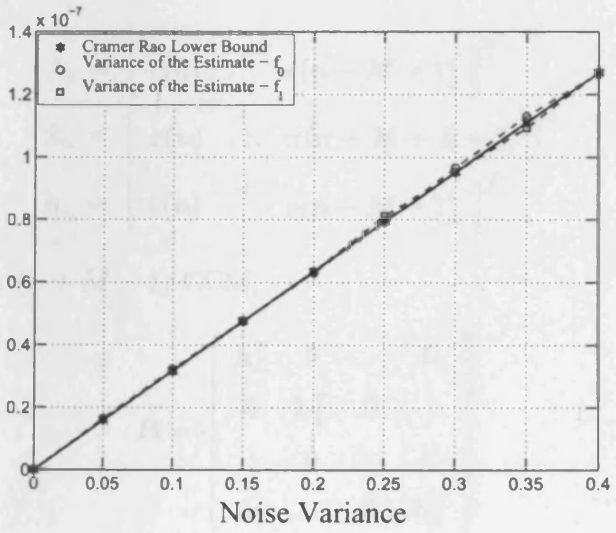

Figure 3.2. Comparison of the variance of the estimates of f_0 and f_1 with the CRLB

3.4 MMSE equalizer design

As discussed earlier, identical FOs from each multipath can be compensated for easily before equalization, distinct FOs are difficult to compensate for easily. Distinct FOs produce time selectivity in the channel that not only degrades the BER performance but increases the computational complexity of the classical equalizers.

3.4.1 Equalizer for channels without FOs

In this section, initially the MMSE equalizer for the communication channel not affected by multiple FOs is considered. Consider the received baseband signal in (6.2.1), for the case when $f_p = 0$. For an equalizer of length M, the received signal vector can then be written as

$$\check{\mathbf{r}}_n = \mathbf{H}\check{\mathbf{x}}_n + \check{\boldsymbol{\eta}}_n, \tag{3.4.1}$$

where

$$\begin{aligned}
\check{\mathbf{r}}_n &= \begin{bmatrix} r(n) & \dots & r(n-M+1) \end{bmatrix}^T, \\
\check{\mathbf{x}}_n &= \begin{bmatrix} x(n) & \dots & x(n-M-L+2) \end{bmatrix}^T, \\
\check{\boldsymbol{\eta}}_n &= \begin{bmatrix} v(n) & \dots & v(n-M+1) \end{bmatrix}^T
\end{aligned}$$

and $\mathbf{H}$ is the $M \times (L+M-1)$ CCM,

$$\mathbf{H} = \begin{bmatrix} \mathbf{h}_L^T & 0 & \dots & \mathbf{0} \\ 0 & \mathbf{h}_L^T & 0 & \vdots \\ \vdots & 0 & \ddots & 0 \\ 0 & \dots & 0 & \mathbf{h}_L^T \end{bmatrix} \tag{3.4.2}$$

The MMSE equalizer, $\mathbf{w}_o$, [30,65] for the estimation of $x(n)$ is found by minimizing the cost function

$$J(\mathbf{w}_o) = |x(n) - \mathbf{w}_o^H \check{\mathbf{r}}_n|^2 \tag{3.4.3}$$

that yields

$$\mathbf{w}_o = \left(\mathbf{H}\mathbf{H}^H + \frac{\sigma_n^2}{\sigma_x^2}\mathbf{I}\right)^{-1}\mathbf{H}\mathbf{z}_v \tag{3.4.4}$$

where $\mathbf{z}_v$ is a coordinate vector, only containing a non-zero component at position v, i.e., $\mathbf{z}_v = \begin{bmatrix} 0 & \dots & 0 & 1 & 0 & \dots & 0 \end{bmatrix}^T$

3.4.2 Equalizer for channels with frequency offsets

In the presence of FOs, the effective CCM $\mathbf{H}$ will vary over time and (3.4.1) will be accordingly modified to

$$\check{\mathbf{r}}_n = (\mathbf{H} \odot \mathbf{\Gamma}_L)\,\check{\mathbf{x}}_n + \check{\boldsymbol{\eta}}_n \triangleq \mathbf{H}_n\check{\mathbf{x}}_n + \check{\boldsymbol{\eta}}_n \tag{3.4.5}$$

where

$$\mathbf{\Gamma}_L = \begin{bmatrix} \boldsymbol{\gamma}_n^T & 0 & \dots & \mathbf{0} \\ 0 & \boldsymbol{\gamma}_{n-1}^T & 0 & \vdots \\ \vdots & 0 & \ddots & 0 \\ 0 & \dots & 0 & \boldsymbol{\gamma}_{n-M+1}^T \end{bmatrix} \tag{3.4.6}$$

and

$$\boldsymbol{\gamma}_k = \begin{bmatrix} e^{j2\pi f_0 k} & \dots & e^{j2\pi f_{L-1} k} \end{bmatrix}^T. \tag{3.4.7}$$

The optimum equalizer derived using (3.4.5), instead of (3.4.1), will thus yield

$$\mathbf{w}_o = \left(\mathbf{H}_n\mathbf{H}_n^H + \frac{\sigma_n^2}{\sigma_x^2}\mathbf{I}\right)^{-1}\mathbf{H}_n\mathbf{z}_v \triangleq \mathbf{R}_n^{-1}\mathbf{H}_n\mathbf{z}_v \tag{3.4.8}$$

which due to the time-varying $\mathbf{H}_n$ will require the inversion of $\mathbf{R}_n$ for each symbol. Such an equalizer may be computationally infeasible. In the following, by fully exploiting the movement of sub-matrices in $\mathbf{R}_n$ a computationally efficient recursive scheme is proposed that does not require the inversion of $\mathbf{R}_n$ after every symbol interval. Generally, for stationary channels, long equalizers provide better performance, however for quasi-stationary channels, very long equalizers are not appropriate due to non-stationarity of the signal that enters into the equalizer. To understand the key

ideas behind the proposed algorithm, for simplicity, consider a simple example with only three channel taps and a length three equalizer. Thus,

$$\mathbf{R}_n = \left[\begin{array}{cc|c} \alpha_{11} & \alpha_{12} & \alpha_{13} \\ \alpha_{12}^* & \alpha_{22} & \alpha_{23} \\ \hline \alpha_{13}^* & \alpha_{23}^* & \alpha_{33} \end{array}\right] \triangleq \left[\begin{array}{cc|c} & \mathbf{A}_n & \alpha_{13} \\ & & \alpha_{23} \\ \hline \alpha_{13}^* & \alpha_{23}^* & \alpha_{33} \end{array}\right] \tag{3.4.9}$$

Note that, due to the structure of $\mathbf{R}_n$,

$$\mathbf{R}_{n+1} = \left[\begin{array}{c|cc} \beta_{11} & \beta_{12} & \beta_{13} \\ \hline \beta_{12}^* & \alpha_{11} & \alpha_{12} \\ \beta_{13}^* & \alpha_{12}^* & \alpha_{22} \end{array}\right] = \left[\begin{array}{c|cc} \beta_{11} & \beta_{12} & \beta_{13} \\ \hline \beta_{12}^* & & \\ \beta_{13}^* & \multicolumn{2}{c}{\mathbf{A}_n} \end{array}\right] \tag{3.4.10}$$

the Hermitian matrix $\mathbf{A}_n$ will appear in both $\mathbf{R}_n$ and $\mathbf{R}_{n+1}$. This structural property will hold for any number of channel coefficients and equalizer taps. For the general case, $\mathbf{R}_n$ is written as

$$\mathbf{R}_n = \left[\begin{array}{cc} \mathbf{A}_n & \mathbf{c}_n \\ \mathbf{c}_n^H & b_n \end{array}\right] \tag{3.4.11}$$

where $\mathbf{A}_n \in \mathcal{C}^{(M-1)\times(M-1)}$, $\mathbf{c}_n \in \mathcal{C}^{(M-1)\times 1}$ and $b_n \in \mathcal{R}$. Provided that the relevant inverses exist, the inverse of a general block matrix can be expressed as (3.4.12) or (3.4.13) (see, e.g., [53,66]).

$$\left[\begin{array}{cc} \mathbf{A} & \mathbf{C} \\ \mathbf{D} & \mathbf{B} \end{array}\right]^{-1} = \left[\begin{array}{c} \mathbf{I} \\ \mathbf{0} \end{array}\right] \mathbf{A}^{-1} \left[\begin{array}{cc} \mathbf{I} & \mathbf{0} \end{array}\right] + \left[\begin{array}{c} -\mathbf{A}^{-1}\mathbf{C} \\ \mathbf{I} \end{array}\right] (\mathbf{B} - \mathbf{D}\mathbf{A}^{-1}\mathbf{C})^{-1} \left[\begin{array}{cc} -\mathbf{D}\mathbf{A}^{-1} & \mathbf{I} \end{array}\right] \tag{3.4.12}$$

$$= \left[\begin{array}{c} \mathbf{0} \\ \mathbf{I} \end{array}\right] \mathbf{B}^{-1} \left[\begin{array}{cc} \mathbf{0} & \mathbf{I} \end{array}\right] + \left[\begin{array}{c} \mathbf{I} \\ -\mathbf{B}^{-1}\mathbf{D} \end{array}\right] (\mathbf{A} - \mathbf{C}\mathbf{B}^{-1}\mathbf{D})^{-1} \left[\begin{array}{cc} \mathbf{I} & -\mathbf{C}\mathbf{B}^{-1} \end{array}\right] \tag{3.4.13}$$

Thus, given $\mathbf{A}_n^{-1}$, one can easily obtain $\mathbf{R}_n^{-1}$ and $\mathbf{R}_{n+1}^{-1}$, avoiding the matrix inversion. As $\mathbf{A}_n$ does not appear in $\mathbf{R}_{n+2}$, it can not be used to find $\mathbf{R}_{n+2}^{-1}$, and the scheme so far thus only allows for a pairwise computational saving, still requiring the inversion

of $\mathbf{A}_{n+1}$ to compute $\mathbf{R}_{n+2}^{-1}$ efficiently. However, further exploiting the structure of $\mathbf{R}_n$, one may compute $\mathbf{A}_{n+1}^{-1}$ efficiently from $\mathbf{R}_{n+1}^{-1}$ using the following lemma.

Lemma 1: *Let*

$$\begin{bmatrix} \mathbf{H}_{11} & \mathbf{H}_{12} \\ \mathbf{H}_{21} & \mathbf{H}_{22} \end{bmatrix} = \begin{bmatrix} \mathbf{A}_{11} & \mathbf{A}_{12} \\ \mathbf{A}_{21} & \mathbf{A}_{22} \end{bmatrix}^{-1} \tag{3.4.14}$$

where $dim\{\mathbf{H}_{kl}\} = dim\{\mathbf{A}_{kl}\}$. *Then, provided that the relevant inverses exist, the inverse of matrix* $\mathbf{A}_{11}$ *can be written as the Schur complement of* $\mathbf{H}_{22}$, *i.e.,*

$$\mathbf{A}_{11}^{-1} = \mathbf{H}_{11} - \mathbf{H}_{12}\mathbf{H}_{22}^{-1}\mathbf{H}_{21} \tag{3.4.15}$$

The proof is given in Appendix 3B. At time n, let us find the inverse of submatrix $\mathbf{A}_n$, and use it respectively to find the inverses of $\mathbf{R}_n$ and $\mathbf{R}_{n+1}$ using (3.4.12) and (3.4.13). Since the inverse of $\mathbf{R}_{n+1}$ is known, the inverse of the new top left hand corner submatrix, $\mathbf{A}_{n+1}$, can be found by using Lemma 1. Once found the inverse of $\mathbf{A}_{n+1}$ can be used to compute the inverse of $\mathbf{R}_{n+2}$ using (3.4.13). This is called a forward and backward recursion method to estimate the transmitted symbols. Therefore, the explicit inverse of the matrix $\mathbf{A}_n$ is needed only once and thereafter, the equalizer is updated for every symbol with the forward and backward recursions method using (3.4.13) and Lemma 1. Note that for this problem, $\mathbf{H}_{22}$ is a scalar.

3.5 Simulations

In order to demonstrate the benefits of employing FOs in equalization, a two path wireless communication channel and an equalizer of length 10 is considered. It is assumed that the channel is quasi-stationary. The FOs have been initially set to 0.003 and 0.005, and at every burst n they have been changed according to the random walk model, $f_l(n) = f_l(n-1) + 0.0001u(n)$, where $u(n)$ is a zero mean real Gaussian noise with unity variance. The complex channel gains h_0 and h_1 have been assumed to be constant throughout a burst, but change between the frames. The training signal is assumed to have a binary alphabet while the data symbols in the burst have been

drawn from an 8-PSK constellation. Here, three scenarios are considered. In the first scenario, the FOs associated with the first and the second paths are set f_0=0.003 and f_1=0.005, and a recursive equalizer is designed as explained previously. In the second scenario, to equalize the channel effects a decision directed scheme is adopted, where the least mean square (LMS) algorithm is used to control the equalizer parameters. Here, the LMS equalizer is initialized with the correct MMSE solution, found at the end of the training interval. In the last scenario an equalizer is designed ignoring the effect of FOs. The results depicted in Figure 3.3 show the superior performance of our proposed scheme over the decision directed scheme and an equalizer not considering the effect of FOs. In all the simulation, a training signal of length 142 is considered for the estimation of the channel parameters including the FOs. The proposed scheme can also be employed in a GSM system. Here, the number of pilot symbols available in a burst is only 26. With this training length the channel can be estimated very efficiently, but to estimate FO this length is insufficient. However, the performance of the FO estimator can be enhanced, by concatenating the pilot symbols from a number of recent past bursts. To illustrate this, GSM burst transmission through a two path time varying channel identical to that used in the previous simulation is simulated. A normal burst in GSM consists of 116 encrypted data symbols and 26 pilot symbols in the middle [43]. At every burst the MGs h_0 and h_1 were estimated using the pilot symbols, but the FOs have been estimated using 142 symbols from the previous burst obtained with the retrieved data symbols together with the pilot symbols, in this way to estimate FOs 5 previous successive bursts are used. To avoid occasional FO estimation error, the FO estimates are filtered through a moving median filter of length five. The BER performance of our proposed scheme for a BPSK modulation scheme is identical to the performance of a GSM communication channel without FOs as shown in Figure 3.4.

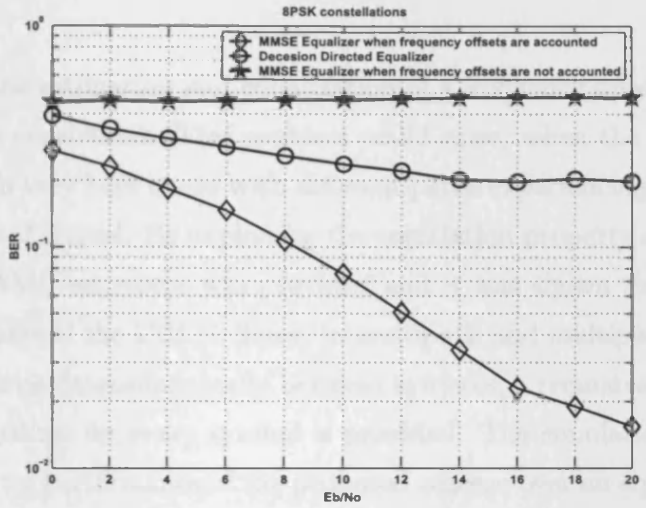

Figure 3.3. Bit error rate performance for MMSE equalizers with and without FO estimation, and a decision directed adaptive equalizer

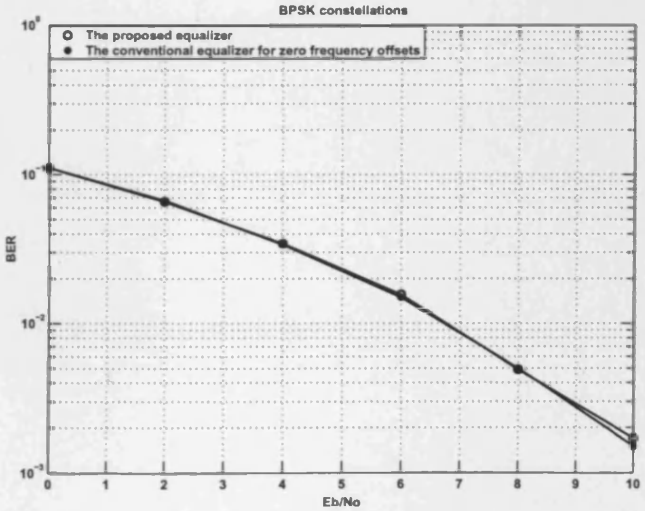

Figure 3.4. Bit error rate performance of MMSE equalizers for a GSM system

3.6 Summary

In this chapter, the estimation and equalization of a frequency selective channel with distinct FOs was considered. This problem could arise, when the receiver or transmitter moves with very high speed with different paths experiencing distinct DSs, due to different angle of arrival. By exploiting the correlation property of the transmitted pilot signal, an AML estimator was provided and it was shown that the estimation error variance attained the CRLB. Since, in multipath and multiple FO scenario, the effective CCM varies deterministically between symbols, a recursive scheme to design the optimum equalizer for every symbol is provided. The simulation results demonstrated the superior performance of the proposed scheme over an equalization scheme that did not consider the effects of multiple FOs.

3.7 Appendices 3

Appendix 3A: Derivation of CRLB for single input single output

In this appendix, the Cramér Rao lower bound for the problem at hand is derived. Let $\bar{\mathbf{r}}(\boldsymbol{\theta}) = \left[\begin{array}{ccc} \bar{r}(n) & \ldots & \bar{r}(n-N+1) \end{array} \right]^T$ and $\boldsymbol{\theta} = \left[\begin{array}{ccc} \mathrm{Re}(\mathbf{h}_L)^T & \mathrm{Im}(\mathbf{h}_L)^T & \mathbf{f}_L^T \end{array} \right]^T$. Under the assumption that $v(n)$ is complex white Gaussian with zero mean and variance σ_v^2, the CRLB can be found using Slepian-Bangs formula (see, e.g., [53]),

$$\left[\mathbf{P}_{CRLB}^{-1}(\boldsymbol{\theta})\right]_{l,p} = 2\sigma_v^{-2}\mathrm{Re}\left\{ \frac{\partial \bar{\mathbf{r}}^H(\boldsymbol{\theta})}{\partial \boldsymbol{\theta}_l} \frac{\partial \bar{\mathbf{r}}(\boldsymbol{\theta})}{\partial \boldsymbol{\theta}_p} \right\} \tag{3.7.1}$$

where $[\mathbf{A}]_{k,p}$ denotes the (k,p)th element of $\mathbf{A}$, and $\mathbf{P} \stackrel{\triangle}{=} E\left\{(\hat{\boldsymbol{\theta}} - \boldsymbol{\theta})(\hat{\boldsymbol{\theta}} - \boldsymbol{\theta})^H\right\} \geq \mathbf{P}_{CRLB}$. Further note that $\frac{\partial \bar{r}(n)}{\partial h_l^r} = e^{j2\pi f_l n}\bar{r}(n-l)$, $\frac{\partial \bar{r}(n)}{\partial h_l^i} = je^{j2\pi f_l n}\bar{r}(n-l)$, and $\frac{\partial \bar{r}(n)}{\partial f_l} = j2\pi n h_l e^{j2\pi f_l n}\bar{r}(n-l)$, where h_l^r and h_l^i are the lth element of $\mathrm{Re}(\mathbf{h}_L)$ and $\mathrm{Im}(\mathbf{h}_L)$.

Appendix 3B: Proof of Lemma 1

Using the block matrix inversion lemma, as expressed in (3.4.12) and (3.4.13), (3.4.14) can be written as (see, e.g., [53,66])

$$\mathbf{H}_{11} = \mathbf{A}_{11}^{-1} + \mathbf{A}_{11}^{-1}\mathbf{A}_{12}\boldsymbol{\Delta}_{\mathbf{A}}^{-1}\mathbf{A}_{21}\mathbf{A}_{11}^{-1} \tag{3.7.2}$$

$$\mathbf{H}_{12} = -\mathbf{A}_{11}^{-1}\mathbf{A}_{12}\boldsymbol{\Delta}_{\mathbf{A}}^{-1} \tag{3.7.3}$$

$$\mathbf{H}_{21} = -\boldsymbol{\Delta}_{\mathbf{A}}^{-1}\mathbf{A}_{21}\mathbf{A}_{11}^{-1} \tag{3.7.4}$$

$$\mathbf{H}_{22} = \boldsymbol{\Delta}_{\mathbf{A}}^{-1} \tag{3.7.5}$$

where $\boldsymbol{\Delta}_{\mathbf{A}} = \mathbf{A}_{22} - \mathbf{A}_{21}\mathbf{A}_{11}^{-1}\mathbf{A}_{12}$ is the Schur complement of $\mathbf{A}_{11}$. Substituting (3.7.5) into (3.7.4), and (3.7.3) into (3.7.2), yields

$$\mathbf{H}_{21} = -\mathbf{H}_{22}\mathbf{A}_{21}\mathbf{A}_{11}^{-1} \tag{3.7.6}$$

$$\mathbf{H}_{11} = \mathbf{A}_{11}^{-1} - \mathbf{H}_{12}\mathbf{A}_{21}\mathbf{A}_{11}^{-1} \tag{3.7.7}$$

Substituting (3.7.6) into (3.7.7) yields

$$\mathbf{H}_{11} = \mathbf{A}_{11}^{-1} + \mathbf{H}_{12}\mathbf{H}_{22}^{-1}\mathbf{H}_{21} \tag{3.7.8}$$

and hence (3.4.15), which concludes the proof.

Chapter 4

PARAMETER ESTIMATION AND EQUALIZATION IN MIMO WITH FREQUENCY OFFSETS

To increase the channel capacity and reliability of a communication system, the information data can be transmitted and received by using a number of transmit and receive antennas [67]. This configuration of the communication system is called a MIMO system. Recent research in communication theory [68] has demonstrated that large gains in capacity and reliability of communications over wireless channels can potentially be achieved by exploiting spatial diversity through MIMO antennas [69–71]. Spatial diversity can be used to either increase the capacity or enhance coverage in a wireless communication system. In the first case, multiple antennas are used at the transmitter and the receiver to form multiple spatial channels to transmit multiple data streams through various spatial modes, which is termed data multiplexing [31, 32, 72]. In the second case, multiple antennas are used to transmit multiple copies of the same data so that a better BER performance can be obtained at very low SNR [73, 74]. This is exploited to increase the coverage in a wireless communication system. Therefore, multiple antennas at both the transmitter and receiver are very likely to play a key role in future high data rate wireless communication systems. Often, MIMO transmission schemes proposed in the literature are based

on somewhat idealized assumptions. Such as most MIMO transmission schemes are designed for frequency-flat channels [33, 73]. However, if there are multipath signals with large propagation delays, then the assumption of frequency-flat channel might not be valid, depending on the symbol duration.

Besson *et al.* [33] discussed the estimation of FOs in MIMO flat fading channels with distinct FOs between each transmitter and receiver. This chapter extend this work for MIMO frequency selective channels that allows distinct FOs for each multipath between each transmit and receive antenna. As discussed in chapter 1, the performance of such multiple antenna based systems may seriously degrade in the presence of FOs. Therefore, it is of importance to determine these FOs and to take them into account for in the equalizer design. In this scenario, to estimate the FOs and MGs, an AML estimator is proposed that exploits the correlation property of the transmitted training sequence. In order to assess the performance of the proposed estimator the corresponding CRLB is determined, and used as a benchmark for the performance of the proposed estimator. Furthermore, multiple FOs introduce deterministic time variations in the channel, which are exploited to design a low complexity MIMO recursive MMSE equalizer to account for symbol-by-symbol variations in the CCM.

4.1 Problem Statement

Consider a MIMO communication system with n_T transmit and n_R receive antennas, where the signal between any two transmit and receive antennas has propagated through a total of L different paths, with each path possibly having different FO. If the sampling rate at the receive antenna k is equal to the symbol transmission rate then the received baseband signal can be written as

$$r_k(m) = u_k(m) + v_k(m), \tag{4.1.1}$$

where

$$u_k(m) = \sum_{l=1}^{n_T} \sum_{p=0}^{L-1} h_{kl}(p) e^{j\omega_{klp} m} x_l(m-p), \tag{4.1.2}$$

for $m = n, \ldots, n-N+1$, $k = 1, \ldots, n_R$, where N is the number of symbols received, $h_{kl}(p)$ and ω_{klp} are respectively the MGs and FOs between the receive antenna k and the transmit antenna l, for the multipath p; these are assumed to be quasi-stationary, i.e., they do not change significantly over an observed data frame, but may change between the frames. Here, $\{x_l(m)\}$ is the training signal sequence, transmitted from the lth transmit antenna and $v_k(m)$ is assumed an additive zero mean circularly Gaussian distributed, spatially and temporally uncorrelated, white noise with variance σ_v^2. Let $\mathbf{X}_{lp} = \text{diag}\left\{ \mathbf{x}_{lp} \right\}$, where $diag\{\mathbf{q}\}$ denotes a diagonal matrix with the vector $\mathbf{q}$ along the diagonal, and

$$\mathbf{x}_{lp} = \left[\begin{array}{ccc} x_l(n-p) & \cdots & x_l(n-p-N+1) \end{array} \right]^T \tag{4.1.3}$$

$$\mathbf{e}_{kl}(p) = \left[\begin{array}{ccc} e^{j\omega_{klp} n} & \cdots & e^{j\omega_{klp}(n-N+1)} \end{array} \right]^T \tag{4.1.4}$$

$$\mathbf{h}_{kl} = \left[\begin{array}{ccc} h_{kl}(0) & \cdots & h_{kl}(L-1) \end{array} \right]^T \tag{4.1.5}$$

where the vector $\mathbf{e}_{kl}(p)$ contains the FO between the receive antenna k and the transmit antenna l, for the multipath p and $\mathbf{h}_{kl}$ is the vector of MGs between the receive antenna k and the transmit antenna l. Furthermore, suppose that

$$\mathbf{V}_{kl} = \left[\begin{array}{ccc} \mathbf{X}_{l0}\mathbf{e}_{kl}(0) & \cdots & \mathbf{X}_{l(L-1)}\mathbf{e}_{kl}(L-1) \end{array} \right], \quad N \times L \tag{4.1.6}$$

$$\mathbf{h}_k = \left[\begin{array}{cccc} \mathbf{h}_{k1}^T & \mathbf{h}_{k2}^T & \cdots & \mathbf{h}_{kn_T}^T \end{array} \right]^T, \quad n_T L \times 1 \tag{4.1.7}$$

$$\mathbf{V}_k = \left[\begin{array}{cccc} \mathbf{V}_{k1} & \mathbf{V}_{k2} & \cdots & \mathbf{V}_{kn_T} \end{array} \right]. \quad N \times n_T L \tag{4.1.8}$$

Using these identities, the N received samples in (4.1.1) can be written in vector form as

$$\begin{aligned} \mathbf{r}_k &= \left[\begin{array}{ccc} r_k(n) & \cdots & r_k(n-N+1) \end{array} \right]^T \\ &= \mathbf{V}_k \mathbf{h}_k + \boldsymbol{v}_k. \end{aligned} \tag{4.1.9}$$

To estimate the various MGs and the FOs, suppose

$$\boldsymbol{\omega}_{kl} = \begin{bmatrix} \omega_{kl0} & \omega_{kl1} & \cdots & \omega_{kl(L-1)} \end{bmatrix}^T \tag{4.1.10}$$

and

$$\boldsymbol{\omega}_k = \begin{bmatrix} \boldsymbol{\omega}_{k1}^T & \boldsymbol{\omega}_{k2}^T & \cdots & \boldsymbol{\omega}_{kn_T}^T \end{bmatrix}^T \qquad n_T L \times 1 \tag{4.1.11}$$

then, the unknown parameter vector, $\boldsymbol{\theta}_k$, corresponding to receive antenna k, to be estimated can be written as $\boldsymbol{\theta}_k = \begin{bmatrix} \mathbf{h}_k^T & \boldsymbol{\omega}_k^T \end{bmatrix}^T$. In the next section, the problem of estimating $\boldsymbol{\theta}_k$ is considered.

4.2 Estimation of Multipath Gains and Frequency Offsets

In this section, an approximate maximum likelihood (AML) estimator is outlined, which fully exploits the structure of the transmitted training sequence. Since the noise, $v_k(n)$, at the receive antenna is spatially uncorrelated, the parameters associated with each receiver can be estimated independently from the received signal. Considering (4.1.9), the likelihood function of $\mathbf{r}_k$ can be written as [30]

$$p(\mathbf{r}_k|\,\boldsymbol{\theta}_k) = \frac{1}{(\pi\sigma_v^2)^N}\, e^{-\frac{(\mathbf{r}_k - \mathbf{V}_k\mathbf{h}_k)^H(\mathbf{r}_k - \mathbf{V}_k\mathbf{h}_k)}{\sigma_v^2}}, \tag{4.2.1}$$

Taking the natural logarithm and ignoring the constant terms, as they will not affect the maximization of the likelihood function, (4.2.1) can be written as

$$\ln p(\mathbf{r}_k|\,\boldsymbol{\theta}_k) = -\frac{1}{\sigma_{v_k}^2}\,(\mathbf{r}_k - \mathbf{V}_k\mathbf{h}_k)^H\,(\mathbf{r}_k - \mathbf{V}_k\mathbf{h}_k)\,. \tag{4.2.2}$$

In order to estimate parameter vector, $\boldsymbol{\theta}_k$, maximization of (4.2.1) is equivalent to the minimization of (4.2.2) (as the minus sign is omitted in the log-likelihood function) with respect to $\mathbf{h}_k$ and yields

$$\hat{\mathbf{h}}_k = (\mathbf{V}_k^H\mathbf{V}_k)^{-1}\mathbf{V}_k^H\mathbf{r}_k, \tag{4.2.3}$$

then, inserting $\hat{\mathbf{h}}_k$ into (4.2.2) yields the cost function to minimize with respect to the FOs

$$J(\omega_{klp}) = \mathbf{r}_k^H\mathbf{r}_k - \mathbf{r}_k^H\mathbf{V}_k(\mathbf{V}_k^H\mathbf{V}_k)^{-1}\mathbf{V}_k^H\mathbf{r}_k. \tag{4.2.4}$$

Note that minimizing (4.2.4) requires an $n_T L$-dimensional minimization. However, choosing the training sequence $\{x_l(n)\}$ such that

$$E\{x_l^*(n-u)x_d(n-v)\} = \delta_{u-v}\delta_{l-d}, \tag{4.2.5}$$

this minimization can be decoupled into $n_T L$ one-dimensional minimizations. Considering (??), note that $\mathbf{V}_k^H\mathbf{V}_k$ will be dominated by the large diagonal terms, with almost negligible contribution from the off-diagonal terms. Thus, $\mathbf{V}_k^H\mathbf{V}_k \approx \sum_{n=0}^{N-1}|x_l(n)|^2\,\mathbf{I} \triangleq \kappa\mathbf{I}$, where κ is constant over the frame considered, enabling us to approximate the minimum of (4.2.4) as the maximum of

$$\begin{aligned} J'(\omega_{klp}) &= \mathbf{r}_k^H\mathbf{V}_k\mathbf{V}_k^H\mathbf{r}_k \\ &= \sum_{l=1}^{n_T}\sum_{p=0}^{L-1}\left|\sum_{n=0}^{N-1} r_k^*(n)x_l(n-p)e^{j\omega_{klp}n}\right|^2 . \end{aligned} \tag{4.2.6}$$

Maximizing $J'(\omega_{klp})$ is equivalent to maximizing all individual terms of the above outer sum. Consider a given path s from the transmit antenna q to the receive antenna k, the contribution of this path to the cost function, $J'(\omega_{klp})$, can be written as

$$\psi_{kqs}(n) = r_k^*(n)x_q(n-s)e^{j\omega_{kqs}n}$$

and using (4.1.1)

$$\psi_{kqs}(n) = h_{kq}^*(s)\,|x_q(n-s)|^2 + c_1(n) + c_2(n), \tag{4.2.7}$$

where

$$\begin{aligned} c_1(n) &= v_k^*(n)x_q(n-s)e^{j\omega_{kqs}n} \\ c_2(n) &= \sum_{l=1}^{n_T}\sum_{\substack{p=0 \\ p\neq s\,|\,l=q}}^{L-1} h_{kl}^*(p)x_l^*(n-p)x_q(n-s)e^{j\Delta\omega_{klp}n}, \end{aligned}$$

and $\Delta\omega_{klp} = \omega_{kqs} - \omega_{klp}$. The first term in $\psi_{kqs}(n)$ corresponds to the signal power for the path s, and as $E\{x_l^*(n-u)x_d(n-v)\} = 0$ for $u \neq v$, or $l \neq d$, it will be significantly larger than the contribution from the interference term, $c_2(n)$, constructed from all

paths except $p \neq s$ when transmit antenna $l = q$. Thus, each of the terms in the outer sum of (4.2.6) will be maximized for $\omega = \omega_{kqs}$, suggesting the AML estimator for ω_{kqs}, for $q = 1, \ldots, n_T$, and $s = 0, \ldots, L-1$, as

$$\phi_{kqs}(\omega) = \left| \sum_{n=0}^{N-1} r_k^*(n) x_q(n-s) e^{j\omega n} \right|^2 \tag{4.2.8}$$

$$\omega_{kqs} = \arg\max_{\omega} \phi_{kqs}(\omega), \tag{4.2.9}$$

which can be efficiently evaluated using the FFT. Once the FOs are estimated, the MGs, $\mathbf{h}_k$, can be estimated by inserting the estimated values of the FOs in (4.2.3). It can be noted that the AML for FOs does not provide the block based solution but for MGs, the AML solution is block based.

4.3 Numerical Example for the Variance of the Estimators

To illustrate the theoretical findings a numerical example is provided. Consider a case with maximum vehicular speed of 250km/h, at a carrier frequency of 1800MHz (RA250 channels as defined in GSM standard [43]), this corresponds to the maximum DS of 0.005 when normalized to the symbol rate of 100kbits/sec, which will be different for different angles of arrivals. For higher carrier frequency or speed, the normalized frequency will further increase. In order to see the performance of the proposed estimator, a case using two transmit and two receive antennas is simulated. Here, it is considered that there are two paths between each transmit and receive antenna, allowing eight different paths and correspondingly eight different FOs. Using the assumption of a quasi-stationary channel, the channel parameters, $h_{kl}(p)$, and the FOs, ω_{klp}, remain constant throughout the training burst interval, but may change according to the Rayleigh distribution between the bursts. BPSK signals are used for training data, the length of the training data from each antenna is 200 samples. The training signals transmitted from each antenna are assumed uncorrelated. In order to estimate the FOs, an FFT based method is used, therefore, the difference between

any two FOs is assumed to be greater than 1/N. In the simulation, parameters are estimated and the variances of the estimators are compared with the corresponding CRLB, which is derived in Appendix 4A. Figures 4.1 and 4.2 depict the variance of the estimators for the MGs and the FOs, respectively. The simulation results show that the proposed estimator attains the CRLB. It can be noticed that the variance of the estimation error sometimes goes slightly below the CRLB. The reason for this can be attributed to the fact that an FFT based grid search method is used to estimate the FOs. The performance of this method relies on the chosen resolution of the FFT and hence the estimate of the FO. Therefore, for the variance of the estimation error to match the theoretical CRLB, the resolution should be infinitely small so that the frequency estimate is unbiased. As a consequence of the non-ideal resolution and hence the bias in the frequency estimate the error variance may sometimes go a little below the theoretical CRLB which assumes exact frequency knowledge.

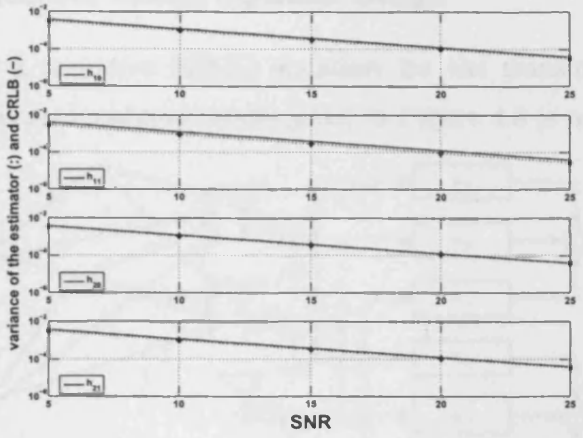

Figure 4.1. Comparison of the variance of the estimates of channel gains (dashed line) with the corresponding CRLB (solid line).

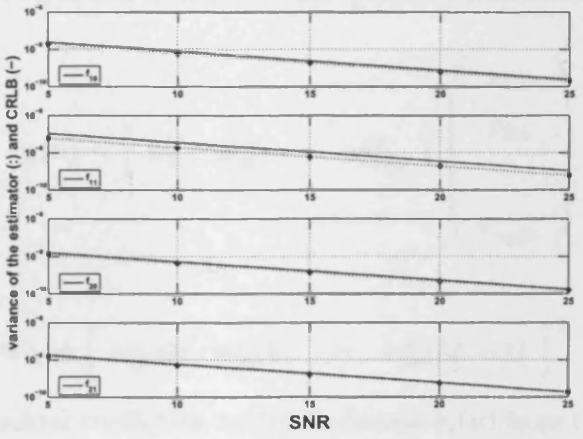

Figure 4.2. Comparison of the variance of the estimates of FOs (dashed line) with the corresponding CRLB (solid line).

4.4 A MIMO Recursive MMSE Equalizer Design

In order to design a recursive MIMO equalizer for the transmitted symbols from antenna l, the equalizer baseband model given in Figure 4.3 is used.

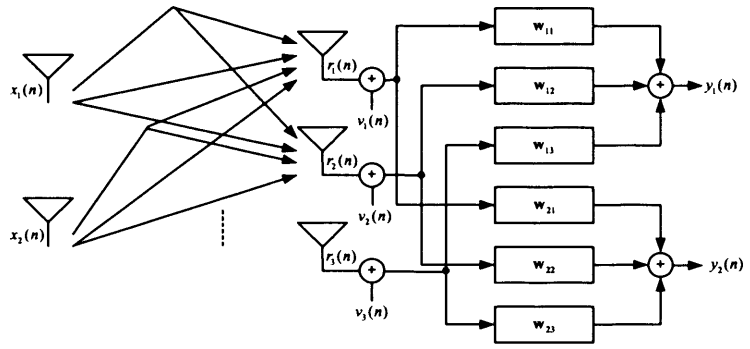

Figure 4.3. A two transmitter and three receiver MIMO transmitter and receiver baseband system.

From the figure, the equalizer output for the symbol transmitted from antenna l can be written as

$$y_l(n) = \begin{bmatrix} \mathbf{w}_{l1}^T & \mathbf{w}_{l2}^T & \cdots & \mathbf{w}_{ln_R}^T \end{bmatrix} \begin{pmatrix} \mathbf{r}_{1m} \\ \mathbf{r}_{2m} \\ \vdots \\ \mathbf{r}_{n_R m} \end{pmatrix} \tag{4.4.1}$$

where

$$\mathbf{w}_{lk} = \begin{bmatrix} w_{lk}^*(0) & w_{lk}^*(1) & \cdots & w_{lk}^*(M-1) \end{bmatrix}^T$$

is the length M equalizer coefficient vector to decode $x_l(n)$ from the received samples, $\mathbf{r}_{km} = \begin{bmatrix} r_k(n) & r_k(n-1) & \cdots & r_k(n-M+1) \end{bmatrix}$, at the antenna k. By rearranging the individual equalizer coefficients and received samples in (4.4.1), the equalizer output can be written as

$$y_l(n) = \mathbf{w}^H \mathbf{r}_m \tag{4.4.2}$$

$$= \mathbf{w}^H \mathbf{H}_c \mathbf{x}_m + \mathbf{w}^H \mathbf{v}_m, \tag{4.4.3}$$

where

$$\mathbf{w} = \begin{bmatrix} \mathbf{w}(0)^T & \mathbf{w}(1)^T & \cdots & \mathbf{w}(M-1)^T \end{bmatrix}^T, \quad 1 \times n_R M$$
$$\mathbf{w}(l) = \begin{bmatrix} w_{11}(l) & w_{12}(l) & \cdots & w_{1n_R}(l) \end{bmatrix}^T, \quad 1 \times n_R$$

$\mathbf{r}_m = \begin{bmatrix} \mathbf{r}^T(n) & \cdots & \mathbf{r}^T(n-M+1) \end{bmatrix}^T$ and $\mathbf{r}(n) = \begin{bmatrix} r_1(n) & \cdots & r_{n_R}(n) \end{bmatrix}^T$. Moreover, $\mathbf{H}_c$ is the $n_R M \times n_T(M+L-1)$ CCM and $\mathbf{x}_m$ is the $n_T(M+L-1) \times 1$ transmitted signal vector and are defined as

$$\mathbf{H}_c = \begin{bmatrix} \mathbf{H}^n & & & \\ & \mathbf{H}^{(n-1)} & & \\ & & \ddots & \\ & & & \mathbf{H}^{(n-M+1)} \end{bmatrix},$$
$$\mathbf{H}^n = \begin{bmatrix} \mathbf{h}_1^n & \mathbf{h}_2^n & \cdots & \mathbf{h}_{n_R}^n \end{bmatrix}^T,$$
$$\mathbf{h}_k^n = \begin{bmatrix} \mathbf{h}_k^n(0)^T & \mathbf{h}_k^n(1)^T & \cdots & \mathbf{h}_k^n(L-1)^T \end{bmatrix}^T,$$
$$\mathbf{h}_k^n(p) = \begin{bmatrix} h_{k1}(p)e^{j\omega_{k1}pn} & \cdots & h_{kn_T}(p)e^{j\omega_{kn_T}pn} \end{bmatrix}^T$$
$$\mathbf{x}_m = \begin{bmatrix} \mathbf{x}^T(n) & \ldots & \mathbf{x}^T(n-M-L+2) \end{bmatrix}^T$$
$$\mathbf{x}(n) = \begin{bmatrix} x_1(n) & \ldots & x_{n_T}(n) \end{bmatrix}^T$$

Finally, $\mathbf{v}_m = \begin{bmatrix} \mathbf{v}^T(n) & \cdots & \mathbf{v}^T(n-M+1) \end{bmatrix}^T$ and $\mathbf{v}(n) = \begin{bmatrix} v_1(n) & \cdots & v_{n_R}(n) \end{bmatrix}^T$.

Remark 1. Here, to estimate the transmitted symbols the condition $n_R M \geq n_T(M+L-1)$ must be satisfied or

$$n_R \geq n_T\left(1 + \frac{L-1}{M}\right), \tag{4.4.4}$$

which implies that in a multipath channel $n_R > n_T$. This result contrasts with the result mentioned in [69] that says $n_R = n_T$. Moreover, $M \geq \left(\frac{n_T}{n_R - n_T}(L-1)\right)$.
The length M equalizer is obtained by minimizing the mean square error cost function

$$J = E\{|y_l(n) - x_l(n-d)|^2\}, \tag{4.4.5}$$

where $l \in (1, 2, ..., n_T)$ and $d \in (0, 1, ..., M + L - 2)$. Therefore,

$$\mathbf{w} = \left(\mathbf{H}_c\mathbf{H}_c^H + \frac{{\sigma_v}^2}{\sigma_x^2}\mathbf{I}\right)^{-1}\mathbf{H}_c\mathbf{z}_v \triangleq \mathbf{R}^{-1}\mathbf{H}_c\mathbf{z}_v, \tag{4.4.6}$$

where $\mathbf{z}_v$ is the $n_T(M + L - 1) \times 1$ coordinate vector, only containing a non-zero element at position v, i.e.,

$$\mathbf{z}_v = \begin{bmatrix} 0 & \cdots & 0 & 1 & 0 & \cdots & 0 \end{bmatrix}^T. \tag{4.4.7}$$

The position of the non-zero element in $\mathbf{z}_v$ determines the equalizer corresponding to the various transmitters $l \in (1, 2, ..., n_T)$ and retrieval delays $d \in (0, 1, ..., M + L - 2)$. For example the one at position $n_T d + l$ will design an equalizer to decode the transmitted signal from antenna l with delay d. The derivation of the equalizer coefficient vector is given in Appendix 4B.

Once $(\mathbf{H}_c\mathbf{H}_c^H + \frac{{\sigma_v}^2}{\sigma_x^2}\mathbf{I})^{-1}\mathbf{H}_c$ is known, the equalizer coefficient values corresponding to the signal transmitted from antenna l can be found by just multiplying with the corresponding $\mathbf{z}_v$. Due to FOs, the CCM $\mathbf{H}_c$ changes after every symbol. Therefore, it is necessary to update the equalizer coefficient values at every symbol, which is typically computationally infeasible. To deal with this problem, exploiting the structural movement of the submatrices in $\mathbf{R}$ a computationally efficient recursive scheme is proposed. This is an extension of the single user result presented in the previous chapter to the multiuser system considered herein. To emphasize the fact that $\mathbf{R}$ changes at every symbol time n, subscript n in (4.4.6), is used as follows

$$\mathbf{w}_n = \mathbf{R}_n^{-1}\mathbf{H}_c(n)\mathbf{z}_v. \tag{4.4.8}$$

and

$$\mathbf{w}_{n+1} = \mathbf{R}_{n+1}^{-1}\mathbf{H}_c(n+1)\mathbf{z}_v. \tag{4.4.9}$$

A close inspection of $\mathbf{H}_c(n)$ reveals that the matrices $\mathbf{R}_n$ and $\mathbf{R}_{n+1}$ can be written as follows

$$\mathbf{R}_n = \left[\begin{array}{c|c} \mathbf{G}_n & \mathbf{C}_n \\ \hline \mathbf{C}_n^H & \mathbf{B}_n \end{array}\right] \tag{4.4.10}$$

$$\mathbf{R}_{n+1} = \left[\begin{array}{c|c} \mathbf{D}_n & \mathbf{E}_n \\ \hline \mathbf{E}_n^H & \mathbf{G}_n \end{array}\right] \tag{4.4.11}$$

where $\mathbf{G}_n \in \mathcal{C}^{n_R(M-1)\times n_R(M-1)}$, $\mathbf{B}_n \in \mathcal{C}^{n_R\times n_R}$, $\mathbf{D}_n \in \mathcal{C}^{n_R\times n_R}$, $\mathbf{C}_n \in \mathcal{C}^{n_R(M-1)\times n_R}$, and $\mathbf{E}_n \in \mathcal{C}^{n_R\times n_R(M-1)}$. Note how the Hermitian matrix $\mathbf{G}_n$ moves from the top left corner to the bottom right corner from time n to $n+1$. Further, if the inverse of $\mathbf{G}_n$, is known, then one could find the inverses of $\mathbf{R}_n$ and $\mathbf{R}_{n+1}$ using the matrix inversion lemma (see, e.g., [53]), yielding a computationally efficient update of $\mathbf{w}$. As $\mathbf{G}_n$ will not appear in $\mathbf{R}_{n+2}$, it can not be used to find the inverse of $\mathbf{R}_{n+2}$. Thus, the scheme so far only allows for a pairwise computational saving, still requiring inversion of $\mathbf{G}_{n+1}$, to find the inverse of $\mathbf{R}_{n+2}$ efficiently. However, further exploiting the structure, one may compute the inverse of $\mathbf{G}_{n+1}$ efficiently from the inverse of $\mathbf{R}_{n+1}$ using the following lemma obtained in the previous chapter.

Let

$$\begin{bmatrix} \mathbf{Q}_{11} & \mathbf{Q}_{12} \\ \mathbf{Q}_{21} & \mathbf{Q}_{22} \end{bmatrix}^{-1} = \begin{bmatrix} \mathbf{H}_{11} & \mathbf{H}_{12} \\ \mathbf{H}_{21} & \mathbf{H}_{22} \end{bmatrix} \tag{4.4.12}$$

Here, $\dim\{\mathbf{H}_{kl}\} = \dim\{\mathbf{Q}_{kl}\}$, where $\dim\{.\}$ denotes the dimension of matrix. Then, provided the relevant inverses exist, the inverse of matrix $\mathbf{Q}_{11}$ can be written as the Schur complement of $\mathbf{H}_{22}$, i.e.,

$$\mathbf{Q}_{11}^{-1} = \mathbf{H}_{11} - \mathbf{H}_{12}\mathbf{H}_{22}^{-1}\mathbf{H}_{21} \tag{4.4.13}$$

Therefore, starting at time n, the inverse of the sub-matrix $\mathbf{G}_n$ is found. The inverses of $\mathbf{R}_n$ and $\mathbf{R}_{n+1}$ are then found using the matrix inversion lemma. Once the inverse

of $\mathbf{R}_{n+1}$ is known, the inverse of $\mathbf{G}_{n+1}$ is found using (4.4.13). Further, the inverse of $\mathbf{G}_{n+1}$ can then be used to find the inverse of $\mathbf{R}_{n+2}$, and so on. This is called a forward and backward recursion method to find the inverse of the matrix $\mathbf{R}_n$ at every symbol time n. Thus, the explicit inverse of the sub-matrix $\mathbf{G}_n$ is needed only once at the start; thereafter, only the inverse of $\mathbf{H}_{22}$ is required after every symbol, which significantly reduces the complexity of finding the inverse of $\mathbf{R}_n$ from $\mathcal{O}(n_R^3\, M^3)$ to $\mathcal{O}(n_R^3)$.

Remark 2. If only one path exists between any two transmit and receive antennas, then the matrix $\mathbf{H}_c(n)\mathbf{H}_c^H(n)$ will be block diagonal, enabling the inverse to be found by taking the inverse of individual blocks in $\mathbf{H}_c(n)\mathbf{H}_c^H(n)$.

Remark 3. For single transmit and single receive antenna schemes with distinct FOs for each path, $\mathbf{H}_{22}$ is only a scalar as shown in Chapter 3. Hence, for this case, the proposed recursive method does not require any explicit matrix inversion, whereas the conventional methods require inversion of an $M \times M$ matrix at every symbol.

4.5 Simulation

In order to demonstrate the benefits of employing FOs in equalization, a MIMO channel is considered. In this simulation a 2 transmit and 3 receive antenna system is considered. The number of multipaths between each transmit and receive antenna is assumed equal to 2. The equalizer is designed using 4 taps. The FOs are initially chosen to be of the order of 10^{-2}, but are changed at every burst according to a random walk model $f_k(n) = f_k(n-1)+0.001u(n)$, where $u(n)$ is the Gaussian random variable with zero mean and variance equal to 1. For simulations, three scenarios are considered. In the first scenario, FOs associated with each multipath are set to zero and the design equalizer is based on the MMSE criterion. In the second scenario, distinct FOs are considered from each multipath and are changed according to a random walk model after each frame. To compensate for the effects of multiple FOs, the proposed recursive equalizer is used that account for FOs in equalizer design. In

the third scenario, a channel with FOs as in the second scenario is considered but the designed MMSE equalizer ignores the effects of FOs in the equalizer design. The bottom curve depicted in Figure 4.4 shows the benchmark performance in the first scenario, while the middle curve shows the performance of the proposed algorithm in the second scenario and finally the top curve shows the performance of an equalizer that does not accounts for FOs. The performance of the proposed recursive equalizer is close to the bench mark performance and in the third scenario the performance of the equalizer not accounting FOs is independent of SNR.

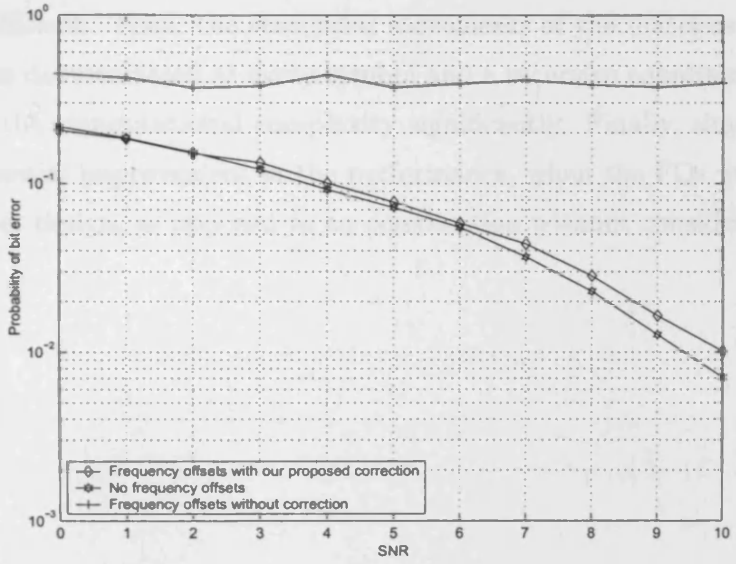

Figure 4.4. Bit error rate performance comparison of the proposed scheme accounting for FOs in the equalizer design with the conventional equalizer scheme ignoring the FOs in the equalizer design. For bench mark the simulation result of a conventional scheme when there is no FO in the channel is also shown.

4.6 Summary

In this chapter, the estimation problem of the MGs and FOs for the frequency selective MIMO channel with distinct FO was addressed. By exploiting the correlation property of the transmitted pilot signal an AML estimator was proposed that decomposed the $n_T L$ dimensional FOs estimation maximization problem into $n_T L$ one dimensional FO estimation maximization problems. The performances of the estimators were validated by comparing their variances with the corresponding CRLB, which was also derived. The estimators were found to be both computationally and statistically efficient. Then, the structural movements of the matrices inside the big matrix $\mathbf{R}_n$ was demonstrated at every symbol and a recursive equalizer was proposed that reduced the computational complexity significantly. Finally, simulation results showed substantial improvement in the performance, when the FOs were considered in the equalizer design, as opposed to an equalization without consideration of FOs.

4.7 Appendices 4

Appendix 4A: Derivation of Cramér Rao Lower Bound for MIMO

This section is devoted to the derivation of the Cramér Rao lower bound for the estimators of MGs and FOs. Stacking all the received samples from time n to $(n - N + 1)$, from all antennas, (4.1.1) can be written in vector form as

$$\mathbf{r} = \mathbf{u} + \boldsymbol{v}, \tag{4.7.1}$$

where

$$\begin{aligned} \mathbf{r} &= \left[\begin{array}{ccc} \mathbf{r}(n)^T & \cdots & \mathbf{r}(n-N+1)^T \end{array} \right] \\ \mathbf{r}(n) &= \left[\begin{array}{ccc} r_1(n) & \cdots & r_{n_R}(n) \end{array} \right]^T \end{aligned}$$

with $\mathbf{u}$ and $\boldsymbol{v}$ formed similarly. Denote the unknown desired vector parameters

$$\boldsymbol{\eta} \triangleq \left[\begin{array}{cccc} \boldsymbol{\eta}_1^T & \boldsymbol{\eta}_2^T & \ldots & \boldsymbol{\eta}_{n_R}^T \end{array} \right]^T, \tag{4.7.2}$$

where

$$\boldsymbol{\eta}_k \triangleq \left[\begin{array}{ccc} Re(\mathbf{h}_k)^T & Im(\mathbf{h}_k)^T & \boldsymbol{\omega}_k^T \end{array} \right]^T. \tag{4.7.3}$$

Since the noise sequence $v_k(n)$ is spatially uncorrelated, the Fisher Information Matrix (FIM) for the estimation of η can be found using Slepian-Bangs formula (see, e.g, [30], [53]).

$$\begin{aligned} \mathbf{F}(k,l) &= \frac{2}{\sigma_v^2} Re\left(\frac{\partial \mathbf{u}^H}{\partial \boldsymbol{\eta}_k} \frac{\partial \mathbf{u}}{\partial \boldsymbol{\eta}_l^T} \right) \\ &= \frac{2}{\sigma_v^2} Re \sum_{n=0}^{N-1} \left(\frac{\partial \mathbf{u}^H(n)}{\partial \boldsymbol{\eta}_k} \frac{\partial \mathbf{u}(n)}{\partial \boldsymbol{\eta}_l^T} \right), \end{aligned} \tag{4.7.4}$$

where

$$\begin{aligned} \frac{\partial \mathbf{u}^H}{\partial \boldsymbol{\eta}_k} &= \left[\begin{array}{c} \frac{\partial \mathbf{u}^H}{\partial Re(\boldsymbol{h}_k)} \\ \frac{\partial \mathbf{u}^H}{\partial Im(\boldsymbol{h}_k)} \\ \frac{\partial \mathbf{u}^H}{\partial \boldsymbol{\omega}_k} \end{array} \right] \quad (3n_T L \times n_R N) \\ \frac{\partial \mathbf{u}}{\partial \boldsymbol{\eta}_l^T} &= \left[\begin{array}{ccc} \frac{\partial \mathbf{u}}{\partial Re(\boldsymbol{h}_l{}^T)} & \frac{\partial \mathbf{u}}{\partial Im(\boldsymbol{h}_l{}^T)} & \frac{\partial \mathbf{u}}{\partial \boldsymbol{\omega}_l{}^T} \end{array} \right] \quad (n_R N \times 3n_T L) \end{aligned}$$

Here, $k, l = 1, 2, ..., n_R$. The FIM can be written as

$$\mathbf{F} = \begin{bmatrix} \mathbf{F}(1,1) & \mathbf{F}(1,2) & \cdots & \mathbf{F}(1,n_R) \\ \mathbf{F}(2,1) & \mathbf{F}(2,2) & \cdots & \mathbf{F}(2,n_R) \\ \vdots & \vdots & \ddots & \vdots \\ \mathbf{F}(n_R,1) & \mathbf{F}(n_R,2) & \cdots & \mathbf{F}(n_R,n_R) \end{bmatrix} \tag{4.7.5}$$

where $\mathbf{F}(k,l)$ denotes the (k,l)th sub-matrix of the FIM corresponding to the parameters $\boldsymbol{\eta}_k$ and $\boldsymbol{\eta}_l$. From (4.7.4), it can be noted that $\mathbf{F}(k,l) = \mathbf{0}$ whenever $k \neq l$. Hence, there is a decoupling between the estimation error in parameters corresponding to two different receive antennas and the FIM is block diagonal, which justifies that the parameters corresponding to each receive antenna can be estimated independently. Let $\mathbf{F}_k = \mathbf{F}(k,k)$, the FIM of size $3n_TL \times 3n_TL$ corresponding to the estimation of $\boldsymbol{\eta}_k = [Re(\mathbf{h}_k)^T \;\; Im(\mathbf{h}_k)^T \;\; \boldsymbol{\omega}_k^T]^T$, then $\mathbf{F}_k$ can be represented as

$$\mathbf{F}_k = \frac{2}{\sigma_v^2} \begin{bmatrix} \mathbf{F}_k[Re(\mathbf{h}_k), Re(\mathbf{h}_k)] & \mathbf{F}_k[Re(\mathbf{h}_k), Im(\mathbf{h}_k)] & \mathbf{F}_k[Re(\mathbf{h}_k), \boldsymbol{\omega}_k] \\ \mathbf{F}_k[Im(\mathbf{h}_k), Re(\mathbf{h}_k)] & \mathbf{F}_k[Im(\mathbf{h}_k), Im(\mathbf{h}_k)] & \mathbf{F}_k[Im(\mathbf{h}_k), \boldsymbol{\omega}_k] \\ \mathbf{F}_k[\boldsymbol{\omega}_k, Re(\mathbf{h}_k)] & \mathbf{F}_k[\boldsymbol{\omega}_k, Im(\mathbf{h}_k)] & \mathbf{F}_k[\boldsymbol{\omega}_k, \boldsymbol{\omega}_k] \end{bmatrix} \tag{4.7.6}$$

and the elements of $\mathbf{F}_k$ can be found using the differentials

$$\frac{\partial u_k(n)}{\partial Re h_{kl}(p)} = e^{j\omega klpn} x_l(n-p) \tag{4.7.7a}$$

$$\frac{\partial u_k(n)}{\partial Im h_{kl}(p)} = j e^{j\omega klpn} x_l(n-p) \tag{4.7.7b}$$

$$\frac{\partial u_k(n)}{\partial \omega_{klp}} = j n h_{kl}(p) e^{j\omega_{klp} n} x_l(n-p) \tag{4.7.7c}$$

Introduce

$$\begin{aligned}
\mathbf{U}_k &= \mathbf{P}_k^H \mathbf{P}_k \\
\mathbf{P}_k &= [\, \mathbf{p}_{k1}(0) \quad \cdots \quad \mathbf{p}_{k1}(L-1) \quad \cdots \quad \mathbf{p}_{kn_T}(L-1)] \\
\mathbf{p}_{kl}(p) &= \mathbf{X}_{lp}\mathbf{e}_{kl}(p) \\
\mathbf{D}_n &= diag\,(0, 1, \cdots, N-1) \\
\mathbf{D}_h &= diag\,(h_k1(0), \cdots h_{k1}(L-1), \cdots, h_{kn_T}(L-1)) \\
\mathbf{T}_k &= \mathbf{P}_k^H \mathbf{D}_n \mathbf{P}_k \mathbf{D}_h \\
\mathbf{S}_k &= \mathbf{D}_h^H \mathbf{P}_k^H \mathbf{D}_n^2 \mathbf{P}_k \mathbf{D}_h \\
\mathbf{B} &= [Re(\mathbf{S}_k - \mathbf{T}_k^H \mathbf{U}_k^{-1} \mathbf{T}_k)]^{-1}
\end{aligned}$$

The individual elements corresponding to the estimation of $\boldsymbol{\eta}_k$ can be found from (4.7.4). Therefore, the initial row of the submatrices in (4.7.6) can be written as

$$\mathbf{F}_k\,[Re(\mathbf{h}_k), Re(\mathbf{h}_k)] = Re\left[\mathbf{P}_k^H \mathbf{P}_k\right] \tag{4.7.8}$$

$$\mathbf{F}_k\,[Re(\mathbf{h}_k), Im(\mathbf{h}_k)] = -Im\left[\mathbf{P}_k^H \mathbf{P}_k\right] \tag{4.7.9}$$

$$\mathbf{F}_k\,[Re(\mathbf{h}_k), \boldsymbol{\omega}_k] = -Im\left[\mathbf{P}_k^H \mathbf{D}_n \mathbf{P}_k \mathbf{D}_h\right] \tag{4.7.10}$$

The second row of matrices can be written as

$$\mathbf{F}_k\,[Im(\mathbf{h}_k), Re(\mathbf{h}_k)] = Im\left[\mathbf{P}_k^H \mathbf{P}_k\right] \tag{4.7.11}$$

$$\mathbf{F}_k\,[Im(\mathbf{h}_k), Im(\mathbf{h}_k)] = Re\left[\mathbf{P}_k^H \mathbf{P}_k\right] \tag{4.7.12}$$

$$\mathbf{F}_k\,[Im(\mathbf{h}_k), \boldsymbol{\omega}_k] = Re\left[\mathbf{P}_k^H \mathbf{D}_n \mathbf{P}_k \mathbf{D}_h\right] \tag{4.7.13}$$

Similarly, the third row of matrices can be written as

$$\mathbf{F}_k\,[\boldsymbol{\omega}_k, Re(\mathbf{h}_k)] = -Im\left[\mathbf{P}_k^H \mathbf{D}_n \mathbf{P}_k \mathbf{D}_h\right]^H \tag{4.7.14}$$

$$\mathbf{F}_k\,[\boldsymbol{\omega}_k, Im(\mathbf{h}_k)] = Re\left[\mathbf{P}_k^H \mathbf{D}_n \mathbf{P}_k \mathbf{D}_h\right]^H \tag{4.7.15}$$

$$\mathbf{F}_k\left[\omega_k, \omega_k\right] = Re[\mathbf{D}_h^H \mathbf{P}_k^H \mathbf{D}_n^2 \mathbf{P}_k \mathbf{D}_h] \tag{4.7.16}$$

In compact form (4.7.6) can be written as

$$\mathbf{F}_k = \frac{2}{{\sigma_v}^2}\begin{bmatrix} Re(\mathbf{U}_k) & -Im(\mathbf{U}_k) & -Im(\mathbf{T}_k) \\ Im(\mathbf{U}_k) & Re(\mathbf{U}_k) & Re(\mathbf{T}_k) \\ -Im(\mathbf{T}_k)^T & Re(\mathbf{T}_k)^T & Re(\mathbf{S}_k) \end{bmatrix} \tag{4.7.17}$$

Note that there is a coupling in the estimation error between the channel parameters and the FOs. The CRLB is obtained as the inverse of the FIM, i.e.,

$$\mathbf{CRLB}(\boldsymbol{\eta}_k) = \mathbf{F}_k^{-1}. \tag{4.7.18}$$

The inverse of $\mathbf{F}_k$ can be calculated by using the matrix inversion lemma, i.e,

$$\begin{aligned} \mathbf{CRLB}(\boldsymbol{\eta}_k) = \frac{{\sigma_v}^2}{2}&\begin{bmatrix} Re(\mathbf{U}_k^{-1}) & -Im(\mathbf{U}_k^{-1}) & \mathbf{0} \\ Im(\mathbf{U}_k^{-1}) & Re(\mathbf{U}_k^{-1}) & \mathbf{0} \\ \mathbf{0} & \mathbf{0} & \mathbf{0} \end{bmatrix} \\ &+ \begin{bmatrix} Im(\mathbf{U}_k^{-1}\mathbf{T}_k) \\ -Re(\mathbf{U}_k^{-1}\mathbf{T}_k) \\ \mathbf{I} \end{bmatrix} \left[Re(\mathbf{S}_k - \mathbf{T}_k^H \mathbf{U}_k^{-1}\mathbf{T}_k)\right]^{-1} \\ &\times \begin{bmatrix} Im(\mathbf{U}_k^{-1}\mathbf{T}_k)^T & -Re(\mathbf{U}_k^{-1}\mathbf{T}_k)^T & \mathbf{I} \end{bmatrix} \end{aligned} \tag{4.7.19}$$

From (4.7.19), the CRLB associated with the FOs becomes

$$\mathbf{CRLB}(\boldsymbol{\omega}_k) = \left[Re(\mathbf{S}_k - \mathbf{T}_k^H \mathbf{U}_k^{-1}\mathbf{T}_k)\right]^{-1}, \tag{4.7.20}$$

and the CRLB for the real and the imaginary parts of the MGs are given as

$$\mathbf{CRLB}[Re(\mathbf{h}_k)] = \left[Re(\mathbf{U}_k^{-1}) + Im(\mathbf{U}_k^{-1}\mathbf{T}_k)\mathbf{B}Im(\mathbf{U}_k^{-1}\mathbf{T}_k)^T\right] \tag{4.7.21}$$

$$\mathbf{CRLB}[Im(\mathbf{h}_k)] = \left[Re(\mathbf{U}_k^{-1}) + Re(\mathbf{U}_k^{-1}\mathbf{T}_k)\mathbf{B}Re(\mathbf{U}_k^{-1}\mathbf{T}_k)^T\right] \tag{4.7.22}$$

Appendix 4B: Derivation of the MMSE Equalizer

Figure 4.3 allows the output of the equalizer, to decode the transmitted signal from antenna l, to be written as

$$\begin{aligned} y_l(n) &= \mathbf{w}^H \mathbf{r}_m \\ &= \mathbf{w}^H \mathbf{H}_c \mathbf{x}_m + \mathbf{w}^H \mathbf{v}_m \end{aligned} \tag{4.7.23}$$

Suppose the equalizer is designed to retrieve the transmitted signal, $x(n)$, with delay d. Then, the mean square error can be written as

$$\begin{aligned} J(\mathbf{w}) &= E\{|y_l(n) - x_l(n-d)|^2\} \\ &= E\{|\mathbf{w}^H \mathbf{r}_m - x_l(n-d)|^2\} \\ &= E\{\mathbf{w}^H \mathbf{r}_m \mathbf{r}_m^H \mathbf{w} - \mathbf{w}^H \mathbf{H}_c \mathbf{x}_m x_l^*(n-d) - x_l(n-d)\mathbf{x}_m^H \mathbf{H}_c^H \mathbf{w} + \sigma_x^2\} \\ &= \mathbf{w}^H \left(\mathbf{H}_c \mathbf{H}_c{}^H \sigma_x^2 + \sigma_v^2 \mathbf{I}\right) \mathbf{w} - E\{\mathbf{w}^H \mathbf{H}_c \mathbf{x}_m x_l^*(n-d) + x_l(n-d)\mathbf{x}_m^H \mathbf{H}_c^H \mathbf{w} - \sigma_x^2\} \end{aligned} \tag{4.7.24}$$

Differentiation with respect to $\mathbf{w}$ yields the MMSE equalizer

$$\mathbf{w} = \left(\mathbf{H}_c \mathbf{H}_c^H + \frac{\sigma_v{}^2}{\sigma_x^2}\mathbf{I}\right)^{-1} \mathbf{H}_c E\left\{ \begin{bmatrix} x_1(n) \\ x_2(n) \\ \vdots \\ x_{n_T}(n) \\ \vdots \\ x_1(n-M-L+2) \\ x_2(n-M-L+2) \\ \vdots \\ x_{n_T}(n-M-L+2) \end{bmatrix} x_l^*(n-d) \right\} \tag{4.7.25}$$

Chapter 5

ITERATIVE EQUALIZATION FOR OFDM SCHEMES

Broadband wireless access technologies can offer bit rates of tens of mega bits per second to residential and business subscribers and are attractive and economical alternatives to broadband wired access technologies [75]. In such environments multipath interference can be severe, which raises the question of what types of anti-multipath measures are necessary. OFDM has been proposed as an effective anti-multipath technique because it offers good performance at low signal processing complexity [76]. Originally, OFDM was anticipated for time invariant channels, such as fixed wire-line telephone systems, where the multipath interference is severe [34]. However, the wireless mobile channels are generally time variant and one of the principal disadvantages of OFDM is its vulnerability to time variant channels. Time selectivity of the channel introduces frequency dispersion, i.e. loss of orthogonality between the sub-carriers. In most of the previous literature on OFDM, the time selectivity of the channels is ignored and time selectivity due only to DS is accounted for that can easily be cancelled before equalization [77–82]. Modern wireless communication systems are expected to operate at high carrier frequencies to provide high data rate services to mobile users. Wireless systems that operate at very high frequencies employ smaller wavelengths, implying that their sensitivity to physical movements grows proportionally [26], and thereby may give rise to a non-sinusoidal time-varying frequency selective channel.

Another reason for time selectivity of the channels is due to the desire to increase the capacity of an OFDM system. In OFDM based systems, data are transmitted in frames, each frame consists of a number of data bits and some extra guard bits are embedded in each frame. These extra bits do not carry any useful information. To increase capacity long length frames are preferred to reduce the loss due to redundant bits in each frame. Channel variation is more likely during such large length frames. Therefore, the primary advantage of OFDM, i.e. interference free operation, can not carry over to important future systems. Consequently, future mobile systems have to deal with time-varying channels. Mitigation of the time selectivity of the channel using an MMSE equalizer is discussed in [24,83], the drawback of these algorithms is their complexity of $\mathcal{O}(N^2)$, which makes them impractical for large N. In [19], Philip Schniter, pre-processed the received signal by multiplying with window coefficients that render the Inter-Carrier-Interference (ICI) response sparse, and thereby squeezes the significant coefficients into the $2D+1$ central diagonals of an ICI matrix. In this work, it is found that $D = f_d N + 1$, where f_d is the normalized Doppler shift in the carrier frequency and N is the number of carriers used to transmit an OFDM symbol. The complexity of this algorithm is $\mathcal{O}(D^2 N)$ and as such increases considerably with the DS.

In previous chapters, equalization of Linear Time Variant (LTV) channels was considered, where the time-variations in MGs of the channel were sinusoidal. In contrast to previous chapters, this chapter considers a Rayleigh fading channel based on Jakes' model [26], where the time selectivity in the channel is non-sinusoidal, however, a modified WSSUS channel model is proposed in [84]. To deal with such time selectivity of the channel, a new approach is proposed, which exploits the sparsity of the CCM. Examining the time domain model of the received OFDM signal reveals that the CCM is sparse and has similar structure to that after preprocessing of the received samples [19]. The number of non-zero elements in a row of the CCM depends on the length of channel taps L, which for a wireless channel may typically varies from 4 to

6 [85]. This characteristic of the CCM can help to design a low complexity OFDM equalizer for time-varying frequency selective channels. In a higher scattering environment, channel shortening algorithms for a doubly selective channel can be used to shorten the channel length, investigation of them will be the part of my future work.

5.1 A Brief Overview of an OFDM System

OFDM is very similar to the well known and used technique of frequency division multiplexing (FDM), it uses the same principle of FDM to allow multiple messages to be sent over a single radio channel. It is different from FDM in several ways. In conventional FDM broadcasting, each radio station transmits on a different frequency and the separation between any two frequencies is kept high so that the carriers do not interfere with each other. However, there is no coordination or synchronization between the stations. On the other hand in OFDM, the data from each source are simultaneously transmitted on different densely packed orthogonal subcarriers that constitute an OFDM signal. All the subcarriers within the OFDM signal are time and frequency synchronized to each other to ensure the interference between the subcarriers is ideally equal to zero. These subcarriers overlap in the frequency domain but do not cause ICI due to the orthogonal nature of the subcarriers.

Figure 5.1 shows the construction of an OFDM signal with eight subcarriers, the binary signals from each information source modulate the amplitude of a different subcarrier, and then all subcarriers are combined together to form an OFDM signal. The baseband frequency of each subcarrier is chosen to be an integral multiple of the inverse of the OFDM signal time so that the subcarriers have an integral number of cycles per symbol. The subcarriers are thereby orthogonal to each other. Note that the phase of all these subcarriers is assumed zero.

In OFDM the overall system bandwidth is broken up into N orthogonal sub-carriers, the data are transmitted on these sub-carriers resulting in a symbol rate that is N times lower than that of a single carrier system. For a fixed channel, orthogonal

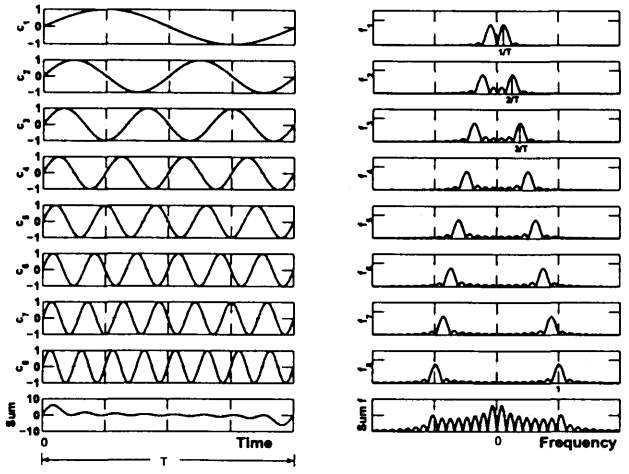

Figure 5.1. Time and frequency response of an 8 carrier OFDM system. Subplots c_1 to c_8 show the subcarriers, f_1 to f_8 show the corresponding magnitudes of the frequency spectrum occupied by each station and the bottom two show the sum of time waveforms and frequency spectrum.

spacing among the carriers prevents the demodulator from seeing frequencies other than their own. OFDM systems transmit low-rate signals simultaneously over a single transmission path. Low symbol rate makes OFDM resistant to the effects of ISI caused by multipath propagation. The effects of ISI on an OFDM signal can be further improved by the addition of a guard period to the start of each symbol in the time domain that yields more robustness to multipath spread. The guard period is generally a cyclic copy of the last bits of the actual data being transmitted. The length of the cyclic prefix is kept at least equal to $L - 1$; under this condition, a linear convolution of the transmitted sequence and the channel is converted to a circular convolution. By doing this the effects of ISI are easily and completely removed provided the length condition is not violated. Moreover, the approach enables the receiver to use the FFT for OFDM implementation [86]. The basic baseband model

of a conventional OFDM system is given in the Figure 5.2. Here, the source data

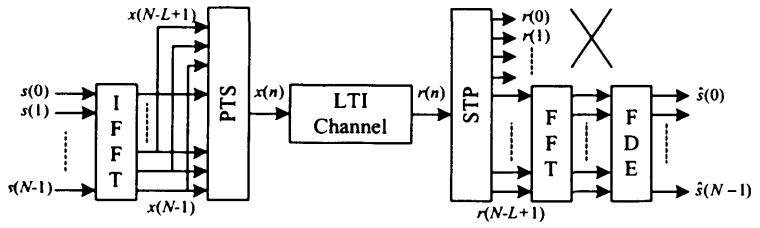

Figure 5.2. A basic baseband OFDM system, transmitting subsequent blocks of N complex data and the receiver removing the cyclic prefix and performing frequency domain equalization.

to be transmitted are converted into blocks, each of N symbols. Then, the Inverse Fast Fourier transform (IFFT) stage converts each block into the time domain block by performing an IFFT operation. Before transmission the last L symbols in the time domain block, termed a cyclic prefix (CP), are prefixed to each time domain block. After the addition of CP the new block is termed as an OFDM symbol. To transmit the symbols serially, the OFDM symbol is passed through the stage called Parallel to Serial (PTS). The transmitted symbols travelled through the channel and at the receiver passed through a stage called Serial to Parallel (STP) that constructs blocks of receive samples each after $N + L$ symbols. The first L samples in each received block contribute to the symbols in the previous OFDM symbol. Therefore, to remove Inter-Block-Interference (IBI) the first L samples from each received block are removed. In order to perform Frequency Domain Equalization (FDE), an FFT is performed on the received time domain samples to convert them into the frequency domain. The frequency domain received samples are passed through the FDE stage that performs MMSE equalization to obtain frequency domain transmitted symbols.

5.2 Problem Statement

The complex OFDM transmission and reception model used in this chapter is given in Figure 5.3. First of all a data block of N symbols is converted into the time domain by applying an IFFT operation, time interleaving is performed and a CP of length L is added at the head of the time interleaved samples. The whole block of data is termed as a random-OFDM symbol. If the $\{s(k)\}$ are the i.i.d symbols to be transmitted and

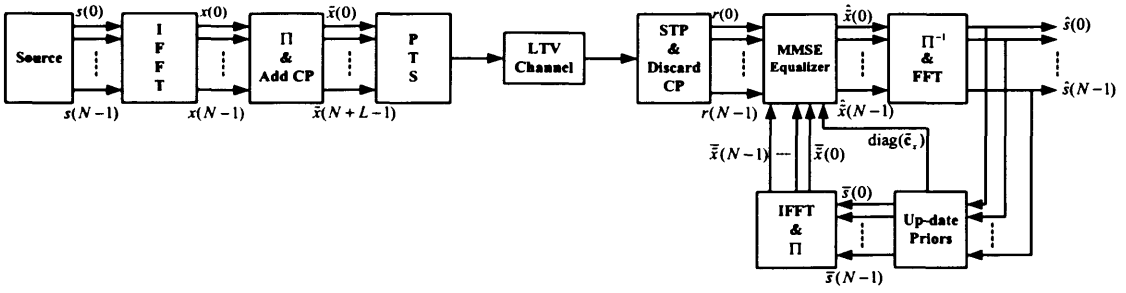

Figure 5.3. A basic baseband OFDM system, transmitting subsequent blocks of N complex data and an iterative detection of the transmitted data.

the $\{x(n)\}$ are the time samples after IFFT operation then the relationship between them can be described by the following N-point DFT operation,

$$x(n) = \frac{1}{\sqrt{N}} \sum_{k=0}^{N-1} s(k) e^{j\frac{2\pi}{N}kn} \tag{5.2.1}$$

where the term $\frac{1}{\sqrt{N}}$ is used to normalize the FFT and IFFT operations. The N samples of the sequence $\{x(n)\}$ in vector form can be written as $\mathbf{x} = \mathbf{F}^H\mathbf{s}$, where $\mathbf{F}$ is the DFT matrix of order N and $\mathbf{s}$ is the frequency domain signal vector. If the signal has propagated through L different paths, then the received baseband signal at time n after removing the cyclic prefix can be written as

$$r(n) = \sum_{l=0}^{L-1} h(n,l)\tilde{x}(\langle n-l \rangle_N) + v(n), \tag{5.2.2}$$

where $\tilde{x}(.)$ denotes the interleaved samples, $h(n,l)$ is the unknown complex MG for the lth channel tap and $v(n)$ is the complex white Gaussian noise at sample time

n. Herein, it is assumed that $h(n,l)$ is a complex Gaussian random variable. The estimation of the parameters of time-variant and time invariant channels is discussed in [83] and [1]. Throughout this chapter, it is assumed as in [19] that perfect knowledge of the channel is available, so only frequency domain transmitted signals are estimated in this work. The received samples in vector form can be written as

$$\mathbf{r} = \mathbf{Hx} + \mathbf{v} = \mathbf{HF}^H\mathbf{s} + \mathbf{v}, \tag{5.2.3}$$

Applying the FFT to (5.2.3), the frequency domain sample vector denoted by R can be written as

$$R = \mathbf{FHF}^H\mathbf{s} + \mathbf{Fv} = \mathbf{H}_{df}\mathbf{s} + \mathbf{Fv} \tag{5.2.4}$$

where, $\mathbf{H}$ is the CCM of size $N \times N$, $\mathbf{H}_{n,l} = h(n, \langle n-l \rangle_N)$ and $\mathbf{H}_{df}$ is the ICI matrix. The MMSE equalizer for the estimation of symbols $\{\tilde{s}(k)\}$ can be found by minimizing $E\{\|\tilde{\mathbf{s}} - \mathbf{Wr}_f\|^2\}$ yielding

$$\mathbf{W} = (\mathbf{H}_{df}^H\mathbf{H}_{df} + \sigma_n^2\mathbf{I}_N)^{-1}\mathbf{H}_{df}^H \tag{5.2.5}$$

where σ_n^2 is the variance of the noise. If in (5.2.4) the channel is LTI then the ICI matrix, $\mathbf{H}_{df}$, is diagonal and to estimate the symbols $\{\tilde{s}(k)\}$, L-MMSE equalization requires the inversion of a diagonal matrix, which is computationally inexpensive.
On the other hand, if the channel is LTV then the matrix $\mathbf{H}_{df}$ is not diagonal, a consequence of which is that ICI is introduced. Hence, L-MMSE equalization requires the inversion of an $N \times N$ Hermitian matrix that needs $\mathcal{O}(N^2)$ operations, which is infeasible for large N and yields poor BER performance [83].
To improve the BER performance, the frequency domain samples can indirectly be estimated from the transmitted time domain samples. In this scheme, the channel effects can be mitigated by using a length M equalizer and M can be much higher than the length of channel. Since the CCM changes after every symbol interval, therefore new equalizer coefficient values are required for each symbol. The computational

complexity to find the length M equalizer is $\mathcal{O}(M^3)$, thereby the computational complexity to estimate N samples will be $\mathcal{O}(NM^3)$. However, as shown in Figure 5.4, if modulo-N indexing is assumed then the structure of $\mathbf{H}$ reveals that the individual symbol $\tilde{x}(n)$ contributes only to the observation samples $r(n)$ to $r(n+L-1)$. Therefore, applying modulo-N indexing in the sequel, it can be noted that these are the only required samples to estimate $\tilde{x}(n)$ and in vector form these received samples can be written as,

$$\mathbf{r}_n = \mathbf{H}_n\tilde{\mathbf{x}} + \mathbf{v}_n, \tag{5.2.6}$$

where

$$\mathbf{r}_n = \begin{bmatrix} r(n) & r(n+1) & \cdots & r(n+L-1) \end{bmatrix}^T,$$

matrix $\mathbf{H}_n$ contains L rows of the matrix $\mathbf{H}$ from n to $n+L-1$ and

$$\mathbf{v}_n = \begin{bmatrix} v(n) & v(n+1) & \cdots & v(n+L-1) \end{bmatrix}^T.$$

5.3 Equalization

Figure 5.3 illustrates the transmitter and the receiver structure used in this chapter, where the equalization has been split into two stages:-

(i) In the first stage the CP is removed and by exploiting the sparsity of the CCM, a length L, MMSE equalizer is designed and transmitted time domain samples are estimated.

(ii) In the second stage performing the FFT on the estimated time domain samples, obtained from first stage, frequency domain symbols are estimated and the corresponding a posteriori values of the means are determined. The second stage passes the a posteriori values of means to the first stage for better estimation of time domain samples. These two stages iteratively exchange their information learned from each other until the specified number of iterations has passed. The first and second stages are separated by a random interleaver and de-interleaver of length N that help to de-correlate the correlated outputs between the stages.

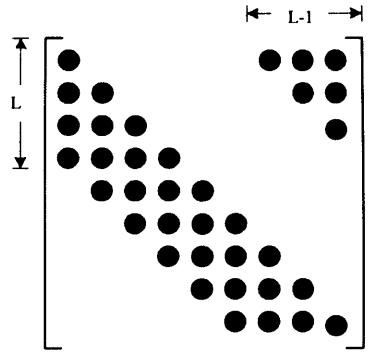

Figure 5.4. Diagonal like structure of the channel convolution matrix, $\mathbf{H}$, showing the sparsity. The dots represent the non-zero elements.

5.3.1 MMSE Equalization

In order to design a length L MMSE equalizer, it is assumed that the noise is temporally uncorrelated and circularly distributed. Therefore $E\{\mathbf{v}_n\} = \mathbf{0}$, $E\{\mathbf{v}_n\mathbf{v}_n{}^H\} = \sigma_n^2\mathbf{I}_L$ and $E\{\tilde{x}(n)\mathbf{v}_n\} = \mathbf{0}$. Moreover, define $\bar{x}(n) = E\{x(n)\}$, $\bar{\mathbf{x}} = E\{\mathbf{x}\}$, $\mathbf{c}_x = [\ c_x(0)\ \ c_x(1)\ \cdots\ c_x(N-1)\ ]$ and $c_x(n) = \mathrm{Cov}[x(n), x(n)]$. The length L MMSE equalizer, $\mathbf{w}_n$, for the estimates of $\tilde{x}(n)$ can be derived by minimizing the cost function,

$$J(\mathbf{w}_n) = E\{|(\tilde{x}(n) - \mathbf{w}_n^H\mathbf{r}_n)|^2\}. \tag{5.3.1}$$

By defining $\hat{\tilde{x}}(n)$ and $\bar{\tilde{x}}(n)$ respectively the estimated and mean values of the interleaved sample $\tilde{x}(n)$, $\bar{\tilde{\mathbf{x}}}$ the mean value of interleaved sample vector $\tilde{\mathbf{x}}$, $\tilde{\mathbf{c}}_x$ is the variance vector of $\{\tilde{x}(n)\}$ and $\mathbf{h}_n$ is the nth column of the matrix $\mathbf{H}_n$ the generalized MMSE equalizer coefficient vector can be found by minimizing (5.3.1) as (derived in Appendix 5A)

$$\mathbf{w}_n = \left(\mathbf{H}_n\mathrm{diag}(\tilde{\mathbf{c}}_x)\mathbf{H}_n^H + \sigma_n^2\mathbf{I}_L\right)^{-1}\mathbf{h}_n\tilde{c}_x(n) \tag{5.3.2}$$

and estimate (derived in Appendix 5B)

$$\hat{\tilde{x}}(n) = \bar{\tilde{x}}(n) + \mathbf{w}_n^H(\mathbf{r}_n - \mathbf{H}_n\bar{\tilde{\mathbf{x}}}). \tag{5.3.3}$$

The estimated samples $\{\hat{\tilde{x}}(n)\}$ are de-interleaved to obtain samples $\{\hat{x}(n)\}$. If the samples $\{x(n)\}$, are known the values of symbols $\{s(k)\}$ can be found as

$$s(k) = \mathbf{i}_k^H \mathbf{F}\mathbf{x} = \mathbf{i}_k^H \mathbf{F} \sum_{n=0}^{N-1} \mathbf{i}_n x(n), \tag{5.3.4}$$

where $\mathbf{i}_k$ is the kth column of an identity matrix of size $N \times N$. Therefore, the equalizer can be translated in terms of $s(k)$ as

$$\mathbf{w}_n = \left(\mathbf{H}_n \mathbf{F}^H \mathrm{diag}(\mathbf{c}_s)\mathbf{F}\mathbf{H}_n^H + \sigma_n^2 \mathbf{I}_L\right)^{-1} \mathbf{H}_n \mathbf{F}^H \mathrm{diag}(\tilde{\mathbf{c}}_s)\mathbf{F}\mathbf{i}_n \tag{5.3.5}$$

and the estimate of $s(k)$ becomes

$$\begin{aligned}
\hat{s}(k) &= \mathbf{i}_k^H \mathbf{F} \sum_{n=0}^{N-1} \mathbf{i}_n \hat{x}(n) \\
&= \mathbf{i}_k^H \mathbf{F} \sum_{n=0}^{N-1} \mathbf{i}_n \left[\bar{x}(n) + \mathbf{w}_n^H (\mathbf{r}_n - \mathbf{H}_n \bar{\mathbf{x}})\right] \\
&= \bar{s}(k) + \mathbf{i}_k^H \mathbf{F} \sum_{n=0}^{N-1} \mathbf{i}_n \mathbf{w}_n^H \left[\mathbf{H}_n \mathbf{F}^H (\mathbf{s} - \bar{\mathbf{s}}) + \mathbf{v}_n\right].
\end{aligned} \tag{5.3.6}$$

Suppose that $\mathcal{V}$ be the vector of dimension $N \times 1$ of frequency domain noise samples, then

$$\mathbf{v}_n = \begin{bmatrix} \mathbf{i}_n^H \\ \mathbf{i}_{n+1}^H \\ \vdots \\ \mathbf{i}_{n+L-1}^H \end{bmatrix} \mathbf{F}^H \mathcal{V} = \mathcal{I}_n \mathbf{F}^H \mathcal{V}.$$

By defining the matrix

$$\mathbf{Q} = \mathbf{F} \sum_{n=0}^{N-1} \mathbf{i}_n \mathbf{w}_n^H \mathbf{H}_n \mathbf{F}^H \tag{5.3.7}$$

and

$$\mathbf{P} = \mathbf{F} \sum_{n=0}^{N-1} \mathbf{i}_n \mathbf{w}_n^H \mathcal{I}_n \mathbf{F}^H \tag{5.3.8}$$

the equation (5.3.6) can be written as

$$\hat{s}(k) = \bar{s}(k) + \mathbf{i}_k^H \mathbf{Q}(\mathbf{s} - \bar{\mathbf{s}}) + \mathbf{i}_k^H \mathbf{P}\mathcal{V}. \tag{5.3.9}$$

The time domain estimated values obtained in the first stage have high probability of error. To estimate any particular transmitted symbol, the estimator cancels the interference from the other (or extrinsic) symbols. In estimation, on the basis of interference cancellation, the performance of the estimator depends on the accuracy of the mean values of the extrinsic symbols. Therefore, the mean values after estimation, i.e. posteriori means, can be found by finding the a posteriori probabilities of the time domain transmitted symbols. Since the transmitted time domain symbols do not have finite constellation points, it is difficult to find their posteriori probabilities. Therefore, time domain estimated samples are converted into the frequency domain where they have finite constellations. From these frequency domain estimated samples the a posteriori means are found, which are then converted into the time domain by an IFFT operation.

5.3.2 Iterative Algorithm

At the start, all the a priori mean values of the symbols $\{s(k)\}$ are initialized to zero so that all samples means are, $\{\bar{x}(n)\} = 0$ and $\text{diag}(\mathbf{c}_s) = \mathbf{I}_N = \text{diag}(\tilde{\mathbf{c}}_x)$. To find the a posteriori values the following important steps are highlighted:

Step 1: To estimate $\tilde{x}(n)$, only extrinsic information is used. Therefore, $\bar{\tilde{x}}(n) = 0$ and $\tilde{c}_x(n) = 1$ and the estimates $\{\hat{\tilde{x}}(n)\}$ are found using (5.3.2) and (5.3.3), then the estimates are de-interleaved to obtain $\{\hat{x}(n)\}$.

Step 2: In the second stage, to obtain the frequency domain estimates, $\{\hat{s}(n)\}$, the FFT is performed on samples $\{\hat{x}(n)\}$.

Step 3: Since the constellation of frequency domain symbols have finite alphabets, in

order to determine the a posteriori values of $\{\bar{s}(k)\}$ and $\{c_s(k)\}$, it is more convenient to work with Log-Likelihood-Ratios (LLR)s. The a priori and a posteriori LLRs of $s(k)$ are defined as [87]

$$L[s(k)] = \ln \frac{Pr\{s(k)=1\}}{Pr\{s(k)=-1\}} \tag{5.3.10}$$

and

$$L[s(k)|_{\hat{s}(k)}] = \ln \frac{Pr\{s(k)=1|_{\hat{s}(k)}\}}{Pr\{s(k)=-1|_{\hat{s}(k)}\}}. \tag{5.3.11}$$

The difference between the a posteriori and a priori LLRs, also called the extrinsic information, of $s(k)$ is

$$\begin{aligned} \triangle L[s(k)] &= L[s(k)|_{\hat{s}(k)}] - L[s(k)] \\ &= \ln \frac{p\{s(k)=1|_{\hat{s}(k)}\}}{p\{s(k)=-1|_{\hat{s}(k)}\}} - \ln \frac{p\{s(k)=1\}}{p\{s(k)=-1\}}. \end{aligned} \tag{5.3.12}$$

Using Bayes' theorem, $p(a|b) = \frac{p(b|a)p(a)}{p(b)}$, (5.3.12) can be written as

$$\begin{aligned} \triangle L[s(k)] &= \ln \frac{p\{\hat{s}(k)|_{s(k)=1}\}p\{s(k)=1\}}{p\{\hat{s}(k)|_{s(k)=-1}\}p\{s(k)=-1\}} - \ln \frac{p\{s(k)=1\}}{p\{s(k)=-1\}} \\ &= \ln \frac{p\{\hat{s}(k)|_{s(k)=1}\}}{p\{\hat{s}(k)|_{s(k)=-1}\}} = L[\hat{s}(k)|_{s(k)}], \end{aligned} \tag{5.3.13}$$

therefore

$$L[s(k)|_{\hat{s}(k)}] = L[s(k)] + L[\hat{s}(k)|_{s(k)}]. \tag{5.3.14}$$

To find $L[\hat{s}(k)|_{s(k)}]$, it is assumed that the probability density function (PDF) of $\hat{s}(k)$ is Gaussian with variance σ_s^2 and can be written as

$$p\{\hat{s}(k)\} = \frac{1}{\sqrt{2\pi\sigma_s^2}} \exp\left(-\frac{(\hat{s}(k)-E\{\hat{s}(k)\})(\hat{s}(k)-E\{\hat{s}(k)\})^H}{2\sigma_s^2}\right). \tag{5.3.15}$$

Therefore, the conditional PDF of $\hat{s}(k)$ becomes

$$p\{\hat{s}(k)|_{s(k)=b}\} = \frac{1}{\sqrt{2\pi\sigma_s^2|_{s(k)=b}}} \exp\left(-\frac{(\hat{s}(k)-m_k(b))(\hat{s}(k)-m_k(b))^H}{2\sigma_s^2|_{s(k)=b}}\right), \tag{5.3.16}$$

where $m_k(b) = E\{\hat{s}(k)|_{s(k)=b}\}$ and $\sigma_s^2|_{s(k)=b} = \text{Cov}[\hat{s}(k), \hat{s}(k)|_{s(k)=b}]$ are respectively the conditional mean and variance of $\hat{s}(k)$. Here, a binary phase shift keying (BPSK) system is considered for which $b = \{+1, -1\}$, for higher constellation systems, such as Quadrature Phase Shift Keying and 8PSK, the derivations are similar. Note $E\{\mathbf{s}|_{s(k)=b}\} = E\{\mathbf{s} + \mathbf{i}_k(b - s(k))\} = \bar{\mathbf{s}} + \mathbf{i}_k(b - \bar{s}(k))$. Therefore from (5.3.9)

$$\begin{aligned} m_k(b) &= E\{\mathbf{i}_k^H \mathbf{Q}(\mathbf{s} - \mathbf{i}_k(s(k) - b) - \bar{\mathbf{s}})\} \\ &= \mathbf{Q}_{k,k} b + \bar{s}(k)(1 - \mathbf{Q}_{k,k}). \end{aligned} \tag{5.3.17}$$

To estimate $\hat{s}(k)$, only the extrinsic information is used, therefore, setting $L[s(k)] = 0$, yields $\bar{s}(k) = 0$ and $c_s(k) = 1$. In (5.3.17), it can be noted that $m_k(b)$ depends on the particular value of b. Similarly, it can be shown that the conditional variance of $\hat{s}(k)$ becomes,

$$\begin{aligned} \sigma_s^2|_{s(k)=b} &= E\{(\hat{s}(k) - m_k(b))(\hat{s}(k) - m_k(b))^H\} \\ &= E\{(\hat{s}(k) - \mathbf{Q}_{k,k} b)(\hat{s}(k) - \mathbf{Q}_{k,k} b)^H\} \\ &= E\{\hat{s}(k)\hat{s}(k)^H|_{s(k)=b}\} - |\mathbf{Q}_{k,k}|^2 \\ &= \mathbf{i}_k^H \mathbf{Q}\ \text{diag}(\mathbf{c}_s)\mathbf{Q}^H \mathbf{i}_k + \sigma_n^2 |\mathbf{P}_{k,k}|^2 - |\mathbf{Q}_{k,k}|^2. \end{aligned} \tag{5.3.18}$$

Unlike the mean, variance of the estimator is independent of b, therefore when writing variance in the sequel the conditional value is omitted. Now everything is available for $L[\hat{s}(k)|_{s(k)}]$, therefore

$$\begin{aligned} L[\hat{s}(k)|_{s(k)}] &= -\frac{(\hat{s}(k) - m_k(+1))^2}{\sigma_s^2} + \frac{(\hat{s}(k) - m_k(-1))^2}{\sigma_s^2} \\ &= 4\frac{Re\{\hat{s}(k)\mathbf{Q}_{k,k}^*\}}{\sigma_s^2} \end{aligned} \tag{5.3.19}$$

Step 4: Once the LLRs are obtained, the a posteriori values for $\bar{s}(k)$ and $c_s(k)$ are obtained as [87]

$$\begin{aligned} \bar{s}(k)|_{\hat{s}(k)} &= Pr\{s(k) = +1|_{\hat{s}(k)}\} - Pr\{s(k) = -1|_{\hat{s}(k)}\} \\ &= \tanh\left(\frac{L[s(k)|_{\hat{s}(k)}]}{2}\right) \end{aligned} \tag{5.3.20}$$

$$c_s(k)|_{\hat{s}(k)} = 1 - \bar{s}(k)|_{\hat{s}(k)}^2. \tag{5.3.21}$$

Step 5: The terms obtained from (5.3.20) and (5.3.21) are transformed into the time domain to determine the a posteriori values of $\{\bar{x}(n)\}$ and $\{c_x(n)\}$. Hence, the resulting values are interleaved to use in (5.3.2) and (5.3.3) in the following iteration.

Step 6: Proceed to step 1 for the next iteration until the desired BER is obtained or the specified number of iterations has elapsed. Table 5.1 shows the overall iterative algorithm used for the simulations.

5.4 Complexity of the Algorithm

Although the size of matrix $\mathbf{H}_n$ is $L \times N$, it contains only $2L-1$ non-zero columns. In each iteration to find the equalizer coefficient values, $\mathbf{w}_n$, the algorithm requires the computation of $(\mathbf{H}_n \text{diag}(\tilde{\mathbf{c}}_x)\mathbf{H}_n^H + \sigma_n^2\mathbf{I}_L)^{-1}\mathbf{h}_n$. The computation of $\text{diag}(\tilde{\mathbf{c}}_x) = \mathbf{F}^H\text{diag}(\tilde{\mathbf{c}}_s)\mathbf{F}$ requires $N\log N$ operations and must be performed once per iteration, given $\text{diag}(\tilde{\mathbf{c}}_x)$ the computation of $\mathbf{H}_n\text{diag}(\tilde{\mathbf{c}}_x)\mathbf{H}_n^H$ requires $\mathcal{O}(L^2)$ operations and must be performed N times per iteration. The size of the matrix $(\mathbf{H}_n\text{diag}(\tilde{\mathbf{c}}_x)\mathbf{H}_n^H + \sigma_n^2\mathbf{I}_L)^{-1}$ is $L \times L$ and it is Hermitian, therefore it will require $\mathcal{O}(L^2)$ operations to be performed N times per iteration. In order to estimate $\hat{\tilde{x}}(n)$, the computation of $\mathbf{H}_n\bar{\tilde{x}}$ requires $\mathcal{O}(L^2)$ operations and must be performed N times per iteration. To find the a posteriori values of $\text{Cov}[\hat{s}(k), \hat{s}(k)]$ the values of $\mathbf{i}_k^H\mathbf{Q}\ \text{diag}(\mathbf{c}_s)\mathbf{Q}^H\mathbf{i}_k$, $\mathbf{Q}_{k,k}$ and $\mathbf{P}_{k,k}; k = 0, 1, ..., N-1$ are required and can be computed explicitly from the expressions for $\mathbf{Q}$ and $\mathbf{P}$ in the computations of $\mathcal{O}(LN)$ or $\mathcal{O}(N\log N)$ [88]. Hence, to estimate N symbols, only $[\mathcal{O}(N\log N) + \mathcal{O}(NL^2)]$ operations are required.

Table 5.1. MMSE-Iterative algorithm for OFDM

$L = zeros(N, 1)$

$\bar{\tilde{\mathbf{x}}} = zeros(N, 1)$

$\text{diag}(\tilde{\mathbf{c}}_x) = \mathbf{I}_N$

while $iter \leq max - iter$

$\mathbf{Q} = zeros(N, N)$

$\mathbf{P} = zeros(N, N)$

$\text{diag}(\tilde{\mathbf{c}}_x) = \mathbf{F}^H \text{diag}(\tilde{\mathbf{c}}_s)\mathbf{F}$

for $n = 1 : N$

$\mathbf{C} = \text{diag}(\tilde{\mathbf{c}}_x)$; $\bar{\tilde{x}}(n) = 0$; $\mathbf{C}(n, n) = 1$

$\mathbf{w}_n = (\mathbf{H}_n \mathbf{C} \mathbf{H}_n^H + \sigma^2 \mathbf{I})^{-1} \mathbf{H}_n \mathbf{i}_n$

$\hat{\tilde{x}}(n) = \bar{\tilde{x}}(n) + \mathbf{w}^H (\mathbf{r}_n - \mathbf{H}_n \bar{\tilde{\mathbf{x}}})$

$\mathbf{Q} = \mathbf{Q} + \mathbf{i}_n \mathbf{w}_n^H \mathbf{H}_n$

$\mathbf{P} = \mathbf{P} + \mathbf{i}_n \mathbf{w}_n^H \mathcal{I}_n$

end

$\mathbf{Q} = \mathbf{F}\mathbf{Q}\mathbf{F}^H$

$\mathbf{P} = \mathbf{F}\mathbf{P}\mathbf{F}^H$

$\hat{\mathbf{x}} = \prod^{-1}(\hat{\tilde{\mathbf{x}}})$; $\hat{\mathbf{s}} = \mathbf{F}^{\mathbf{H}} \hat{\mathbf{x}}$

for $k = 1 : N$

$\sigma_s^2(k) = \mathbf{i}_k^H \mathbf{Q}\ \text{diag}(\mathbf{c}_s) \mathbf{Q}^H \mathbf{i}_k + \sigma_n^2 |\mathbf{P}_{k,k}|^2 - |\mathbf{Q}_{k,k}|^2$

$\triangle L(k) = \frac{4Re(\hat{s}(k)\mathbf{Q}_{k,k}^*)}{\sigma_s^2(k)}$

$L(k) = L(k) + \triangle L(k)$

$\bar{s}(k) = \tanh(L(k)/2)$

$c_s(k) = 1 - \bar{s}(k)^2$

end

$\bar{\mathbf{x}} = \mathbf{F}^H \bar{\mathbf{s}}$; $\bar{\tilde{\mathbf{x}}} = \prod(\bar{\mathbf{x}})$

end

5.5 Simulation

In this section, the performance of the proposed MMSE-iterative algorithm is compared with the L-MMSE equalizer and Match Filter Bound (MFB). For all simulations, the length of the CP is kept equal to the order of the channel and number of carriers is equal to the number of symbols in an OFDM block. A 4-tap wireless fading channel model is used in which each channel tap is represented by a complex Gaussian random variable. The real and imaginary parts of each channel tap are independently generated with the Doppler spectrum based on Jakes' model. At all DSs, it is assumed that the channel is known. At low DSs the channel variations are very small while an increase in DS increases the time variations in the channel. Here, it is assumed that $\sum_{l=0}^{L-1} \sigma_l^2 = 1$, where σ_l^2 is the variance of the lth path. The transmitted frequency domain symbols $\{s(k)\}$ are BPSK. The MFB is obtained by assuming all the transmitted frequency domain symbols $\{s(l)|_{l \neq k}\}$ are known. For the MFB the interference due to other symbols is cancelled completely and hence provides the best achievable performance.

In Figures 5.5 and 5.6 the convergence of the iterative algorithm for the block length of 32 is shown. It can be noticed that the algorithm takes five iterations to converge and there is no significant improvement in the BER performance after 5 iterations. Moreover, an increase in the DS increases the time selectivity of the channel, which effects the time diversity gain. For example, for the same block length of 32, in the figures it can be noted that an increase in DS from 0.01 to 0.05 yields an improvement of 2dB in SNR. The comparison of the BER and Symbol Error Rate (SER) performances of the proposed algorithm with the L-MMSE and MFB is depicted in Figures 5.7 and 5.8. Here, it can be seen that the proposed algorithm outperforms the L-MMSE equalizer and the performance difference as compared to the MFB is less than 1dB. Moreover, as the DS increases the performance difference between the proposed algorithm and the MFB also increases slightly. The performance of the proposed algorithm when the interleaver is not exploited is also shown. The algorithm without

the interleaver outperforms the L-MMSE equalizer, but it is poor when compared to the MFB.

For the OFDM block length of 64, Figures 5.9 and 5.10 compare the BER and SER performances of the iterative algorithm with the L-MMSE and MFB. As compared to the block length of 32, more extrinsic information is available in the block length of 64 to estimate any arbitrary transmitted symbol. Therefore, in the figures approximately 2dB improvement in the SNR can be noticed.

To find the posteriori mean and variance of the frequency domain symbols, the posteriori variance of the estimator, $\text{cov}(\hat{s}(k), \hat{s}(k))$, is required. By sacrificing some performance gain, the computations of calculating the variance of estimator can be saved. Therefore, if the variance of the estimator is supposed equal to one, it will decrease the overall computational complexity. Figures 5.9 and 5.10 also show the simulation results when $\text{Cov}(\hat{s}(k), \hat{s}(k))|_{\hat{s}(k)} = 1$ for all k. The performance gap is less than 1dB.

Finally, Figure 5.11 shows the improvement in the BER performance, for a fixed value of SNR, as the DS or the number of carriers in an OFDM block is increased.

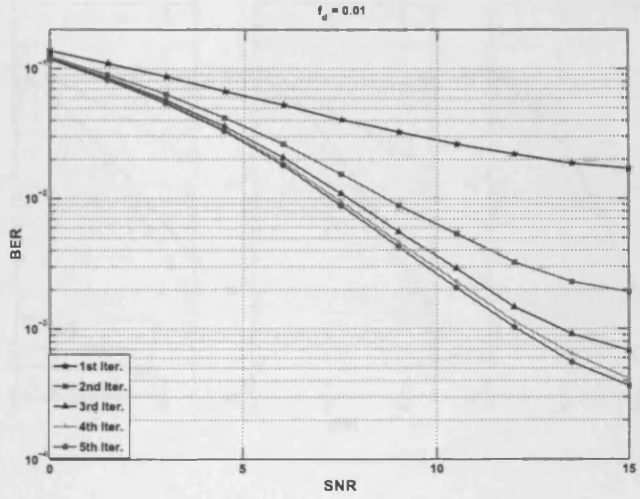

Figure 5.5. Bit-error-rate performance of the MMSE-iterative algorithm after different numbers of iterations at DS of 0.01.

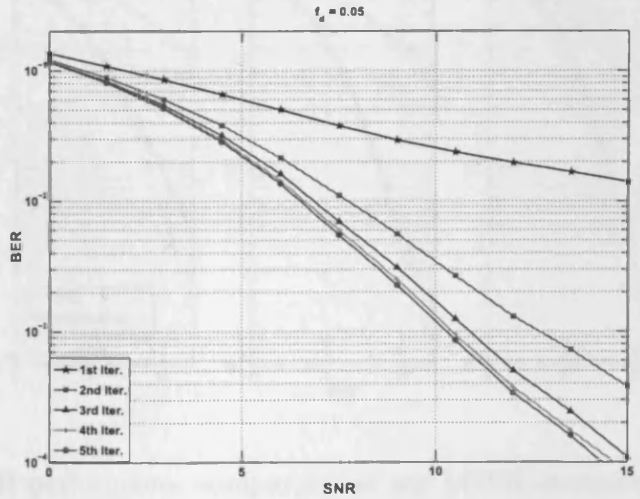

Figure 5.6. Bit-error-rate performance of the MMSE-iterative algorithm after different numbers of iterations at DS of 0.05.

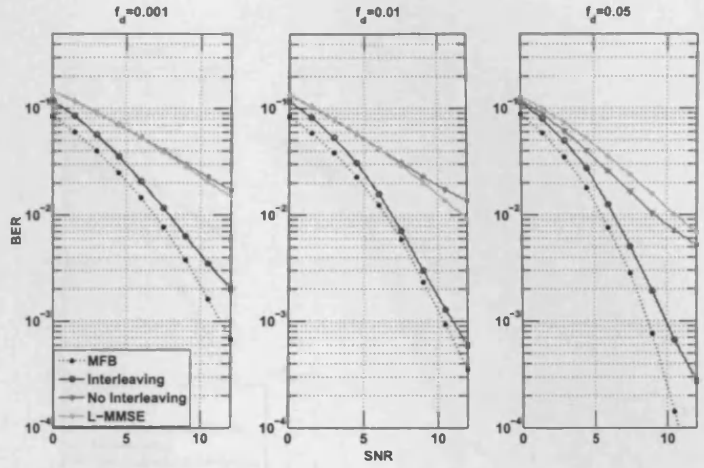

Figure 5.7. BER performance comparison of the MMSE-iterative algorithm, after five iterations and at different DSs, with the L-MMSE equalizer and MFB.

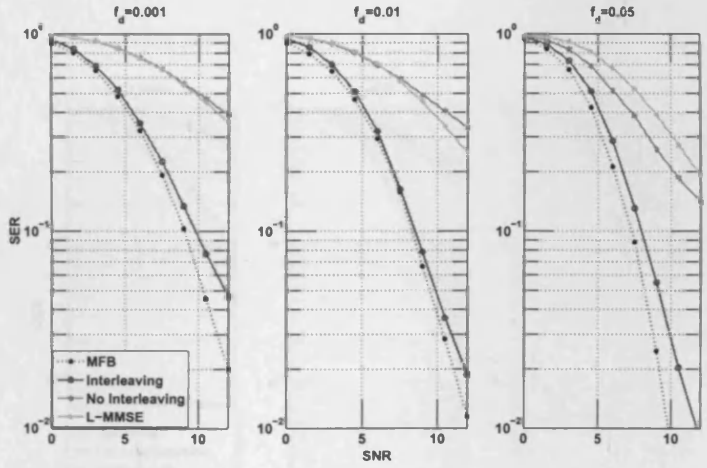

Figure 5.8. SER performance comparison of the MMSE-iterative algorithm, after five iterations and at different DSs, with the L-MMSE equalizer and MFB.

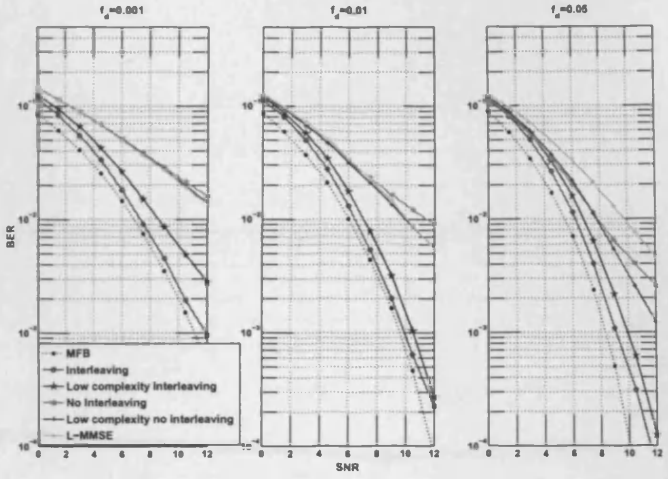

Figure 5.9. BER performance comparison of the MMSE-iterative algorithm, after five iterations and at different DSs, with the L-MMSE equalizer and MFB.

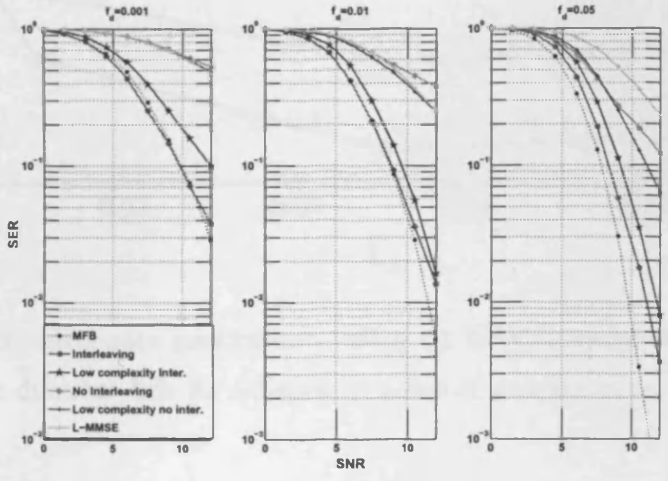

Figure 5.10. SER performance comparison of the MMSE-iterative algorithm, after five iterations and at different DSs, with the L-MMSE equalizer and MFB.

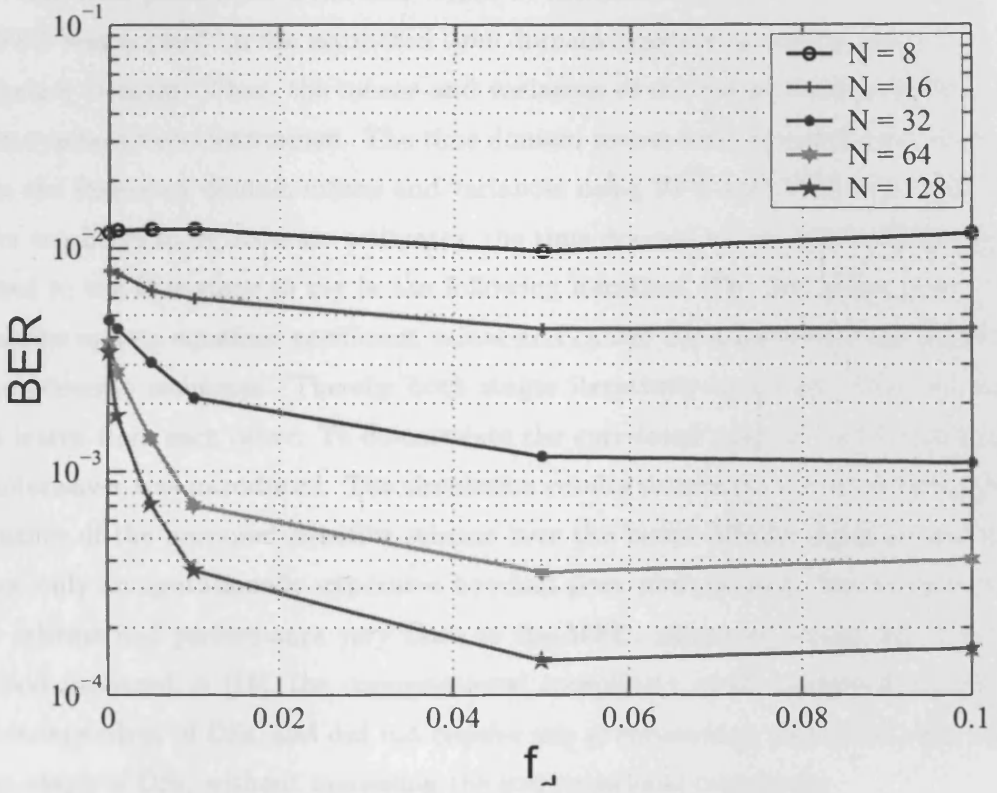

Figure 5.11. Bit-error-rate performance using an MMSE-iterative algorithm after five iterations at different DSs for different number of carriers in an OFDM block.

5.6 Summary

In this chapter, the design of a low complexity OFDM iterative receiver, for a doubly selective channel, was studied. The equalization was divided into two stages; the first stage estimated the transmitted time domain symbols, with a length L MMSE equalizer, and then passed the estimated values to the second stage. In the second stage, an FFT was applied on the estimated time domain symbols to convert them into the frequency domain. Then, the means and variances of the transmitted frequency domain symbols were determined. The time domain means and variances were obtained from the frequency domain means and variances using FFT and IFFT operations. In order to obtain more accurate estimates, the time domain means and variances were passed to the first stage to use in the following iteration. The first stage used these values to update equalizer coefficient values and cancel the interference and provided more accurate estimates. Thereby both stages iteratively exchanged their information learnt from each other. To de-correlate the correlated outputs from both stages an interleaver was introduced. The simulation results demonstrated the superior performance of the proposed iterative scheme over the linear MMSE equalization, that is not only computationally expensive but had poor performance. Importantly, the new scheme had performance very close to the MFB. Moreover, unlike the iterative method proposed in [19], the computational complexity of the proposed algorithm was independent of DSs, and did not require any preprocessing and could work for a large range of DSs, without increasing the computational complexity.

5.7 Appendices 5

Appendix 5A: Derivation of General MMSE Equalizer

From (5.2.6) it can be written as

$$\mathbf{r}_n = \mathbf{H}_n\mathbf{x} + \mathbf{v}_n,$$

to estimate time domain samples $\{x(n)\}$, the MMSE equalizer can be found by minimizing the cost function

$$\begin{aligned} J(\mathbf{w}_n) &= E\{|x(n) - \mathbf{w}_n^H\mathbf{r}_n|^2\} \\ &= E\{x(n)x^*(n) - x(n)\mathbf{r}_n^H\mathbf{w}_n - \mathbf{w}_n^H\mathbf{r}_n x^*(n) + \mathbf{w}_n^H\mathbf{r}_n\mathbf{r}_n^H\mathbf{w}_n\}. \end{aligned} \quad (5.7.1)$$

To minimize the cost function, $J(\mathbf{w}_n)$, differentiate with respect to $\mathbf{w}_n$ and equate to zero to yield

$$E\{\mathbf{r}_n x^*(n)\} = E\{\mathbf{r}_n\mathbf{r}_n^H\}\mathbf{w}_n \quad (5.7.2)$$

$$E\{(\mathbf{H}_n\mathbf{x} + \mathbf{v}_n)x^*(n)\} = E\{(\mathbf{H}_n\mathbf{x} + \mathbf{v}_n)(\mathbf{H}_n\mathbf{x} + \mathbf{v}_n)^H\}\mathbf{w}_n \quad (5.7.3)$$

$$\mathbf{H}_n E\{\mathbf{x}x^*(n)\} = \left(E\{\mathbf{H}_n\mathbf{x}\mathbf{x}^H\mathbf{H}_n^H + \mathbf{v}_n\mathbf{v}_n^H\}\right)\mathbf{w}_n \quad (5.7.4)$$

$$\mathbf{H}_n \mathrm{Cov}[x(n), x(n)]\mathbf{i}_n = \left(\mathbf{H}_n E\{\mathbf{x}\mathbf{x}^H\}\mathbf{H}_n^H + E\{\mathbf{v}_n\mathbf{v}_n^H\}\right)\mathbf{w}_n \quad (5.7.5)$$

$$\mathbf{h}_n c_x(n) = [\mathbf{H}_n \mathrm{Cov}(\mathbf{x}, \mathbf{x})\mathbf{H}_n^H + \sigma_v^2\mathbf{I}_L]\mathbf{w}_n \quad (5.7.6)$$

and therefore the equalizer coefficient vector can be determined as

$$\mathbf{w}_n = (\mathbf{H}_n \mathrm{diag}(\mathbf{c}_x)\mathbf{H}_n^H + \sigma_v^2\mathbf{I}_L)^{-1}\mathbf{h}_n c_x(n)$$

Appendix 5B: Derivation of General Estimator

The samples $\{x(n)\}$ can be estimated by

$$\hat{x}(n) = \mathbf{w}_n^H \mathbf{r}_n \tag{5.7.7}$$

and the expected value of the estimator can be written as

$$E\{\hat{x}(n)\} = \mathbf{w}_n^H \mathbf{H}_n \bar{\mathbf{x}} \tag{5.7.8}$$

If the estimator is unbiased then $E\{\hat{x}(n)\} = x(n)$, therefore, subtracting (5.7.8) from (5.7.7) yields

$$\hat{x}(n) = \bar{x}(n) - \mathbf{w}_n^H (\mathbf{r}_n - \mathbf{H}_n \bar{\mathbf{x}}) \tag{5.7.9}$$

Chapter 6

ITERATIVE EQUALIZATION FOR A SINGLE CARRIER WITH CYCLIC PREFIX SCHEME

OFDM is an attractive technique for achieving high bit rate transmission over wireless channels and provides low complexity channel equalization over severe time invariant multipath environments [89, 90]. However, an OFDM signal has very high Peak to Average Power Ratio (PAPR) that has limited its application, since high PAPR requires an expensive transmitter power amplifier [91]. In the worst case scenario, peak transmitted power may be up to N times the average power, where N is the number of subcarriers used to transmit the OFDM block [92]. These large peaks cause saturation in power amplifiers. The conventional methods to reduce the PAPR are to use a linear power amplifier or back off the operating point of a non-linear power amplifier. Both of these methods result in a significant power efficiency penalty. To reduce PAPR the work in [91, 93] deliberately clips the OFDM signal before amplification, which mitigates the PAPR but introduces some performance degradation. Cimini in [94, 95] has presented a suboptimal strategy to tackle this problem.
Single Carrier with Cyclic Prefix (SCCP) is a closely related transmission scheme that possesses most of the benefits of OFDM but does not have PAPR problem, thereby eliminating the need for an expensive transmitter power amplifier that can operate

linearly over a wide range of signal amplitudes. On top of that the use of single carrier transmission has several attractive features, which are given below [76,90,96]:

1. When combined with CP, its performance with FDE is similar to that of OFDM, even for very long channel delay spread.

2. Single carrier modulation is a well proven technology in many existing wireless and wire-line applications and its radio frequency requirements are well known.

Therefore, this chapter provides the application of iterative algorithm, presented in the last chapter for OFDM, for SCCP systems.

6.1 A Brief Overview of the SCCP System

The basic baseband model of a conventional SCCP transmission and reception system is shown in Figure 6.1. Here, similar to OFDM, the data are transmitted in blocks and a CP is appended at the beginning of each data block. By doing this the effects of IBI are completely removed. Moreover, for an SCCP system, this approach enables the receiver to use the FFT and IFFT for FDE [86]. The data block is passed through a PTS stage to transmit the symbols serially. At the receiver $N + L - 1$ successive samples are collected and passed through an STP stage. Then, the first $L - 1$ received samples are removed that contribute to the symbols from the previous block. In FDE, the received time samples are converted into frequency domain and an MMSE equalization is performed to estimate the frequency domain transmitted symbols. If the channel is LTI then due to the presence of a diagonal ICI matrix the computational complexity of the equalization is $\mathcal{O}(N)$. To obtain the transmitted time domain symbols an inverse FFT is performed on the estimated frequency domain symbols. The relationship between the time and frequency domain symbols is given in (5.2.1). However, similar to OFDM an SCCP system is very sensitive to time selectivity of the channel that disturbs the orthogonality of the ICI matrix. For FDE, the time selectivity increases the computational complexity and

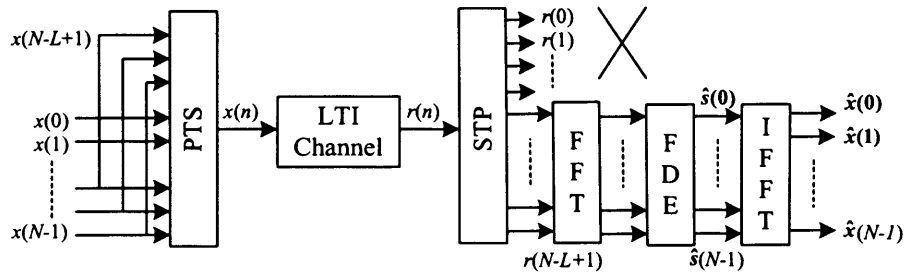

Figure 6.1. A basic baseband SCCP scheme, transmitting subsequent blocks of N data symbols and the receiver is performing frequency domain equalization, where L is the support of channel.

decreases the BER performance due to the emergence of the off diagonal terms in the ICI matrix. FDE for SCCP in a frequency selective channel is discussed in [76,90,97]. In most of the algorithms given in these papers, it is assumed that the channel is only frequency selective. In order to perform FDE in SCCP systems operating over a doubly selective channel, Schniter *et al.* [88], pre-processed the time domain received signal by multiplying with window coefficients that squeeze the significant coefficients in the ICI matrix into the $2D+1$ central diagonals. Here, it is found that $D = f_d N+1$, where f_d is the DS due to the relative motion between the transmitter and receiver and N is the number of symbols used to transmit an SCCP block of data. The complexity of this algorithm increases as the DS increases. In contrast to this work, as discussed in previous chapter, examining the time domain model of the received SCCP signal too reveals that the CCM is already sparse and has similar structure to that after preprocessing of the received samples [19,88].

6.2 Problem Statement

The iterative SCCP communication system used in this chapter is given in Figure 6.2. Before deriving the receiver, an intuitive explanation of its operation is discussed. Initially, all data to be transmitted are converted into blocks and a CP is added in

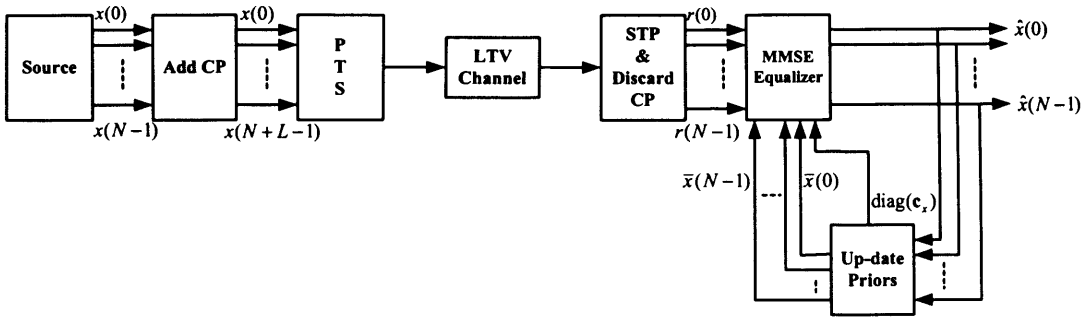

Figure 6.2. A baseband iterative SCCP system, transmitting subsequent blocks of N data symbols and the receiver is performing iterative time domain equalization.

each block. Each block of data is passed through a PTS stage to transmit each symbol in the block serially over the channel. At the receiver the signal is passed through the STP stage and the CP part is removed. Herein, in contrast to a conventional SCCP system no FFT and IFFT is performed on the received time samples. Then, an MMSE equalizer estimates the transmitted time domain symbols. The estimated values are used to find the means and variances of the transmitted symbols. By assuming the current estimated values are correct, their effects are cancelled when estimating the current symbol. This operation is done iteratively to obtain more accurate values. If the number of symbols in an SCCP block is N and the signal has propagated through L different paths, then, considering the sampling rate equal to the symbol transmission rate, the received baseband signal sampled at discrete time n, after removing the CP can be written as

$$\begin{aligned} r(n) &= \sum_{l=0}^{L-1} h_{n,l} x(\langle n-l \rangle_N) + v(n) \\ &= \frac{1}{\sqrt{N}} \sum_{k=0}^{N-1} s(k) e^{j\frac{2\pi}{N}kn} \sum_{l=0}^{L-1} h_{n,l} e^{-j\frac{2\pi}{N}kl} + v(n), \end{aligned} \tag{6.2.1}$$

where $h_{n,l}$ is the complex MG for the lth channel tap, $x(n)$, $v(n)$ and $s(k)$ are respectively the transmitted time domain symbols, the zero mean circularly complex white Gaussian noise at sample time n and the frequency domain transmitted symbols at

frequency k. By assuming the perfect knowledge of CIR, the N received samples in vector form can be written as

$$\mathbf{r} = \mathbf{H}\mathbf{x} + \mathbf{v} = \mathbf{H}\mathbf{F}^H\mathbf{s} + \mathbf{v}. \tag{6.2.2}$$

For FDE, the received time domain sample vector, $\mathbf{r}$, is multiplied with the FFT matrix that yields the frequency domain samples

$$\mathbf{F}\mathbf{r} = \mathbf{F}\mathbf{H}\mathbf{F}^H\mathbf{s} + \mathbf{F}\mathbf{v} = \mathbf{H}_{df}\mathbf{s} + \mathbf{F}\mathbf{v}, \tag{6.2.3}$$

where $\mathbf{H}$ is the CCM of size $N \times N$, the nth row and lth column entry of the matrix $\mathbf{H}$ can be written as $\mathbf{H}_{n,l} = h_{n,\langle n-l\rangle_N}$. Similarly, as defined in the previous chapter, $\mathbf{F}$ is the FFT matrix of size $N \times N$, $\mathbf{H}_{df}$ is the ICI matrix and $\mathbf{s}$ is a vector of frequency domain transmitted symbols. The MMSE equalizer for the estimation of $\mathbf{s}$ can be found by minimizing $E\{\|\mathbf{s} - \mathbf{W}\mathbf{F}\mathbf{r}\|^2\}$ yielding

$$\mathbf{W} = (\mathbf{H}_{df}^H\mathbf{H}_{df} + \sigma_n^2\mathbf{I}_N)^{-1}\mathbf{H}_{df}^H \tag{6.2.4}$$

where $\mathbf{W}$ is an equalizer coefficient matrix to decode all the frequency domain transmitted symbols and σ_n^2 is the variance of the noise. For frequency domain equalization, if in (6.2.3) the channel is LTI then the matrix $\mathbf{H}_{df}$ will be diagonal. Thereby, in order to estimate the sequence of samples $\{s(k)\}$, the L-MMSE equalizer requires the inversion of a diagonal matrix that is computationally inexpensive. Furthermore, to estimate the sequence of transmitted symbols $\{x(n)\}$, an IFFT is performed on the sequence of estimated samples $\{s(k)\}$.

On the other hand, in a LTV channel the matrix $\mathbf{H}$ is not circulant, therefore the matrix $\mathbf{H}_{df}$ is not diagonal, a consequence of which is that ICI is introduced. Hence the L-MMSE equalizer requires the inversion of an $N \times N$ matrix that needs $\mathcal{O}(N^2)$ operations, which is infeasible for large N and yields poor BER performance [83]. However, as shown in Figure 5.4, if modulo-N indexing is assumed, then the structure of $\mathbf{H}$ reveals that the individual symbol $x(n)$ contributes only to the observation

samples $r(n)$ to $r(n+L-1)$. Therefore, considering modulo-N indexing in the sequel, it can be noted that these are the only samples required to estimate $x(n)$ and in vector form these received samples can be written as,

$$\mathbf{r}_n = \mathbf{H}_n\mathbf{x} + \mathbf{v}_n, \tag{6.2.5}$$

where

$$\mathbf{r}_n = \begin{bmatrix} r(n) & r(n+1) & \cdots & r(n+L-1) \end{bmatrix}^T,$$

matrix $\mathbf{H}_n$ contains L rows of the matrix $\mathbf{H}$ from n to $n+L-1$ and

$$\mathbf{v}_n = \begin{bmatrix} v(n) & v(n+1) & \cdots & v(n+L-1) \end{bmatrix}^T.$$

6.3 Symbol Estimation

Similar to OFDM in the last chapter, to estimate the transmitted time domain symbols, the sparsity present in the CCM is exploited to design a length L MMSE equalizer. As discussed in Chapter 5, in OFDM the time domain transmitted symbols have a high number of unknown constellation points as a consequence of the IFFT operation on the symbols to be transmitted. Therefore, it was impractical to find the LLRs of the time domain samples and frequency domain samples were obtained in order to find the LLRs. In contrast, in SCCP, the transmitted time domain symbols have finite constellation points. Therefore, the LLRs can be found without using frequency domain samples. On this basis, next a low complexity MMSE-iterative algorithm is described.

6.3.1 MMSE Equalizer

To find the MMSE equalizer for an SCCP system, the derivations of the previous chapter are followed. The noise is assumed temporally uncorrelated, circularly distributed and zero mean, therefore $E\{\mathbf{v}_n\} = \mathbf{0}$, $E\{\mathbf{v}_n\mathbf{v}_n{}^H\} = \sigma_n^2\mathbf{I}_L$ and $E\{x(n)\mathbf{v}_n\} = \mathbf{0}$. Further, define $\bar{x}(n) = E\{x(n)\}$, $\bar{\mathbf{x}} = E\{\mathbf{x}\}$, $\mathbf{c}_x = \begin{bmatrix} c_x(0) & c_x(1) & \cdots & c_x(N-1) \end{bmatrix}$ and

$c_x(n) = \text{Cov}[x(n), x(n)]$. The MMSE equalizer, $\mathbf{w}_n$, of length L for the soft estimates of $x(n)$ can be derived by minimizing the cost function,

$$J(\mathbf{w}_n) = E\{|x(n) - \mathbf{w}_n^H \mathbf{r}_n|^2\}, \tag{6.3.1}$$

which yields the MMSE equalizer coefficient vector, $\mathbf{w}_n$, and estimator $\hat{x}(n)$ as derived in Appendix 5A and 5B,

$$\mathbf{w}_n = \left(\mathbf{H}_n \text{diag}(\mathbf{c}_x)\mathbf{H}_n^H + {\sigma_x}^2 \mathbf{I}_L\right)^{-1} \mathbf{h}_n c_x(n) \tag{6.3.2}$$

$$\hat{x}(n) = \bar{x}(n) + \mathbf{w}_n^H(\mathbf{r}_n - \mathbf{H}_n \bar{\mathbf{x}}) \tag{6.3.3}$$

with the assumption that $\{\bar{x}(n) \neq 0\}$, the mean values of the estimates of the individual symbols can not be equal to zero, in (6.3.2) $\mathbf{h}_n$ is the nth column of $\mathbf{H}_n$. For better estimates the a posteriori mean values $\{\bar{x}(k)\}$ can be found to cancel their effects when finding any particular transmitted symbol. The posteriori mean values require the a posteriori probabilities, which are found in the next section.

6.3.2 Iterative Algorithm

For better estimates, it is intended to determine the a posteriori values of $\{\bar{x}(n)\}$ and $\{c_x(n)\}$ to use in (6.3.2) and (6.3.3) in the next iteration. To find these values the following steps are required to form the proposed iterative algorithm.

Step 1: In the first iteration, all mean values are initialized to zero i.e. $\{\bar{x}(n)\} = 0$ that corresponds to $\text{diag}(\mathbf{c}_x) = \mathbf{I}_N$, then, the estimate $\hat{x}(n)$ is obtained using (6.3.2) and (6.3.3).

Step 2: As mentioned in the previous chapter, with the assumption of BPSK signals, it is more convenient to work with the LLRs rather than the probabilities [98]. The a priori and a posteriori LLRs of $x(n)$ are defined as

$$L[x(n)] = \ln \frac{(Pr\{x(n) = 1\}}{Pr\{x(n) = -1\})} \tag{6.3.4}$$

and

$$L[x(n)|_{\hat{x}(n)}] = \ln\frac{(Pr\{x(n)=1|_{\hat{x}(n)}\}}{Pr\{x(n)=-1|_{\hat{x}(n)}\})}. \tag{6.3.5}$$

The difference between the a posteriori and a priori LLRs (which is the extrinsic information) of $x(n)$, as derived in the previous chapter, is

$$\begin{aligned}\triangle L[x(n)] &= L[x(n)|_{\hat{x}(n)}] - L[x(n)] = L[\hat{x}(n)|_{x(n)}] \\ &= \ln\frac{p\{\hat{x}(n)|_{x(n)=1}\}}{p\{\hat{x}(n)|_{x(n)=-1}\}}.\end{aligned} \tag{6.3.6}$$

In order to find the extrinsic LLR, $L[\hat{x}(n)|_{x(n)}]$, it is assumed that the probability density function (PDF) of $\hat{x}(n)$ is Gaussian with variance σ_x^2 and can be written as

$$p\{\hat{x}(n)\} = \frac{1}{\sqrt{2\pi}\sigma_x}\exp\left(-\frac{(\hat{x}(n)-E\{\hat{x}(n)\})(\hat{x}(n)-E\{\hat{x}(n)\})^H}{2\sigma_x^2}\right). \tag{6.3.7}$$

Therefore the conditional PDF, when the transmitted signal $x(n) = b \in \{+1, -1\}$, of $\hat{x}(n)$ becomes

$$p\{\hat{x}(n)|_{x(n)=b}\} = \frac{1}{\sqrt{2\pi}\sigma_x}\exp\left(-\frac{(\hat{x}(n)-m_n(b))(\hat{x}(n)-m_n(b))^H}{2\sigma_x^2|_{x(n)=b}}\right), \tag{6.3.8}$$

where $m_n(b) = E\{\hat{x}(n)|_{x(n)=b}\}$ and $\sigma_x^2|_{x(n)=b} = \mathrm{Cov}[\hat{x}(n), \hat{x}(n)|_{x(n)=b}]$, which are the conditional mean and variance of $\hat{x}(n)$.

Throughout the iterative receiver process, to estimate $x(n)$ only the extrinsic information is used. Which implies that, when estimating $x(n)$, the a priori information is set as $\bar{x}(n) = 0$ and $c_x(n) = 1$ in equations (6.3.2) and (6.3.3). Hence, the conditional

mean can be determined by using (6.3.3) as

$$\begin{aligned} E\{\hat{x}(n)|_{x(n)=b}\} &= E\left\{\bar{x}(n) + \mathbf{w}_n^H\left(\mathbf{r}_n - \mathbf{H}_n\bar{\mathbf{x}}\right)\right\}|_{x(n)=b} \\ &= \mathbf{w}_n^H\mathbf{H}_n \begin{bmatrix} \bar{x}(0) \\ \cdots \\ b + \bar{x}(n) - \bar{x}(n) \\ \cdots \\ x(N) \end{bmatrix} - \mathbf{w}_n^H\mathbf{H}_n\bar{\mathbf{x}} \\ &= \mathbf{w}_n^H\mathbf{H}_n\mathbf{i}_n b + \mathbf{w}_n^H\mathbf{H}_n\bar{\mathbf{x}} - \mathbf{w}_n^H\mathbf{H}_n\bar{\mathbf{x}} \\ &= \mathbf{w}_n^H\mathbf{h}_n b \end{aligned} \tag{6.3.9}$$

It should be noted that $m_n(b)$ depends on the particular value of b. Similarly, it can be shown that the conditional variance of $\hat{x}(n)$ becomes

$$\begin{aligned} \sigma_x^2|_{x(n)=b} &= E\{\hat{x}(n)\hat{x}^H(n)|_{x(n)=b}\} - m_n(b)m_n(b)^H \\ &= E\{\hat{x}(n)\hat{x}^H(n)|_{x(n)=b}\} - \mathbf{w}_n^H\mathbf{h}_n\mathbf{h}_n^H\mathbf{w}_n \end{aligned} \tag{6.3.10}$$

within which the term

$$E\{\hat{x}(n)\hat{x}^H(n)|_{x(n)=b}\} = \mathbf{w}_n^H(\mathbf{H}_n\mathrm{diag}(\mathbf{c}_x)\mathbf{H}_n^H + \sigma_n^2\mathbf{I}_L)\mathbf{w}_n|_{x(n)=b} \tag{6.3.11}$$

Substituting (6.3.2) in (6.3.11) yields $E\{\hat{x}(n)\hat{x}^H(n)|_{x(n)=b}\} = \mathbf{w}_n^H\mathbf{h}_n$. Therefore (6.3.10) becomes

$$\sigma_x^2|_{x(n)=b} = \mathbf{w}_n^H\mathbf{h}_n - \mathbf{w}_n^H\mathbf{h}_n\mathbf{h}_n^H\mathbf{w}_n. \tag{6.3.12}$$

Note that unlike the mean the variance of the estimator is independent of b, and the difference between the a posteriori and the a priori LLR of $x(n)$ becomes

$$\begin{aligned}\triangle L\left[x(n)\right] &= \ln\frac{\left[\exp\left(-\frac{(\hat{x}(n)-m_n(+1))^2}{\sigma_{\tilde{x}}^2|_{x(n)=+1}}\right)\right]}{\left[\exp\left(-\frac{(\hat{x}(n)-m_n(-1))^2}{\sigma_{\tilde{x}}^2|_{x(n)=-1}}\right)\right]} \\ &= -\frac{(\hat{x}(n)-\mathbf{w}_n^H\mathbf{h}_n)^2}{\sigma_{\tilde{x}}^2|_{x(n)=+1}} + \frac{(\hat{x}(n)+\mathbf{w}_n^H\mathbf{h}_n)^2}{\sigma_{\tilde{x}}^2|_{x(n)=-1}} \\ &= 4\frac{Re\{\hat{x}(n)\}}{1-\mathbf{h}_n^H\mathbf{w}_n}. \end{aligned} \tag{6.3.13}$$

Therefore, the a posteriori LLR of $x(n)$

$$L\left[x(n)|_{\hat{x}(n)}\right] = L\left[x(n)\right] + \triangle L\left[x(n)\right]. \tag{6.3.14}$$

Step 3: Exploiting (6.3.14) and using the property $Pr\{x(n)=1|_{\hat{x}(n)}\} + Pr\{x(n)=-1|_{\hat{x}(n)}\} = 1$ the posteriori values for $\bar{x}(n)$ and $c_x(n)$ are obtained as

$$\begin{aligned}\bar{x}(n)|_{\hat{x}(n)} &= Pr\left\{x(n)=+1|_{\hat{x}(n)}\right\} - Pr\left\{x(n)=-1|_{\hat{x}(n)}\right\} \\ &= \tanh\left(\frac{L\left[x(n)|_{\hat{x}(n)}\right]}{2}\right) \end{aligned} \tag{6.3.15}$$

and

$$\begin{aligned}c_x(n)|_{\hat{x}(n)} &= \sum_{b\in\{+1,-1\}} (b-\bar{x}(n)|_{\hat{x}(n)})^2 Pr(x(n)=b|_{\hat{x}(n)}) \\ &= 1-\bar{x}(n)|_{\hat{x}(n)}^2. \end{aligned} \tag{6.3.16}$$

Note that equations (6.3.15) and (6.3.16) update the values of $\bar{x}(n)$ and $c_x(n)$ in (6.3.2) and (6.3.3) in Step 1.

Step 4: Steps 1 to 3 are repeated until the specified number of iterations has elapsed. The Table 6.1 shows the overall iterative algorithm used for the simulations.

Table 6.1. MMSE-Iterative algorithm for SCCP

$L = zeros(N, 1)$
$\bar{\mathbf{x}} = zeros(N, 1)$
$\text{diag}(\mathbf{c}_x) = \mathbf{I}_N$
while $iter \leq max - iter$
  for $n = 1 : N$
  $\bar{x}(n) = 0 \; ; \quad c_x(n) = 1$
    $\mathbf{w}_n = (\mathbf{H}_n \text{diag}(\mathbf{c}_x)\mathbf{H}_n^H + \sigma^2\mathbf{I})^{-1}\mathbf{h}_n$
    $\hat{x}(n) = \bar{x}(n) + \mathbf{w}^H(\mathbf{r}_n - \mathbf{H}_n\bar{\mathbf{x}})$
    $\triangle L(k) = \frac{4Re\{\hat{x}(n)\}}{1-\mathbf{h}_n^H\mathbf{w}_n}$
    $L(k) = L(k) + \triangle L(k)$
    $\bar{x}(n) = \tanh(L(k)/2)$
    $c_x(n) = 1 - \bar{x}(n)^2$
  end

6.4 Complexity of the Algorithm

6.4.1 Linear Time Variant Channel

In each iteration, to find the equalizer coefficient values $\mathbf{w}_n$, the algorithm requires the inversion of $[\mathbf{H}_n\text{diag}(\mathbf{c}_x)\mathbf{H}_n^H + \sigma_n^2\mathbf{I}_L]$ that needs $\mathcal{O}(L^2)$ operations and must be performed N times per iteration. Although the dimensions of matrix $\mathbf{H}_n$ are $L \times N$, it contains only $2L - 1$ non-zero columns. The product term inside the matrix $\mathbf{H}_n\text{diag}(\mathbf{c}_x)\mathbf{H}_n^H$ can be computed in $\mathcal{O}(L^2)$ operations as a consequence of the sparsity within the channel convolution matrix. Once $\mathbf{w}_n$ is obtained the estimation of $\hat{x}(n)$ requires the computation of $\mathbf{H}_n\bar{\mathbf{x}}$ that also needs $\mathcal{O}(L^2)$ operations and must be repeated N times per iteration. Therefore, to estimate N symbols only $\mathcal{O}(NL^2)$ computations per iteration are required.

6.4.2 Linear Time Invariant Channel

In an LTI channel the FDE requires $\mathcal{O}(2N\log_2 N)$ operations, while the proposed algorithm requires $\mathcal{O}(L^2N)$ operations per iteration. Therefore, the complexity of the proposed algorithm for a small length of channel ($\leq$5) is identical to the complexity of the FDE but the performance is better.

6.5 Simulation

In this section, the performance of the proposed low complexity MMSE-iterative algorithm is compared with the L-MMSE equalizer and MFB. The length of the CP is kept equal to the length of the channel. A 4-tap wireless fading channel model is used in which each channel tap is represented by a complex Gaussian random variable. The real and imaginary parts of each channel tap are independently generated with the Doppler spectrum based on Jakes' model. Here, it is assumed that $\sum_{l=0}^{L-1}\sigma_l^2 = 1$, where σ_l^2 is the variance of the lth path. The transmitted symbols $\{x(n)\}$ are BPSK. The MFB is obtained from the model given in (6.2.2) by assuming the symbols $\{x(l)|_{l\neq n}\}$ are known. In Figures 6.3 and 6.4 respectively, the convergence of the proposed iterative algorithm is analyzed for slow and fast time varying channels, for the SCCP block length of 32. From the figures it can be seen that the algorithm converges after five iterations and there is no significant change after five iterations. Moreover, for fast time varying channels it converges slightly faster. Figures 6.5 and 6.6 respectively compare the BER and SER performance of the iterative algorithm with the L-MMSE equalizer and MFB for the SCCP block length of 32. At low DS, for example $f_d = 0.001$, the channel changes very slowly and in this case the performances of the iterative method and the L-MMSE equalizer are close to each other. However, as the large DS introduces significant time selectivity into the channel the proposed algorithm outperforms the L-MMSE equalizer. Figure 6.7 repeats the simulation in Figure 6.5 for the SCCP block length of 64. By comparing the results of these figures, it can be concluded that using long length SCCP blocks of data

appears to yield better performance. For example, considering the performance of the iterative algorithm for the SCCP block length of 32 and 64 for the DS of 0.05. The algorithm for the SCCP block length of 64 yields 1dB gain in SNR. The reason for this gain is due to the fact that to estimate a symbol $x(n)$, more extrinsic information is available. In Figure 6.8, the performance of the proposed algorithm is compared with the FDE for the case of an LTI channel. Even in the case of an LTI channel, the iterative method outperforms the FDE by at least 1dB.

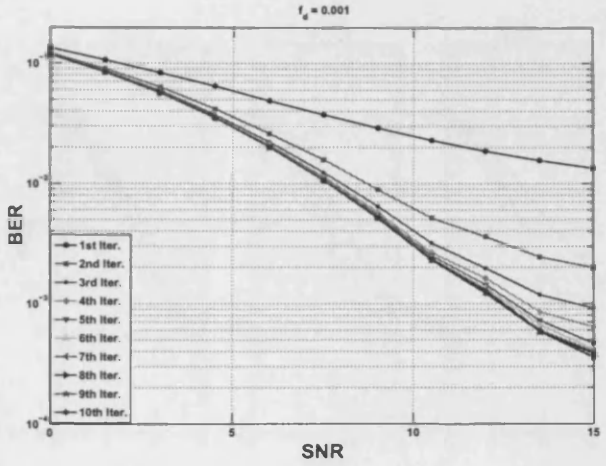

Figure 6.3. BER performance of the iterative algorithm after different number of iterations at slow fading $f_d = 0.001$.The number of symbols in a SCCP block is 32.

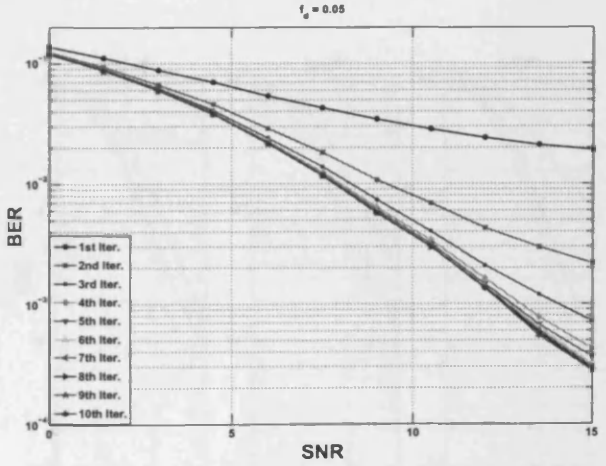

Figure 6.4. BER performance of the iterative algorithm after different number of iterations at fast fading $f_d = 0.05$. The number of symbols in a SCCP block is 32.

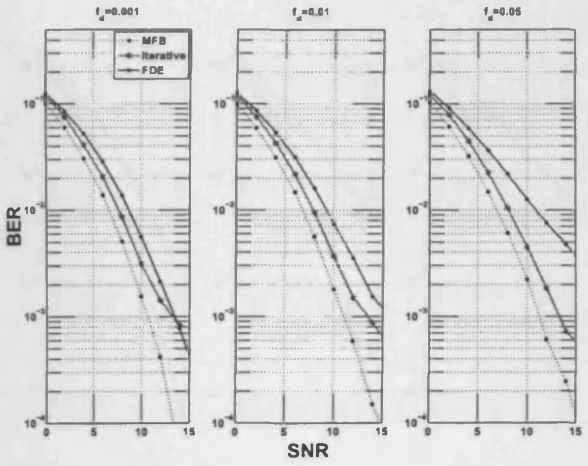

Figure 6.5. Bit error rate performance comparison of the proposed iterative algorithm after five iterations with the L-MMSE equalizer and MFB at different DSs. The number of symbols in one block is 32 and the length of the channel is 4.

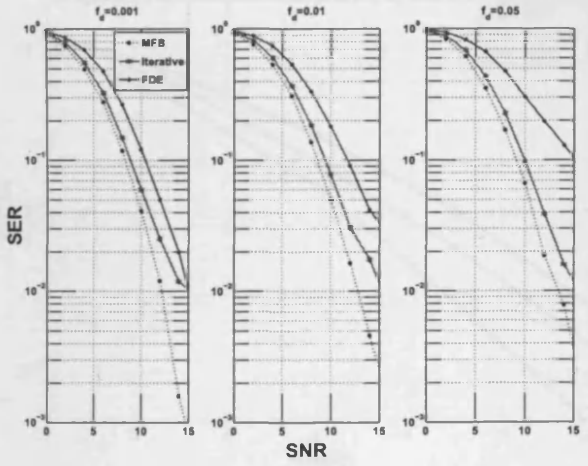

Figure 6.6. Symbol error rate performance comparison of the proposed iterative algorithm after five iterations with the L-MMSE equalizer and MFB at different DSs. The number of symbols in one block is 32 and the length of the channel is 4.

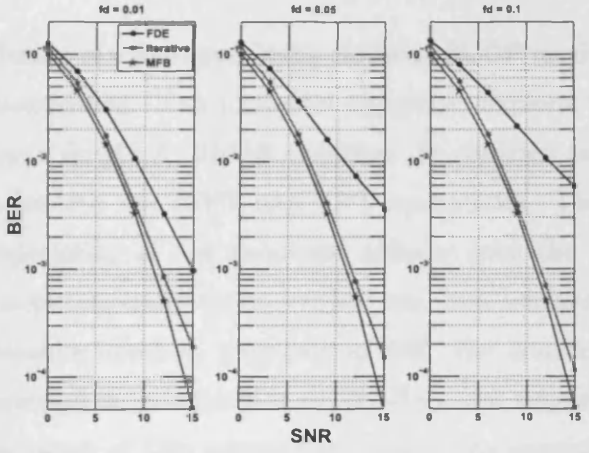

Figure 6.7. BER performance comparison of the proposed iterative algorithm after five iterations with the L-MMSE equalizer and MFB at different DSs. The number of symbols in one block is 64 and the length of the channel is 4.

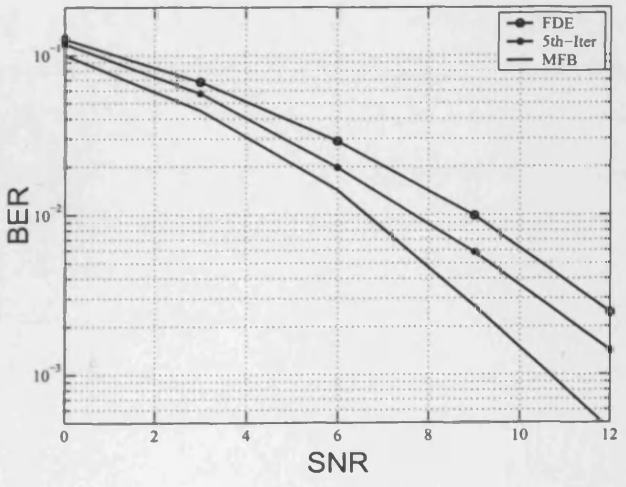

Figure 6.8. BER performance comparison of the proposed iterative algorithm for an LTI channel after five iterations with the FDE and MFB. In both equalizations, the number of symbols in one block is 32 and the length of the channel is 4.

6.6 Summary

In this chapter the design of a low complexity iterative SCCP receiver for LTV and LTI channels has been considered. The proposed algorithm exploits the sparsity present in the CCM to design a length L MMSE equalizer. In contrast to FDE, the proposed algorithm does not involve the IFFT and FFT operations. The simulation results demonstrate the superiority of the proposed scheme over the L-MMSE equalizer, which is not only computationally expensive but has poor performance. On the other hand, unlike the iterative method proposed in [88], the computational complexity of the proposed algorithm is independent of DS, does not require preprocessing and can work for a large range of DSs without increasing the computational complexity significantly. The computational complexity of the proposed algorithm depends on the length of the channel that can be reduced by applying channel shortening algorithms.

Chapter 7

CONCLUSION AND FUTURE WORK

7.1 Conclusion

With the advent of multimedia services in mobile communication the demand for high data rate is continuously increasing. High data rate transmission on a bandlimited channel gives rise to ISI, the effects of which can be mitigated by employing an equalizer at the receiver. On the other hand, for high data rate transmission the signals are transmitted on very high frequencies that in a mobile environment introduces significant DSs in the carrier frequencies, which is one of the main reasons for time variations in frequency selective channels. Time variation in frequency selective channels degrades the BER performance of communication systems and increases the computational burden on the receiver. In fast time-varying channels with higher order modulation schemes, adaptive equalizers may not perform well. Therefore, block based equalizers are preferred but they require the channel parameters. In fast time-varying channels the estimation of channel parameters becomes a challenging problem. Therefore, in this thesis the parameter estimation and equalization techniques for doubly selective channels have been developed and analyzed.

This thesis started with a simple time-varying deterministic channel, where the relative motion between the transmitter and receiver was very high and various multipaths experienced different DSs due to different angle of arrival. Distinct DSs introduced

sinusoidal time-variations in each multipath of the channel. At first, the equalization of a wireless SISO channel that allowed multipath with distinct DSs was considered. For this scenario, to mitigate the effects of the channel, the equalizer coefficient values required the knowledge of CSI and FOs. To estimate the FOs using MLE was an L dimensional maximization problem, where L is the support of the channel. However, exploiting the correlation property of the transmitted training sequence the L dimensional maximization problem was split into L one dimensional maximization problems. To validate the performance of FOs and CSI estimators, the CRLB was derived and the performance of the estimators was compared with this bound. The estimators were found to be statistically efficient. Moreover, distinct FOs could not be compensated for prior to equalization (as in conventional equalizations), therefore, they were accounted for in the equalizer design. By doing this, the equalizer design required the inversion of an $M \times M$ matrix to decode each symbol, where M was the number of equalizer taps. To reduce the computational burden on the receiver, a novel equalization structure was proposed that exploited the deterministic structural movements of the matrices in CCM, using matrix inversion lemmas and a corollary derived from these matrix inversion lemmas. The proposed algorithm did not require the inversion of an $M \times M$ matrix, rather the inversion of an $(M-1) \times (M-1)$ matrix was performed only at the start of the frame, for rest of the symbols no inversion was required.

Then the equalization of a SISO channel with multipath and multiple FOs was extended for multi-user transmission systems where the channel was modelled as a multiple-input and multiple-output frequency selective system. Here, estimation of FOs was an $n_R L$ dimensional problem. But due to uncorrelated training symbols from each transmit antenna, the problem was split into $n_R L$ one dimensional maximization problems. Here, again due to distinct DSs, the equalizer required the inversion of an $n_R M \times n_R M$ matrix. But, exploiting the structural movements of the matrices as in the SISO system the computational complexity was reduced significantly. In this

case, at the start of the frame the inversion of a $(M-1)n_R \times (M-1)n_R$ matrix was required, but for rest of the symbols in the frame, only the inversion of an $n_R \times n_R$ matrix was required.

In the rich scattering environment or when there was motion of physical objects between the transmitter and the receiver, the CCM did not change deterministically and the structural movements of the matrices could not be seen. In this scenario the channel was assumed to follow the Rayleigh fading model. Therefore, in the next step, the equalization of a general doubly selective channel was studied. For the equalization of a doubly selective channel, an OFDM scheme was considered, since it is more sensitive to the time selectivity of the channel. Here, it was assumed that the channel was known at the receiver. In OFDM, a time-varying channel introduced ICI that increased the computational complexity to $\mathcal{O}(N^3)$ and degraded the BER performance of the receiver. For an OFDM doubly selective channel, using the time and frequency samples a low complexity iterative algorithm was proposed. This algorithm exploited the sparsity present in the CCM to design a length L MMSE equalizer to decode the transmitted time domain samples, where L was the number of multipaths. The time domain samples were estimated on the basis of interference cancellations. Here, the time domain samples did not have finite constellation due to the IFFT operation therefore, it was difficult to find the mean values. In order to find the mean values, the estimated time domain samples were passed to the second stage where the frequency domain symbols were found. As the frequency domain symbols had finite constellations, it was easy to find the mean values. Mean values obtained in the second stage were converted into the time domain and passed back to the first stage. Both of these stages shared their information learnt from each other iteratively and worked independently. To make the outputs of each stage independent of each other, a random interleaver and a de-interleaver were introduced.

Finally, the iterative equalization of a Rayleigh fading channel for a SCCP system was considered. In contrast to the equalization of an OFDM channel, this algorithm worked only with time domain samples. In an SCCP system, at the transmitter no IFFT is performed on the signals to be transmitted, therefore, the transmitted time domain samples have finite constellations. In the proposed algorithm for SCCP, at the receiver, in contrast to conventional FDE, no FFT and IFFT was performed. To estimate the time domain samples a length L MMSE equalizer is designed and time domain samples were obtained by cancelling the interfering symbols obtained in the previous iteration. From the estimated time domain symbols the a posteriori probabilities were found and used to find the a posteriori means of the transmitted symbols. In the following iteration these mean values were used to cancel the interfering symbols when estimating symbols for obtaining more accurate values.

7.2 Future Work

The work presented in this thesis can be extended in a number of directions, including specific issues related to the algorithms presented. The proposed low complexity equalization presented in first two contribution chapters can be extended to the DFE, wherein, exploiting the structural movement in the convolution matrix could be challenging, but the DFE could provide a much better performance. Moreover, the presented FO estimation and correction can be employed in Ultra Wide Band (UWB), where the problem is more challenging due to wide spectrum of the signal.

In the last two chapters iterative algorithms are presented and a critical issue of estimation of time-varying channels was ignored. In our on-going work, the estimation of time-varying channels is being considered.

The proposed iterative algorithms also resemble turbo equalization, in on-going work the performance gap between the turbo equalization and the proposed algorithm when

coding is applied is being considered.
Here, the computational complexity of the algorithm increases linearly with the length of the channel. This can limit the application of the algorithm only to small length channels. In on-going work, it is being tried to develop algorithms that do not increase the computational complexity linearly with the channel length. Time domain channel shortening algorithms for doubly selective channels can also be found.

The work of iterative equalization could also be extended to MIMO OFDM.

BIBLIOGRAPHY

[1] S. Ahmed, S. Lambotharan, A. Jakobsson, and J. A. Chambers, "Parameter estimation and equalization techniques for communication channels with multi-path and multiple frequency offsets," *IEEE Trans. Commun.*, vol. 53, pp. 219–223, Feb. 2005.

[2] S. Ahmed, S. Lambotharan, A. Jakobsson, and J. A. Chambers, "MIMO frequency selective channels with multiple frequency offsets: Estimation and detection techniques," *IEE Commun. Proceedings*, pp. 489– 494, Aug. 2005.

[3] S. Ahmed, S. Lambotharan, A. Jakobsson, and J. A. Chambers, "Parameter Estimation and Equalization Techniques for MIMO Frequency Selective Channels with Multiple Frequency Offsets," *European Signal Processing Conference, Vienna, Austria*, Sep. 2004.

[4] S. Ahmed, S. L. M. Sellathurai, and J. A. Chambers, "Low Complexity Iterative Method of Equalization for OFDM in wireless channels with Multiple Frequency Offsets," *European Signal Processing Conference, Antalya, Turkey*, Sep. 2005.

[5] S. Ahmed, M. Sellathurai, and J. A. Chambers, "Low complexity iterative method of equalization for OFDM in doubly selective channels," *sumitted to IEEE Trans. Wireless Commun.*, Jul. 2005.

[6] S. Ahmed, M. Sellathurai, and J. A. Chambers, "Low complexity iterative method of equalization for OFDM in time varying channels," *accepted for 39th Asilomar*

Conference on Signals, Systems and Computers, Pacific Groves, California USA., Oct. 2005.

[7] S. Ahmed, M. Sellathurai, S. Lambotharan, and J. A. Chambers, "Parameter estimation and equalization techniques for communication channels with multi-path and multiple frequency offsets," *accepted for IEEE Signal Processing Letters.*

[8] E. Ayanoglu, K. Y. Eng, M. J. Karol, Z. L. P. Pancha, M. Veeraraghavan, and C. B. Woodworth, "Mobile Infra-structure," *Bell-Labs Technical Journal*, pp. 143–161, 1996.

[9] T. Ojanpera and R. Prasad, *Wideband CDMA for Third Generation Mobile Communications.* Artech House, 1998.

[10] S. Ohmori, Y. Yamao, and N. Nakajima, "The future generation of mobile communications based on broadband access technologies," *IEEE Commun. Magazines*, vol. 38, pp. 134–149, Dec. 2000.

[11] T. S. Rappaport, *Wireless Communications Principles and Practice.* Upper Saddle River, N.J.: Prentice-Hall, 2002.

[12] R. Pirhonen, T. Rautava, and J. Penttinen, "TDMA convergence for packet data services," *IEEE Personnel Communication Magazine*, vol. 6, pp. 68–73, June 1999.

[13] M. Zeng, A. Annamalai, and V. K. Bargava, "Harmonization of third-generation mobile systems," *IEEE Commun. Magazines*, pp. 94–104, Dec. 2000.

[14] H. Holma and A. Toskala, *WCDMA for UMTS.* New York, N.Y.: John Wiley and Sons, Inc., 2004.

[15] W. Mohr and W. Konhauser, "Access network evaluation beyond third generation mobile communications," *IEEE Commun. Magazines*, vol. 38, pp. 122–133, Dec. 2000.

[16] B. D. Woerner, J. H. Reed, and T. S. Rappaport, "Simulation issues for future wireless modems," *IEEE Commun. Magazines*, pp. 42 – 53, Jul. 1994.

[17] J. G. Proakis, *Digital Communications.* McGraw-Hill, Inc., 1989.

[18] S. Qureshi, "Adaptive equalization," *IEEE Proceedings*, vol. 73, pp. 1349–1387, Sep. 1985.

[19] P. Schniter, "Low-Complexity Equalization of OFDM in Doubly Selective Channels," *IEEE Trans. on Signal Processing*, vol. 52, pp. 1002–1010, April 2004.

[20] H. Viswanathan and R. Krishnamoorthy, "A frequency offset estimation technique for frequency selective fading channels," *IEEE Commun. Letters*, vol. 5, pp. 166–168, April 2001.

[21] P. Stoica and O. Besson, "Training sequence design for frequency offset and frequency selective channel estimation," *IEEE Trans. Commun.*, vol. 51, pp. 1910– 1917, Nov. 2003.

[22] K. E. Scott and E. B. Olasz, "Simultaneously clock phase and frequency offset estimation," *IEEE Trans. Commun.*, vol. 43, pp. 2263–2270, July 1995.

[23] H. Murata and S. Yoshida, "Maximum-likelihood sequence estimation receiver with joint frequency offset and delay profile estimation technique ," *Global Telecommunications Conference (GLOBECOM 98).*, vol. 6, pp. 3455 – 3459, Nov. 1998.

[24] X. Cai and G. B. Giannakis, " Low-complexity ICI Suppression for OFDM over Time and Frequency-Selective Rayleigh Fading Channels ," *Asilomar Conference on Signals, Systems and Computers*, vol. 2, pp. 1822 – 1826, Nov 2002.

[25] S. Haykin, *Communication Systems.* John Wiley and Sons, Inc.

[26] W. C. Jakes, *Microwave Mobile Communications.* Wiley IEEE Press, May, 1994.

[27] C. Toker, "Signal Processing Algorithms and Architectures for Communication Transceivers," *PhD thesis, University of London*, Sep. 2004.

[28] M. Morelli, U. Mengali, and G. M. Vitetta, "Further results in carrier frequency estimation for transmissions over flat fading channels," *IEEE Commun. Letters*, vol. 2, pp. 327–330, Dec. 1998.

[29] L. Krasny, H. Arslan, D. Koilpillai, and S. Chennakeshu, "Doppler spread estimation for wireless mobile radio systems," *IEEE Commun. Letters*, vol. 5, pp. 197 – 199, May 2001.

[30] S. M. Kay, *Fundamentals of Statistical Signal Processing, Estimation Theory.* Englewood Cliffs, N.J.: Prentice-Hall, 1993.

[31] A. Paulraj and C. Papadias, "Space time processing for wireless communications," *IEEE Signal Processing Magazine*, vol. 14, pp. 49–83, Nov. 1997.

[32] A. Naguib, N. Seshadri, and A. R. Calderbank, "Increasing data rate over wireless channels," *IEEE Signal Processing Magazine*, vol. 17, pp. 76–92, May 2000.

[33] O. Besson and P. Stoica, "On parameter estimation of MIMO flat-fading channels with frequency offsets," *IEEE Trans. Signal Processing*, vol. 51, pp. 602–613, March 2003.

[34] J. A. C. Bingham, *ADSL, VDSL, and Multicarrier Modulation.* New York: John Wiley and Sons, Inc., 2000.

[35] T. Starr, J. M. Cioffi, and P. J. Silverman, *Understanding Digital Subscriber Line Technology.* Upper Saddle River, N.J.: Prentice-Hall, 1999.

[36] R. W. Lucky, "Automatic equalization for digital Communication," *Bell System Technical Journal*, vol. 46, pp. 547–588, Nov. 1965.

[37] J. G. Proakis and J. Miller, "An adaptive receiver for digital signaling through channels with inter-symbol-interference," *IEEE Trans. on Inform. Theory*, vol. 15, pp. 484–497, Jul. 1969.

[38] S. Qureshi, "Adaptive equalization," *IEEE Transaction on Signal Processing*, vol. 20, pp. 9–16, Mar. 1982.

[39] J. G. Proakis, "Adaptive equalization for TDMA digital mobile radio," *IEEE Trans. on Vehicular Technology*, vol. 40, pp. 333–341, May 1991.

[40] G. D. Forney, "The Viterbi algorithm," *IEEE Proceedings*, vol. 61, pp. 268–278, Mar. 1978.

[41] H. Chen, R. Perry, and K. Buckley, "On MLSE algorithms for unknown fast time-varying channels," *IEEE Trans. Commun.*, vol. 51, pp. 730–734, May 2003.

[42] J. T. Chen, A. Paulraj, and U. Reddy, "Multichannel maximum-likelihood sequence estimation (MLSE) equalizer for GSM using a parametric channel model," *IEEE Trans. Commun.*, vol. 47, pp. 53–63, Jan. 1999.

[43] "Multiplexing and multiple access on radio path," *3GPP TS 45.002 (V5.9.0)*, April 2003.

[44] V. D. Trajkovic, P. B. Rapajic, and R. A. Kennedy, "Low-complexity iterative decoding with decision-aided equalization for magnetic recording channels," *To appear in IEEE Signal Processing Letters.*

[45] W. Zi-Ning and J. M. Cioffi, "Low-complexity iterative decoding with decision-aided equalization for magnetic recording channels," *IEEE Journal on Selected Areas in Commun*, vol. 19, pp. 699 – 708, Apr. 2001.

[46] C. A. Belfiori and J. H. Park, "Decision feed-back equalizer," *IEEE Proc.*, vol. 67, pp. 1143–1156, Aug. 1979.

[47] A. C. Raul, P. B. Schniter, J. Balakrishnan, and C. R. Johnson, "Tutorial on decision feed-back equalizer," *(www.ece.osu.edu/schniter/research.html)*, pp. 1–20, Jul. 1998.

[48] B. Widrow and S. D. Stearns, *Adaptive Signal Processing.* Englewood Cliffs, N.J.: Prentice-Hall, 1985.

[49] A. R. S. Bahai and M. Sarraf, "A frequency offset estimation technique for nonstationary channels," *International Conference on Acoustics, Speech, and Signal Processing (ICASSP)*, vol. 5, pp. 3897 – 3900, April 1997.

[50] A. R. S. Bahai and M. Sarraf, "A frequency offset estimation technique for wireless channels," *First IEEE Signal Processing Workshop on Signal Processing Advances in Wireless Commun.*, pp. 397 – 400, April 1997.

[51] W. Y. Kuo and M. P. Fitz, "Frequency offset compensation of pilot symbol assisted modulation in frequency flat fading," *IEEE Trans. Commun.*, vol. 45, pp. 1412 – 1416, Nov. 1997.

[52] A. V. Oppenheim and R. W. Schafer, *Discrete-Time Signal Processing.* Prentice-Hall, 1989.

[53] P. Stoica and R. Moses, *Introduction to Spectral Analysis.* Upper Saddle River, N.J.: Prentice Hall, 1997.

[54] B. Porat, *A Course in Digital Signal Processing.* New York, N.Y.: John Wiley and Sons, Inc., 1997.

[55] A. Eriksson, P. Stoica, and T. Soderstrom, "Asymptotical analysis of MUSIC and ESPRIT frequency estimates," *IEEE International Conference on Acoustics, Speech and Signal Processing (ICASSP)*, vol. 4, pp. 556 – 559, Apr. 1993.

[56] S. Haykin, *Adaptive Filter Theory (2nd edition).* Englewood Cliffs, N.J.: Prentice Hall, Inc., 1991.

[57] G. Strang, *Linear algebra and its applications, 3rd Ed.* Thomson Learning, Inc, 1988.

[58] E. Serpedin, A. Chevreuil, G. B. Giannakis, and P. Loubaton, "Blind channel and carrier frequency offset estimation using periodic modulation precoders," *IEEE Trans. Signal Processing*, vol. 48, pp. 2389–2405, Aug. 2000.

[59] Y. Ma and Y. Huang, "Blind estimation of carrier frequency offset for OFDM in unknown multi-path channels," *IEE Electronics Letter*, vol. 39, pp. 128–130, Jan. 2003.

[60] M. Ghogho and A. Swami, "Blind frequency-offset estimator for OFDM systems transmitting constant-modulus symbols," *IEEE Commun. Letters*, vol. 6, pp. 343 – 345, Aug. 2003.

[61] S. Haykin and M. Moher, *Modern Wireless Communications.* Upper Saddle River, N. J.: Prentice Hall, Inc., 2005.

[62] D. K. Hong, Y. J. Lee, D. Hong, and C. Kang, "Robust frequency offset estimation for pilot symbol assisted packet CDMA with MIMO antenna system," *IEEE Commun. Letters*, vol. 6, pp. 262–264, June 2002.

[63] L. Krasny, H. Arslan, D. Koilpillai, and S. Chennakeshu, "Optimal and suboptimal algorithms for Doppler spread estimation in mobile radio systems," *IEEE International Symposium on Personal, Indoor and Mobile Radio Communications (PIMRC 2000)*, vol. 2, pp. 1295 – 1299, Sep. 2000.

[64] A. R. S. Bahai and M. Sarraf, "Frequency offset estimation in frequency selective fading channels," *Vehicular Technology Conference (VTC)*, vol. 3, pp. 1719 – 1723, May 1997.

[65] Markku, J. Heihhila, P. Komulainen, and J. Lilleberg, "Interference suppression in

CDMA downlink through adaptive channel equalization," *IEEE Vehicular Technology Conference, 1999-Fall.*

[66] T. Kailath and A. H. Sayed, *Fast Reliable Algorithms for Matrices with Structure.* Philadelphia, USA: SIAM, 1999.

[67] M. A. Jensen and J. W. Wallace, "A review of antennas and propagation for MIMO wireless communications," *IEEE Trans. Antennas and Propagation*, pp. 2810–2824, Nov. 2004.

[68] C. E. Shannon and W. Weaver, *The Mathematical Theory of Communication.* Urbana: University of Illinois Press, 1962.

[69] J. Mietzner and P. A. Hoeher, "Boosting the performance of wireless communication systems: theory and practice of multiple-antenna techniques," *IEEE Communications Magazine*, pp. 40 – 47, Oct. 2004.

[70] G. J. Foschini and M. G. Gans, "On limits of wireless communications in a fading environment when using multiple antennas," *Wireless Personal Communications*, pp. 311–335, Mar. 1998.

[71] I. E. Telatar, "Capacity of multi-antenna Gaussian channels," *European Transactions on Telecommunications*, pp. 585–595, Nov. 1999.

[72] G. J. Foschini, "Layered space-time architecture for wireless communication in a fading environment when using multi-element antennas," *Bell Labs. Technical Journal*, pp. 41–59, Autumn 1996.

[73] S. M. Alamouti, "A simple transmit diversity technique for wireless communications," *IEEE Transaction on Selected Areas in Communications*, vol. 16, pp. 1451–1458, Oct. 1998.

[74] V. Tarokh, H. Jafarkhani, and A. R. Calderbank, "Space time block codes from orthogonal design," *IEEE Transactions on Information Theory*, vol. 45, pp. 1456–1467, July 1999.

[75] D. E. A. Clarke and T. Kanada, "Broadband: The last mile," *IEEE Commun. Magazine*, vol. 31, pp. 94–100, Mar. 93.

[76] H. Sari, G. Karam, and I. Jeanclaude, "Frequency domain equalization of mobile radio and terrestrial broadcast channels," *In Proc. Globcom Conference, San Francisco*, pp. 1–5, Nov. 1994.

[77] M. Morelli and U. Mengali, "An improved frequency offset estimator for OFDM applications," *IEEE Commun. Letters*, vol. 45, pp. 75–77, Mar. 1999.

[78] M. Morelli, "Timing and frequency synchronization for the uplink of an OFDMA System," *IEEE Trans. Commun.*, vol. 52, pp. 296 – 306, Feb. 2004.

[79] J. J. Beek, P. O. Borjesson, M. L. Boucheret, D. Landstrom, J. M. Arenas, and P. Odling, "A time and frequency synchronization scheme for multiuser OFDM," *IEEE Journals on Selected Areas of Commun.*, vol. 17, pp. 1378 – 1389, Nov. 1999.

[80] J. C. Lin, "Maximum-likelihood frame timing instant and frequency offset estimation for OFDM communication over a fast Rayleigh-fading channel," *IEEE Trans. Vehicular Technology*, vol. 52, pp. 1049 – 1062, July 2003.

[81] J. J. Beek, P. O. Borjesson, and M. Sandell, "Non-data-aided carrier frequency offset estimation for OFDM and downlink DS-CDMA systems," *IEEE Trans. Signal Processing*, vol. 45, pp. 1800–1805, Jul. 1997.

[82] P. H. Moose, "A technique for orthogonal frequency division multiplexing frequency offset correction," *IEEE Trans. Commun.*, vol. 42, pp. 2908–2914, Oct. 1994.

[83] Y. S. Choi, P. J. Voltz, and F. A. Cassara, "On Channel Estimation and Detection for Multi-carrier Signals in Fast and Selective Rayleigh Fading Channels ," *IEEE Trans. Commun*, vol. 49, pp. 1375 – 1387, Aug 2001.

[84] Y. R. Zheng and C. Xiao, "Simulation models with correct statistical properties for Rayleigh fading channels," *IEEE Trans. Commun.*, pp. 920–928, June. 2003.

[85] B. Sklar, "Rayleigh fading channels in mobile digital communication systems Part II: Mitigation," *IEEE Commun. Magazine*, vol. 35, pp. 102–109, Jul. 1997.

[86] G. L. Stuber, J. R. Barry, S. W. Mclaughlin, and M. A. Ingram, "Broadband MIMO-OFDM wireless Commun.," *Proc. IEEE*, vol. 92, pp. 271 – 294, Feb. 2004.

[87] M. Tüchler, R. Koetter, and A. C. Singer, "Turbo equalization: Principles and new results," *IEEE Trans. Commun.*, vol. 50, pp. 754–766, May. 2002.

[88] P. Schniter and H. Liu, "Iterative Equalization for Single-Carrier Cyclic-Prefix in Doubly-Dispersive Channels," *Asilomar Conference on Signals, Systems and Computers*, vol. 1, pp. 502 – 506, Nov. 2003.

[89] I. Koffman and V. Roman, "Broadband wireless access solutions based on OFDM access in IEEE 802.16," *IEEE Communications Magazine*, pp. 96–103, Apr. 2002.

[90] H. Sari, G. Karam, and I. Jeanclaude, "Transmission techniques for digital terrestrial TV broadcasting," *IEEE Communications Magazine*, vol. 33, pp. 100–109, Feb. 1995.

[91] X. Li and L. J. C. Jr., "Effects of clipping and filtering on the performance of OFDM," *IEEE Commun. Lett.*, vol. 2, p. 131133, May 1998.

[92] M. E. R. Khan and K. M. Ahmed, "A novel technique for peak to average power ratio reduction in OFDM systems," *Canadian Conference on Electrical and Computer Engineering*, vol. 1, pp. 165–168, May 1996.

[93] R. O. Neill and L. N. Lopes, "Envelope variations and spectral splatter in clipped multicarrier signals," *in Proc. PIMRC95*, p. 7175, Jun. 1995.

[94] J. L. J. Cimini and N. R. Sollenberger, "Peak-to-average power ratio reduction of an OFDM signal using partial transmit sequences," *IEEE Commun. Letters*, vol. 4, pp. 86–88, Mar. 2000.

[95] J. L. J. Cimini and N. R. Sollenberger, "Peak-to-average power ratio reduction of an OFDM signal using partial transmit sequences," *IEEE International Conference on Communications*, vol. 1, pp. 511–515, Jun. 1999.

[96] G. Kadel, "Diversity and equalization in frequency domain - A robust and flexible receiver technology for broadband mobile communications system," *IEEE Vehicular Technology Conference*, vol. 2, pp. 894 – 898, May 1997.

[97] D. Falconer, S. L. Ariyavisitakul, A. B. Seeyar, and B. Edison, "Frequency Domain Equalization for Single-Carrier Broadband Wireless Systems," *IEEE Commun. Magazine*, pp. 58–66, Apr. 2002.

[98] R. Koetter, A. C. Singer, and M. Tuchler, "Turbo equalization," *IEEE Signal Processing Magazine*, vol. 21, pp. 67 – 80, Jan. 2004.